REFERENCE ONLY

UNIVERSITY OF LONDON THESIS

Degree PhD Year 2006 Name of Author HARRIS R K

COPYRIGHT

This is a thesis accepted for a Higher Degree of the University of London. It is an unpublished typescript and the copyright is held by the author. All persons consulting the thesis must read and abide by the Copyright Declaration below.

COPYRIGHT DECLARATION

I recognise that the copyright of the above-described thesis rests with the author and that no quotation from it or information derived from it may be published without the prior written consent of the author.

LOANS

Theses may not be lent to individuals, but the Senate House Library may lend a copy to approved libraries within the United Kingdom, for consultation solely on the premises of those libraries. Application should be made to: Inter-Library Loans, Senate House Library, Senate House, Malet Street, London WC1E 7HU.

REPRODUCTION

University of London theses may not be reproduced without explicit written permission from the Senate House Library. Enquiries should be addressed to the Theses Section of the Library. Regulations concerning reproduction vary according to the date of acceptance of the thesis and are listed below as guidelines.

A. Before 1962. Permission granted only upon the prior written consent of the author. (The Senate House Library will provide addresses where possible).

B. 1962 - 1974. In many cases the author has agreed to permit copying upon completion of a Copyright Declaration.

C. 1975 - 1988. Most theses may be copied upon completion of a Copyright Declaration.

D. 1989 onwards. Most theses may be copied.

This thesis comes within category D.

☑ This copy has been deposited in the Library of UCL

☐ This copy has been deposited in the Senate House Library, Senate House, Malet Street, London WC1E 7HU.

Functional Analysis of PfSUB2: a Malaria Merozoite Serine Protease

Philippa Kate Harris

Division of Parasitology

National Institute of Medical Research

London, NW7 1AA

A thesis submitted in part fulfilment of the requirement of University College London for the degree of Doctor of Philosophy

2005

UMI Number: U592892

All rights reserved

INFORMATION TO ALL USERS
The quality of this reproduction is dependent upon the quality of the copy submitted.

In the unlikely event that the author did not send a complete manuscript
and there are missing pages, these will be noted. Also, if material had to be removed,
a note will indicate the deletion.

UMI U592892
Published by ProQuest LLC 2013. Copyright in the Dissertation held by the Author.
Microform Edition © ProQuest LLC.
All rights reserved. This work is protected against
unauthorized copying under Title 17, United States Code.

ProQuest LLC
789 East Eisenhower Parkway
P.O. Box 1346
Ann Arbor, MI 48106-1346

Malaria is caused by members of the apicomplexan parasite genus *Plasmodium.* Of the four species that infect humans, *P. falciparum* is associated with the most severe forms of the disease. *P. falciparum* has a complicated life cycle involving two hosts. The disease in humans is associated with the red blood cell (RBC) cycle. Merozoites invade a RBC, replicate asexually within it, and cause the RBC to rupture releasing daughter merozoites into the blood stream to repeat the cycle. Invasion relies on an actinomyosin motor within the parasite and is also associated with the proteolytic shedding of a number of merozoite surface proteins, including the essential proteins AMA1 and MSP1. Both are shed by a merozoite surface 'sheddase' called MESH. The leading candidate for MESH is PfSUB2, an essential membrane-bound subtilisin-like protease (subtilase). In this project I have used transfection of the parasite to explore the role of PfSUB2 within the asexual blood stage life cycle of *P. falciparum*. PfSUB2 has been epitope tagged by targeted homologous recombination, and shown to initially accumulate in apical organelles called micronemes. Following merozoite release PfSUB2 is capped to the rear of the parasite in an actin-dependent manner and following invasion is detected distributed around the plasma membrane of the intracellular parasite. This pattern of trafficking is similar to that predicted for MESH. The tagged PfSUB2 has been purified from parasite extracts and the activity assessed. I have also attempted to over-express PfSUB2 from an episome within the parasite. As part of this work I have begun to characterise the *pfsub2* promoter. A region at the 5' region of the gene has been shown to display promoter activity.

This work would not have been possible without the help of many people. Firstly, I would like to thank my supervisor Mike Blackman for his excellent guidance. I would also like to thank the rest of the lab for their support, in particular Fiona Hackett for help in the early days, Rebecca O'Donnell for transfection and parasite advice and Sharon Yeoh for the PfSUB2 alignment. Peter Fletcher was responsible for manufacturing all the peptides used in this work and performed the mass spectroscopy.

On a personal note I would like to thank my family for their continuing support. Last but not least I would like to thank Tom for putting up with me and for his useful suggestions on practical techniques.

List of Tables **Page**

List of Figures: **Page**

Abbreviations:

AMA1	- Apical Membrane Antigen 1
APP	- Amyloid Precursor Protein
BDM	- Butane-2,3-monoxime
BSA	- Bovine Serum Albumin
CAT	- Chloramphenicol Acetyl Transferase
DAPI	- 4,6-diamidino-2-phenylindole
dATP	- Adenine Triphosphate
ddH_2O	- double distilled water
DMF	- Dimethyl Formamide
DMSO	- Dimethyl Sulphoxide
ER	- Endoplasmic Reticulum
ECL	- Enhanced Chemiluminescent solution
FITC	- Fluorescein
GDP	- Gross Domestic Product
GFP	- Green Fluorescent Protein
GPI	- Glycosyl-phosphatidylinositol
HA	- Haemagglutinin
6-IATR	- 6-iodoacetamidotetramethylrhodamine
IFA	- Immunofluorescence assay
IMC	- Inner Membrane Complex
IPTG	- Isopropyl beta D thiogalactopyranoside
JAS	- Jasplakinolide
MESH	- Merozoite Surface Sheddase
MESNA	- sodium 2-mercaptoethanesulphonate
MPP	- Microneme Protein Protease
MSP1	- Merozoite Surface Protein 1
OD	- Optical Density

PBST	- PBS Tween
PCR	- Polymerase Chain Reaction
PfSUB2	- *P. falciparum* subtilisin-like serine protease 2
PV	- Parasitophorous Vacuole
RBC	- Red Blood Cell
RP-HPLC	- Reversed Phase - High Performance Liquid Chromatography
SDM	- Site Directed Mutagenesis
SDS	- Sodium Dodecyl Sulphate
SDS-PAGE	- SDS Polyacrylamide Gel Electrophoresis
TCEP	- Tris(carboxyethyl)phosphine
TGF	- Transforming Growth Factor
TLC	- Thin Layer Chromatography
TRAP	- Thrombospondin Related Anonymous Protein

1. Introduction

1.1 Malaria

The phylum Apicomplexa comprises a wide array of obligate intracellular parasites including *Toxoplasma gondii*, the causative agent of toxoplasmosis, and *Plasmodium* the causative agent of malaria. *P. falciparum* is one of four species of *Plasmodium* which infect humans and is the species primarily associated with mortality. Malaria is found in tropical and sub-tropical areas of the world and causes an estimated 300-500 million cases and 2.3 million deaths per year although recent work by Snow *et al.* suggests that the number of cases is vastly underestimated, particularly in areas outside Africa [1, 2]. Unsurprisingly, the burden placed on countries with endemic malaria is reflected economically; the increase in gross domestic product (GDP) between 1965-1990 for countries with severe malaria was 0.4% compared with 2.3% average growth in other countries [3].

The disease seen in vertebrates infected with *Plasmodium* is associated with replication of the asexual erythrocytic stage (see below). In infection with *P. falciparum* the clinical outcome varies from an asymptomatic infection to the more severe forms of the disease, such as severe anaemia and cerebral malaria, often resulting in death. There are drugs, such as the first-line antimalarial chloroquine, that can be used to treat malaria infections. However the emergence of drug resistant forms of the parasite means that the first-line drugs are no longer very effective and alternatives are required. The drugs required to treat chloroquine-resistant *P. falciparum* malaria are over ten times more expensive than chloroquine and cannot be afforded by many of the countries most affected [4]. There is a pressing need for new antimalarials and the identification of novel chemotherapeutic targets. Indeed Breman argues that without effective intervention the number of cases in children under 5 in endemic areas could double by 2020 [5].

1.2 Life cycle

The *P. falciparum* life cycle, illustrated in Figure 1.1, requires two hosts; an *Anopheles* mosquito for the sexual reproductive stages and a human host for the asexual reproductive stages. In brief, a mosquito takes up male and female gametocytes in a blood meal which undergo fertilization in the insect midgut to form ookinetes. These cells penetrate the midgut wall and form oocysts. The parasite undergoes replication within the oocyst which then ruptures releasing sporozoites. Sporozoites exhibit gliding motility and migrate through tissues to the salivary glands from where they enter the vertebrate host at the mosquito's next blood meal. The sporozoites invade hepatocytes, undergo schizogony and differentiate into merozoites. The merozoites are released into the blood stream and invade red blood cells (RBCs). Within the RBC the parasite progresses through a number of morphologically distinct stages called ring, trophozoite and schizont. The RBC then ruptures and releases daughter merozoites which initiate another cycle of replication by invading new RBCs. The length of time from merozoite invasion to release varies amongst *Plasmodium* species, and in *P. falciparum* is 48 hours. *P. falciparum* merozoites must attach and invade erythrocytes efficiently as the invasive half-life is very short [6]. During the erythrocytic replication cycle gametocytes are also formed which the mosquito takes up during a blood meal and the cycle continues.

1.3 The merozoite

The merozoite, as seen in Figure 1.2, is an ovoid cell which varies in size between *Plasmodium sp.* and in *P. falciparum* is approximately 1.6 µm long and 1.0 µm wide [7]. The surface of the parasite is covered in a coat of bristle-like filaments [8]. The parasite cell wall consists of a three-layered pellicle with a plasma membrane and two inner membranes known as the inner membrane complex (IMC). The apical prominence of the cell contains the rhoptries, twin pear shaped organelles, and the smaller micronemes, clustered around the rhoptry ducts. The

Figure 1.1 The *P. falciparum* lifecycle

Schematic representation of the *P. falciparum* lifecycle. In brief, male and female gametocytes undergo fertilization in the insect midgut to form ookinetes (1). These penetrate the midgut wall and form oocysts. The parasite undergoes replication within the oocyst which then ruptures releasing sporozoites (2). These migrate to the salivary glands and enter the vertebrate host at the mosquito's next blood meal. Sporozoites invade hepatocytes, undergo schizogony and differentiate into merozoites which are released into the blood stream (3). Within the RBC the parasites undergo schizogony and form daughter merozoites (4). The RBC ruptures and merozoites are released which initiate another cycle of replication. Gametocytes are also formed during this cycle which the mosquito takes up in a blood meal.

This figure is taken from 'Malaria', Edited by A.J Knell for The Wellcome Trust, Oxford University Press (1991).

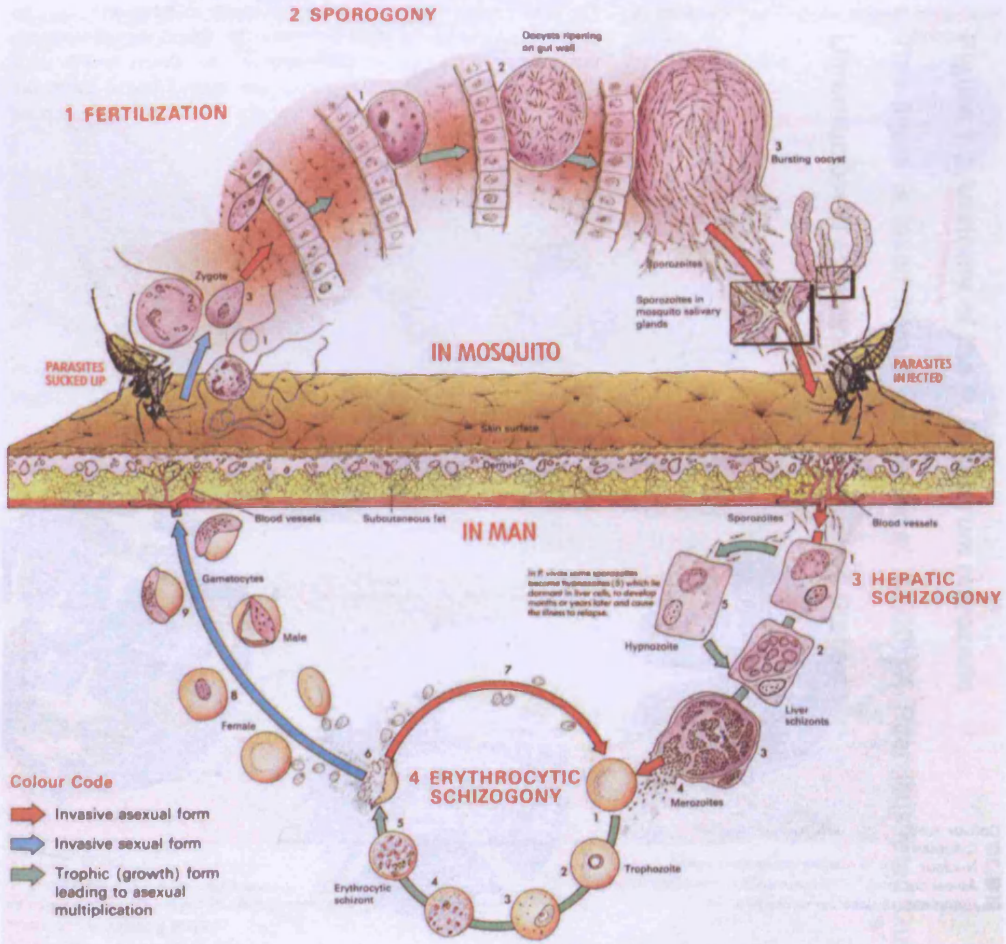
2 SPOROGONY
Oocysts ripening on gut wall
1 FERTILIZATION
3 Bursting oocyst
Zygote
Sporozoites
Sporozoites in mosquito salivary glands
IN MOSQUITO
PARASITES SUCKED UP
PARASITES INJECTED
Skin surface
Dermis
Blood vessels
Subcutaneous fat
IN MAN
Sporozoites
Blood vessels
Gametocytes
Male
Female
3 HEPATIC SCHIZOGONY
Hypnozoite
Liver schizonts
Merozoites
4 ERYTHROCYTIC SCHIZOGONY
Trophozoite
Erythrocytic schizont
Colour Code
Invasive asexual form
Invasive sexual form
Trophic (growth) form leading to asexual multiplication

Figure 1.2 Anatomy of the *P. falciparum* merozoite

This figure is taken from Bannister *et al*, (2000) 'A Brief Illustrated Guide to the Ultrastructure of *P. falciparum* Asexual Blood Stages'.

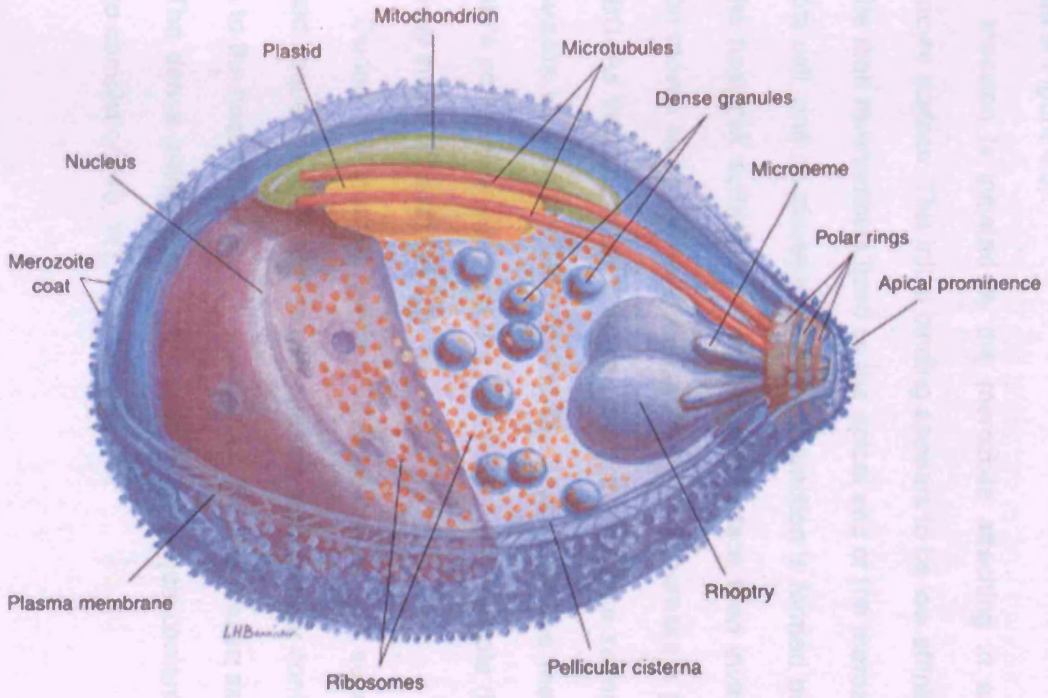
Mitochondrion
Plastid
Microtubules
Dense granules
Nucleus
Microneme
Polar rings
Merozoite coat
Apical prominence
Plasma membrane
Rhoptry
Ribosomes
Pellicular cisterna

dense granules lie separately within the apical cytoplasm of the merozoite.

1.4 Invasion of the RBC

Merozoite invasion of the erythrocyte is a very rapid process undergoing completion within a few seconds [9]. Despite this limitation the steps comprising the process of invasion have been well defined at the microscopic level and these are outlined in Figure 1.3.

Invasion is initiated by the merozoite attaching in any orientation to the erythrocyte surface. This initial binding appears to be low affinity and reversible. The parasite then re-orientates itself so the apical end of the merozoite is in contact with the host cell, and an electron-dense tight junction is formed between the merozoite and the host cell surface. The erythrocyte surface then invaginates and the tight junction moves along the merozoite surface as the parasite is propelled forward into the RBC. As the tight junction moves along the parasite surface the protein coat of the parasite is shed [8]. Once inside the erythrocyte the membrane fuses at the parasite's posterior end forming the parasitophorous vacuole (PV), which surrounds the newly invaded merozoite.

During this invasion process the contents of the secretory organelles are released sequentially. Firstly the micronemes secrete their contents as the parasites attach to the host cell and this is followed by rhoptry release as the parasite invades [10]. The dense granules only appear to release their contents once invasion has gone to completion [10, 11].

1.5 Invasion is driven by a parasite actinomyosin motor

Erythrocyte invasion by *Plasmodium* merozoites is blocked in the presence of cytochalasin, an inhibitor of actin polymerisation and butane-2,3-dione monoxime

Figure 1.3 The erythrocytic cycle of *P. falciparum*

The *P. falciparum* merozoite (a) attaches in any orientation and then (b) re-orientates so its apical end is in contact with the RBC surface. (c); the tight junction is formed and the contents of the secretory organelles released. (d); the tight junction sweeps over the parasite surface as it enters the RBC. (e); merozoite surface proteins are shed and the parasite enters the cell enclosed in the PV.

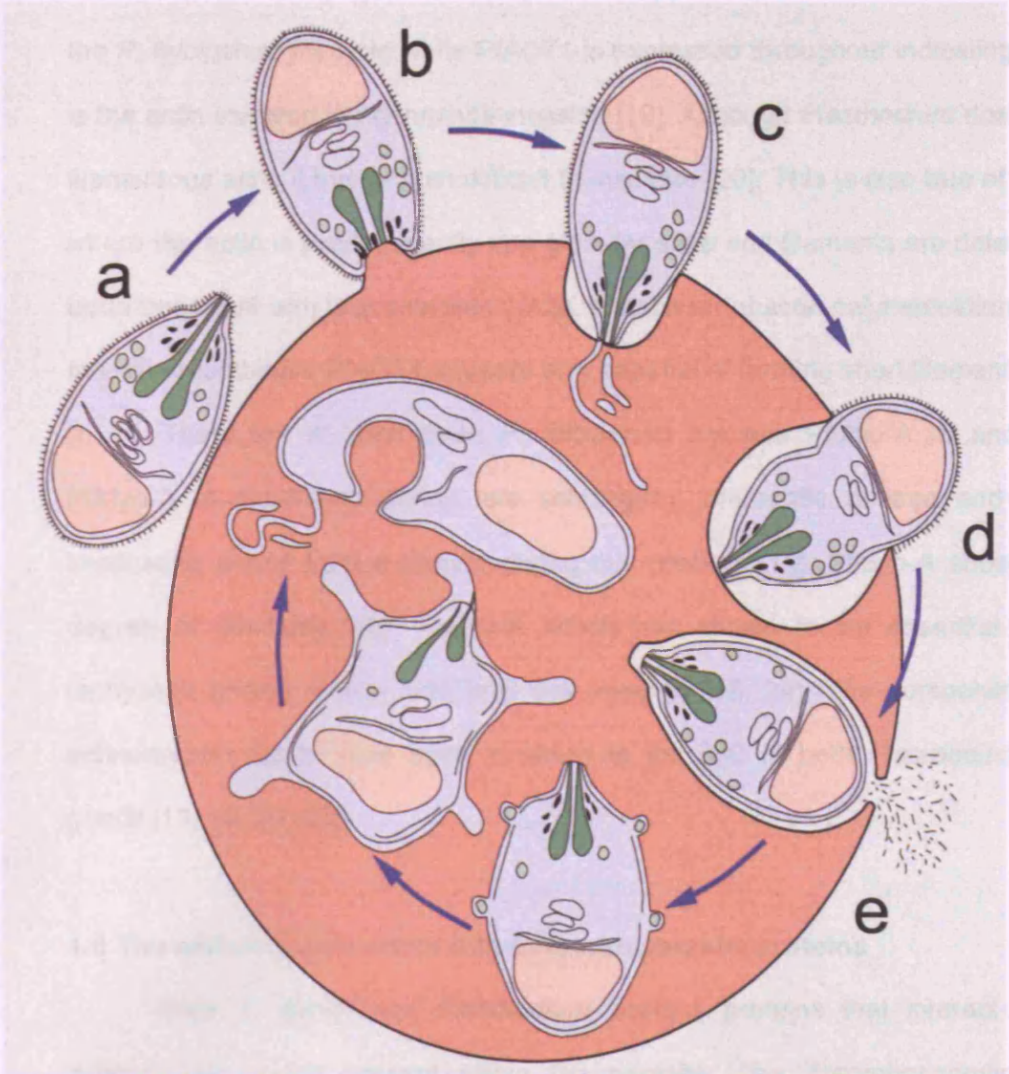
a
b
c
d
e

(BDM), an inhibitor of the myosin ATPase [12, 13]. These compounds have also been shown to inhibit the invasion of host cells by *T. gondii* tachyzoites and other apicomplexa such as *Eimeria tenella* [14-16]. These results implicate an actinomyosin motor as being involved in the invasion of host cells by apicomplexa [17].

P. falciparum possesses two actin genes coding for *P. falciparum* actin 1 (Pf-ACT1) and PfACT2 [18]. PfACT2 expression appears limited to the sexual stages of the *P. falciparum* lifecycle while PfACT1 is expressed throughout indicating that this is the actin involved in erythrocyte invasion [19]. Although *Plasmodium* does contain filamentous actin it has proven difficult to visualise [20]. This is also true of *T. gondii* where the actin is predominantly in a globular state and filaments are detected only upon treatment with jasplakinolide (JAS), a stabiliser of actin polymerisation [21, 22]. *In vitro* recombinant PfACT1 appears only capable of forming short filaments [23].

There are at least three *P. falciparum* myosins PfMyo-A, B and C [17]. PfMyo-A is expressed during late schizogony, merozoite release and invasion implicating a role for the protein during this process [13]. PfMyo-A shows a high degree of similarity with TgMyo-A which has shown to be essential for both tachyzoite gliding motility and host cell invasion [13, 24]. The components of an actinomyosin motor have been localised to the IMC in both *Plasmodium* and *T. gondii* [13, 15, 22, 25].

1.6 The actinomyosin motor interacts with parasite proteins

Both *T. gondii* and *Plasmodium* express proteins that interact with the actinomyosin motor present within the parasite. The Thrombospondin-Related Anonymous Protein (TRAP) family are integral membrane proteins containing a number of adhesive domains that are found throughout apicomplexa [26]. Members of this protein family have been shown to be crucial for the invasion process [27-30]. The first member to be described was TRAP, found on the surface of *P. falciparum*

sporozoites, but also detected during the erythrocytic stage indicating a general role in invasion [31]. Other examples of this protein family include the paralog PfCTRP, expressed in the ookinete stage and MIC2 expressed in *T. gondii* tachyzoites [30, 32]. TRAP and MIC2 have been shown to interact with glycosaminoglycans (GAGs) present on cell surfaces indicating that their role may be in adhesion to the host cell [33, 34].

TRAP and MIC2 initially accumulate in the micronemes of the parasites before release onto the cell surface and subsequent capping to the posterior of the cell [28, 32, 34-36]. The cytoplasmic domain of TRAP family members contain a number of conserved residues, including a number of acidic residues and a tryptophan, and the function of this region appears conserved amongst apicomplexa [28, 37]. These conserved residues present in the cytoplasmic tail are responsible for an interaction with aldolase, an enzyme known to bind F-actin and shown to interact with parasite actin [38-40]. This interaction means that TRAP and MIC2 are bound to the actinomyosin motor via aldolase and it is presumably this interaction that is responsible for the capping of the proteins during invasion.

As invasion proceeds MIC2 and TRAP are shed from the parasite surface [28, 32, 36]. The shedding of MIC2 constitutes a C-terminal cleavage by the action of a serine protease named microneme protein protease 1 (MPP1) and is essential for the parasite to detach from the host cell surface and invade [41, 42]. The mechanism of shedding of these proteins is likely to be conserved as TRAP expressed in *T. gondii* also undergoes C-terminal cleavage [43].

The capping and interaction with the actinomyosin motor of parasite proteins has led to a 'capping' model being proposed for cell invasion in *T. gondii,* and other related Apicomplexa [44, 45]. Transmembrane proteins, such as MIC2 and TRAP, move from the anterior to the posterior end of the parasite where they are shed. The transmembrane proteins adhere to the host cell on their ectoplasmic side, and are linked to the sub-membranous actinomyosin complex, so the rearward movement of

these proteins drives entry into the host cell. Final parasite release from the host cell surface and entry into the cell is coupled with eventual proteolytic removal of the adhesins. This proteolysis is likely to be essential for invasion to go to completion [41].

1.7 Protein shedding from the merozoite surface

The invasion of erythrocytes by the *Plasmodium* merozoite is also associated with surface adhesions that undergo shedding from the parasite membrane. Erythrocyte binding protein-175 (EBA-175) is a member of the ebl family of proteins that binds to glycophorin A, the dominant glycoprotein on the surface of the RBC [46-48]. The cytoplasmic tail of EBA-175 is essential for function of the protein but can be replaced with the TRAP tail despite no obvious homology between the two domains [49]. Parasites without EBA-175 are able to invade erythrocytes efficiently, albeit with a different ligand pathway [47].

Apical Membrane Antigen 1 (AMA1) is an integral membrane protein expressed late in the erythrocytic cycle of all the species of *Plasmodium* so far studied [19]. The protein is also expressed and shown to have a role during sporozoite invasion of hepatocytes [50]. The *pfama1* gene cannot be knocked out in the blood stages indicating that AMA1 is essential to the parasite [51]. Erythrocyte invasion and hepatocytes invasion can be blocked by anti-AMA1 antibodies and this has led to the development of AMA1 vaccines with varying degrees of success [50, 52-54]. There is a homologue, TgAMA1, present in *T. gondii* tachyzoites that also appears essential to the parasite [55].

In late schizogony PfAMA1 initially accumulates as an 83 kDa molecule in the micronemes where it undergoes N-terminal processing to form a 66 kDa protein [56-59]. This form relocates over the surface of the parasite upon merozoite release and is then shed [57]. The shedding of AMA1 is caused by a serine protease and may be essential for invasion [57, 60].

The structure of AMA1 is comprised of three domains characterised by the disulphide bonding pattern [61]. The recently solved crystal structure revealed that domains I and II resemble PAN domains, found in proteins with diverse adhesion functions and believed to be involved in binding interactions [62, 63]. AMA1 has been shown to bind to erythrocytes and may be involved in the re-orientation of the parasite on the host cell surface [64-66]. A conditional knock out of TgAMA1 has been achieved and the parasites are able to glide and initially attach to the host cell but are inhibited in their ability to intimately attach to host cells, release rhoptry contents and invade [67].

Merozoite Surface Protein 1 (MSP1) is another parasite surface protein believed to play a role in parasite adhesion to the RBC, in this case via erythrocyte proteins such as band 3 erythrocyte protein and spectrin [68, 69]. MSP1 is thought to be essential as attempts to knock out the *pfmsp1* gene have been unsuccessful [70]. The ability to block *Plasmodium* infection with anti-MSP1 antibodies has led to interest in the protein as a vaccine candidate [71].

MSP1 is attached to the parasite membrane by its C-terminus via a glycosyl-phosphatidylinositol (GPI) anchor [72]. The protein is synthesised as a 200 kDa precursor protein that undergoes extensive processing to give fragments called $MSP1_{83}$, $MSP1_{30}$, $MSP1_{38}$ and $MSP1_{42}$ which form a non-covalent complex on the merozoite surface [73]. During invasion the $MSP1_{42}$ fragment undergoes secondary processing, by the action of a serine protease, which releases the bulk of the protein but leaves a 19 kDa fragment ($MSP1_{19}$) bound to the parasite surface which is then carried into the RBC [74, 75]. If the secondary processing of MSP1 is blocked the parasites are unable to invade indicating that this cleavage is essential for invasion [6, 75].

The sites at which AMA1 and MSP1 shedding occur have no sequence similarity and the MSP1 site lies many residues further away from the membrane than the AMA1 site [60, 76]. However the two epidermal growth factor (EGF) domain

structure of $MSP1_{19}$, conserved amongst *Plasmodium*, means that the cleavage site probably lies in close proximity to the GPI anchor and at a similar distance to the membrane from the AMA1 cleavage site [6, 70, 77, 78]. Intriguingly Howell *et al.* demonstrated that the shedding of AMA1 was sensitive to the exact set of inhibitors, including specific compounds discovered from library screens, as MSP1 secondary processing [60]. It is highly unlikely that the parasite possesses two enzymes with identical inhibition profiles but rather that MSP1 and AMA1 are shed from the merozoite surface by the action of a single serine protease [60].

1.8 Sheddases

Sheddases are a group of enzymes that cleave integral membrane proteins or GPI anchored proteins releasing the protein from the membrane [79]. Proteins cleaved in this way include β-Amyloid precursor (APP), the protein involved in Alzheimer's disease, and transforming growth factor-α (TGF-α) [80]. The conformation and steric availability of a sheddase cleavage site is thought to be more important than the specific sequence [80-83]. A stalk of minimum length is also required [80]. Although sheddases are often metalloproteases there is growing evidence for alternative classes of enzymes, such as serine proteases, cleaving in this way [79, 84].

Because of its apparent sequence independent substrate recognition, the enzyme responsible for the shedding of both AMA1 and MSP1 from the parasite surface is considered to be a sheddase and has been named MErozoite surface SHeddase (MESH). Since, as described above, AMA1 and MSP1 shedding may be essential for the parasite to invade [6, 57, 60, 75], MESH therefore represents an attractive drug target candidate. However, at present the identity of MESH is unknown.

1.9 Serine proteases

Serine proteases are a large and diverse class of proteases that can be grouped into 6 clans [85]. The two largest of these are the chymotrypsin-like and subtilisin-like clans. Wu *et al.* identified members of both chymotrypsin-like and subtilisin-like clans within the *P. falciparum* genome alongside a number of more unusual serine proteases [86]. There appear to be only two chymotrypsin-like serine proteases both of which are homologues of DegP [86]. DegP protease (also known as HtrA) is a member of a family of serine proteases involved in cell fate and it is likely that the *P. falciparum* chymotrypsin-like proteases play a similar role within the parasite [87].

Plasmodium has eight putative rhomboids, a novel group of serine proteases, that cleave substrates at an intramembrane site [88-90]. These enzymes require a glycine/alanine motif, believed to destabilise the helix arrangement, in the transmembrane domain of substrates to allow cleavage [91]. These enzymes have been more extensively studied in *T. gondii* which has 6 rhomboids (TgROM1-6), four of which are expressed in the tachyzoite stage [92, 93]. MMP1, the enzyme responsible for the cleavage of MIC2, has recently been shown to be a rhomboid and this enzyme is likely to cleave other microneme proteins such as TgMIC6 and TgMIC12 [43, 91, 94]. Although TgROM2 has been shown to cleave the transmembrane domains of TgMIC2 and TgMIC12 *in vitro*, TgROM5 is considered to be MMP1 and has been localised to the posterior end of the cell [92, 93].

A number of transmembrane domains of *Plasmodium* proteins contain a rhomboid cleavage motif including members of the ebl family such as EBA-175 [95]. The rhomboid cleavage of MIC2 suggests that other members of this protein family, such as TRAP, may also undergo intramembrane cleavage from the parasite surface. A small proportion of PfAMA1 undergoes inefficient rhomboid cleavage and in the presence of compounds that inhibit the action of MESH this proportion is increased [60, 96]. This indicates that while AMA1 is not the physiological substrate

the parasite expresses active rhomboids. However, TgAMA1 is shed exclusively by the action of a rhomboid indicating differences in the shedding of membrane proteins between *P. falciparum* and *T. gondii* [96]. Rhomboids are not capable of cleaving GPI-anchored proteins, such as MSP1, indicating the need for proteases other than rhomboids to cleave *Plasmodium* surface proteins. As yet there is no evidence for a sheddase, such as MESH, in *T. gondii* and it may be that surface proteins in this parasite are removed solely by the action of intramembrane cleavage.

Subtilisins are characterised by an Asp/His/Ser catalytic triad surrounded by characteristic sequence motifs [97, 98]. The proteins are produced as inactive zymogens before autocatalytic cleavage to remove a propeptide and reveal an active protease [98-101]. Subtilisin propeptides are involved in the folding of the protein, which is critical for the formation of an active protease, and can also act as specific potent inhibitors of their respective enzyme [102-108]. There are 3 subtilisin-like serine protease genes found within the *P. falciparum* genome, called subtilisin-like serine protease 1 (PfSUB1), PfSUB2 and PfSUB3. The function of none of these proteases is known.

PfSUB1 is expressed during the erythrocytic cycle with maximum expression at the schizont stage and is located in the dense granules of the parasite [19, 109]. Attempts to knock out the *sub1* gene in both *P. berghei* and *P. falciparum* have been unsuccessful suggesting an essential role for the protein within the parasite [110, 111]. PfSUB1 can be expressed in a recombinant active form allowing study of the enzyme's substrate specificity [112]. The site of MSP1 cleavage is a leucine-asparagine bond and it has been shown that PfSUB1 cannot cleave this motif [76, 112]. PfSUB1 therefore cannot be responsible for the secondary cleavage of MSP1 and therefore cannot be MESH.

PfSUB3 is transcribed in gametocytes and sporozoites as well as during the erythrocytic cycle indicating a role throughout the lifecycle [19]. The *pfsub3* gene

has recently been knocked out in blood stage parasites and, while there was a slight growth defect in blood stage parasites, the shedding of MSP1 and AMA1 appeared normal indicating that PfSUB3 is not MESH [113].

1.10 PfSUB2

PfSUB2 is a large putative type I integral membrane protein expressed during the erythrocytic stage of the *P. falciparum* life cycle, specifically 40-48 hours post merozoite invasion and represented schematically in Figure 1.4 [19, 114]. Orthologues of PfSUB2 are found in all the species of *Plasmodium* so far studied and an alignment is shown in Figure 1.5 [115]. PfSUB2 is found as a very small proportion of the total protein content of the merozoite and is thought to be located in the dense granules at the apical end of the merozoite [114, 116].

The PfSUB2 primary sequence comprises a putative N-terminal secretory signal peptide, followed by a hydrophilic domain, a subtilase catalytic domain, transmembrane domain and finally a cytoplasmic domain [114]. The protein undergoes extensive post-translational processing. It is first expressed as a 160 kDa form which is rapidly converted to a 74 kDa intermediate form, before further processing to a 72 kDa form [114]. The localisation of PfSUB2 and time of expression suggest a role for the protein in erythrocyte invasion. The presence of a putative transmembrane domain may mean that the mature form(s) of PfSUB2 exist as a membrane-bound protease.

The protein appears to be essential as attempts to disrupt the *sub2* gene in both *P. falciparum* and *P. berghei* have been unsuccessful [115, 117]. PfSUB2 has also been detected in gametocytes and the orthologue PbSUB2 has been detected in the mosquito stages of the lifecycle, during ookinete invasion of the mosquito mid-gut cell, further suggesting a general role in invasion [118, 119].

For a number of reasons, PfSUB2 is the best candidate for MESH, the sheddase responsible for the cleavage of MSP1 and AMA1 from the merozoite

Figure 1.4 PfSUB2

Schematic representation of the putative domain structure of PfSUB2. The protein has a signal peptide, relatively large propeptide, catalytic domain, transmembrane domain and cytoplasmic domain. The predicted processing sites are indicated.

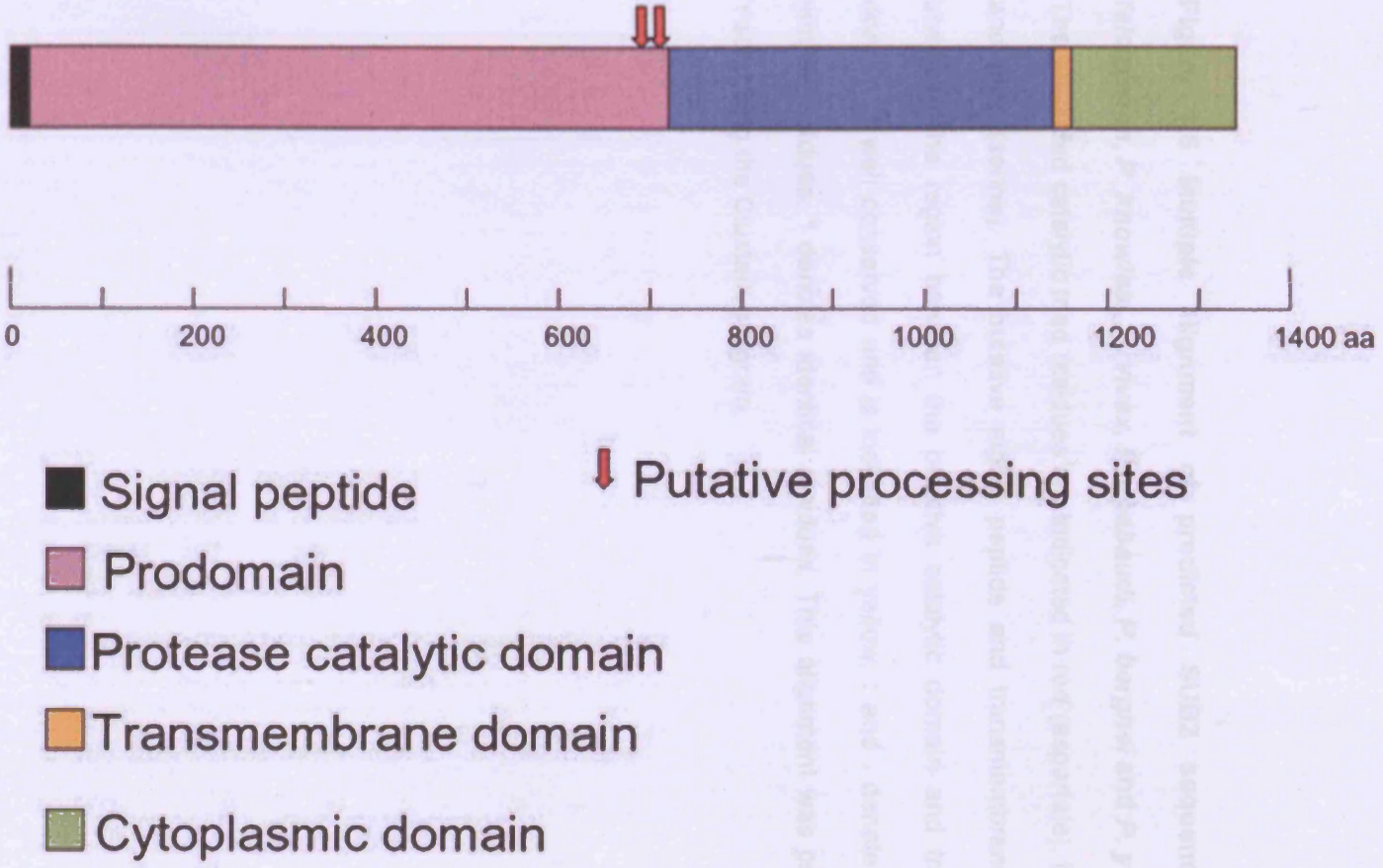
0
200
400
600
800
1000
1200
1400 aa
Signal peptide
Prodomain
Protease catalytic domain
Transmembrane domain
Cytoplasmic domain
Putative processing sites

Figure 1.5 Multiple alignment of predicted SUB2 sequences from *P. falciparum*, *P. knowlesi*, *P. vivax*, *P. chabaudi*, *P. berghei* and *P. yoelii*

The predicted catalytic triad residues are indicated in red (aspartate), blue (histidine) and pink (serine). The putative signal peptide and transmembrane domain are shaded. The region between the putative catalytic domain and transmembrane domain is well conserved and is indicated in yellow. : and . denote conserved or similar residues, * denotes identical residues. This alignment was produced by S. Yeoh using the ClustalX program.


Signal peptide
Falciparum MLNIIYVVSLILIKFIFYKECNNNNNYYLSNIELYNYKLRKR-NRILNNNINDRKSFLSDLEQNYKPLFDIYELSANFEKRRKELEKKTKGEENEIEKKKENDLEEKKENEIEKKKENDL 119
Knowlesi MLSLLYVLWLMLMNIFFQYDWHR--KKILSELGNYNVKLVKRKSRILSDSKTGRINFLDEIKESYRPLFDVYELSAKFEKLRNTKEKEEEKRGRQKQKQKKKKKKKKNDHIEEEEQ--- 115
Vivax MLSSLYVLPLILVNILFQNDWHR--KKILSELGNYNVKLVKR-SRVLSNRTTGRINFLDEIKESYKPLFDVYELSAEFEKLRNAKGKGEEKRGRKK----KKKKKKKNDHIGGGD---- 109
Chabaudi MLRTFYVLSLILIEFILHKGQYN--KHILSTN-LKNYNFVDKDHRILVSDIEDSEKHIEDIKDAYKPIFNIYEISAEFHKKKYIANKKKKQKDGSE-----QSIEKKINSEGDERSQ--- 109
Berghei MLRTFYVLSLMLIEFILHNGQYN--KHICSKN-SKKYNFVGKKHRILVSDIEDRENHIEGIADIYKPIFNIYEISAEFHKKKNIADKKKKRKYGIN-----QSIEKRRIAEENERRQ--- 109
Yoelii MLRTFYVLSLMLIEFILHKGQYN--KHICSKN-LKKYNFVGKKHRILASIIEDREKQVEDITDGYKPIFNIYEISAAFHKKKDIADKKKRRRYGNQ-----QSIENRRIAEENERRL--- 109
Falciparum EKEYNDVINLLELSLSSEYKELN--------ADVS------NNDNSGHEENNKHKLNKKNSSNYKNDK----------SLDELIKG---------- 181
Knowlesi -DKKTPSLNLIQLSSTQSDETEHIKKRISKPFPIALAHRRKPISIKKHAADSIHMLNDGKSDKEGDARMNVNNDADVFTKLVNEGNIEDFGKLGEDEQGETKERNLKSQSFQGDDTEEVN 234
Vivax -DKETPRLNLIKLSATQPDGGEHTQKGKSTEAPIREAHSGKSTGINKRAANFIQMLNDGNSNGRGDAEMGVENEPDTFSKLINEGNIEDFDHLEKDEP-EGEEEKKQEEAGEAEAGAAEG 227
Chabaudi -LNQNEGITSLELSDRHP---------- 126
Berghei -LNKTEGTQFLELSNRYPN----------IGKQNSQQNKVNEINNQNAASNSNDNI----------GNDNI---------- 159
Yoelii -SNQLDDIQFIELSNKYPN----------IGKQNSQQNKVNKINNQNGASNSNDNI----------RNDE---------- 158
Falciparum ----------AILKLKQNPNIKNKNMLDYDKIFKIIKEKLINKNLASNKIK----------GGDNEKLKEEKKQSDISTN------VEVKKDIIN---------- 250
Knowlesi SVVKEGRHSNERKREDKNDDEDDQDVEGKADQETIQKTDQRAEQEANQR-------AVQETNQREEQEANQREEQEANQREEQEADEESNQRAEQEANQREEQEADEES---------- 336
Vivax KEKGEEAERKEEQEEAKQPQEQEQRDHKSMREEESQSASREEERQSNMRESPPGGESPQEGGDNIEGGTEVAARKGGDKSKGQEREGEKNLMASKKEGVKAEKPSEEGSPSGHSLQGEGA 347
Chabaudi ----------DAENDDHDDLIEERDDTLEQEDSAENNDGILP----------RGKIYEQDEENKNIY----------TIPSDENS---------- 181
Berghei --------GNDNIGNDEDDDEDDDEDLIEGRKDNLEEDDLIEKNDSNLP----------RGKMHEKEEKNKNIN----------TTPGNESS---------- 223
Yoelii ----------DEDEGEDEDEDDDLIEGRKDNLEEDDLVEKNGANLK----------RGNMHGQEEKNKNIN----------TTPGNENN---------- 217
Falciparum -----DQLNKGIPTKIENKDDMINKESNKEDITNEGKSNSLNNLNTLNNDGNIITKVYDHYTIVTNSNDILNDISIDASDISKNSIGGINIPFNENDNSSFTHQRYIVLSNNGEKKYKIV 365
Knowlesi --------NQRAEQEADEESNQRAEQEADE-EADQEAEYELKEGENV-AQQDIIVQEFDHYKIVTNSHDILNDIYVDASDISKLSIGSINIAYSEQNKTSFTHQRHIVLNNRGNKKYRVV 446
Vivax EEAPAASPAEDSDEKKEEEEEEEEEEEEED-SNDQGREYQLNDGNSV-AQEDIITQEFDHYTIVTNSNDVLNDIRVDASDISKLSIESINIPYSEANKTSFTHQRHIVLTNKGNKKYRVV 465
Chabaudi --------NEKVYDKKSD-ISLKDKIDYKE-RGYGN----FKSKEKN-LDENIKTYTFDHYKIITNSENILNDIKVDASDISKLSINSLNIEYNEKNKAEYTHQRHIILSNEGNRRYKIF 286
Berghei --------NKNVNDKKKNGISLKDKIDNKQ--NNGG----LKEKGNN-LDDNIKTYTFDHYKIITNSDNILNDIKVDASDISKLSINSINIEYNEKNKAEYTHQRHIVLSNNGNRRYKIF 328
Yoelii --------SKNVNDNKKSGISLKDKIDNNE-QHNSG----LKGTTKY-LDDNIKTYTFDHYKLITNSDNILNDIKVDASDISKLSINSLSIEYNEVNKTEYTHQRHIVLTNKGNRRYKIF 323
Falciparum LMTKNPKFMDMDGIYDEEEKKESLIELNQKVNKEENTN--LYDGTGTLYYGKKSKKEKENTQQKGGNNPNVDINILNNNNNNNNNNNNNSNNNSNSMNDEEINYNNNNNKESPSMFRRFI 483
Knowlesi LMTKNPKFTELEDEESENAATNTFIEKEKVERKKTSDGHGEEDNDRTNLYGGKGTLDFSKAYRSNRK----------GSGRQVGNPNVEMYSAGDT----SGGGIRGTINRLFSFL 548
Vivax LMTKNPKFIELEDEPDEKAENNTFIERESMEQKRTPNGRGEHTSDRTNLYGGKGTLDFSKVYSGNGR----------GSGREVENPHVETHTGGGT----GEGGIRATINRLFSFL 567
Chabaudi LMTKNPKFTKTDDIPQP---EMNFIQTKAVQNEGATEE--EDKYYNENLYSGFGTLDFEKGYSKTKKK------IDNGHASGVNDQNSNHQNIEKNDSHE----NEKHNHGFIGKVRSFF 391
Berghei LMTKNPKFTKTEDIEEP---GMSFIQTETGENEDEKED--EENYLNENLYSGFGTIDYENDYSKKKKK------IESEHASGLNDKISNSQNIEKSGSHE----NEKYNHGYIEKIRSFF 433
Yoelii LMTKNPKFTKTEDIEEP---EMSFIQTETGENTNEKED--EENYLNENLYSGFGTIDYENGYSKKKKK------INSEHASELNDKISNSQNIEKSDSHE----NEKYNHGFIGKIQSFF 428
Falciparum NFLSFSGNENETEDTLIYHNKN---------DNSYKNKKEGTGKNNDNNDPNNNNNKKILLNVDKLVDQYLLNLKNNHTSKQELILVLKGELDLHSKNMKNVINNAKKNLEKYFKEHFKE 594
Knowlesi SFKGNPDESASGTDPSKDSGGR-----SGDNEDQKGNANEGGNRHGSIPQDDRTHDLNEILSVDKLVDQYLLNLKNNTPDKQELILVLRGDLDLHSPYMKLVIKRSNAKFEQHIKRNFEQ 663
Vivax TFGGNPGESARGAGESKDGGGKKESANGGGDRHHHHYRHDLQSRDNRRSRHDRTKDLNEILSADKLVDQYLLNLKNNTPERQELIFVLRGDLDLHSTYMRRVIKRSNAKFEEHIKKNFQQ 687
Chabaudi SFLSVS---NSQKDDNIESGKK---------NEESNNADSKTRLNEKTDDTTRKDSLNEFLSVDKLTDQYLLNLKNKNVKEQELILIFQGDLDLHSKEMRKVIDEANAKLTNYLNMHFKD 499
Berghei SFLSMP---SSKKDDSIGSEKK---------TEERSNTDSKAKLNKKTNDMAKKNNSNAFLSVDKIIDQYLLNLKNKNMKEQELIFIFHGNLDLHSKEMKTVINEANAKFTKYINMHFKD 541
Yoelii SFLSIP---SSKKDDSIGSEKK---------SEERNNVDSKPKLNKKPNDTAKKNNSNKILTVDKVTDQYLLNLKNKNMKEQELIFIFHGDLDLHSKKMKTIINEANVKFTKYINMHFKD 536


Falciparum FDKISYDISTPINFLCIFIPTLFDMNNMDLLKQALLILHNDLHEYVENWSFSSTYHTYEADYIKE---------Q-DS----------VYDRSPK----------KKY 672
Knowlesi IDKIVYDISSPINFLCFFVPTIFDMNNFHLLKEALMVLHKELERYMENWSFSNTYVTLDAPQIQGDGSGASADWRNDSQKKDAPIEGGAGSQADHHG-------KDHAEG-SQYRKGRKF 775
Vivax VDSIVYDVSSPINFLCFFVPTVFDMSNFHMLKEALLVLQKELERYMENWSFSNTYVTLDAPHVGGEG-GASAGAGHDG-RKDAHMGSRAGDQADGHADDRETGHTDHREGGAPHGKPRKF 805
Chabaudi IKNMNYDISSPINFVCFFIPTVFDISNLNILKEALIMSHNELKDYIDNWNFSNTYIAFDRNYEDEDI----KKEDIDN----------VMNKLNEHG----------EKY 585
Berghei VKNIRYDISSPINFVCFFIPIIFDMSNLKILKEALIILNNELKDYIDNWNFSNTYVAFDNNYENE---------DIDN----------VMNKLNENM----------EKY 622
Yoelii VKNIRYDISSPINFVCFFIPIIFDMSNLKILKEALIILHNELKNYIDNWNFSNTYIAFDTDYENE---------DIDN----------AMNKLNENM----------KKY 617
Cat. Domain->
Falciparum IKASKKLYNNKYSFLNKFLNIEPLILFAKKLNSKRSNIEKEILNFLPKELRDYSTWNLSIIRVFNAWFLAGYGNKNVKVCVVDSGADIKHVDLNGNLYIPEYNEKYEMTQDFYNFMVKNP 792
Knowlesi IKKKKKLYNGKYSFLRKIWSFDTISAFAAKMKKKNTDIENEILNFLPKELREYSTWNLSVIRVFNAWFLAGYGNKNVKVCIIDSGIDKNHVDLMKNVYIPEYSEQYEMTEDFYDFMVKNP 895
Vivax VKKKKNLYNVKYSFLRKFWSFDSIIAFARKMNKKNMDIEKEILNFLPKELREYSTWNLSVIRVFNAWFLAGYGNKNVKVCIIDSGVDKNHIDLMKNVYIPEYSEQYEMTQDFYDFMVKNP 925
Chabaudi IKKPKKLYNIKYSFLRKIWGLESIISLYKGKNKKEADIEERILNALPKELKEYSTWNLSFIRVFNAWLLSGYGNKNVKICVIDSGIDKNHIDLASNVYIPKYSDKYEMTDEFFDFMVQNP 705
Berghei IKKPKKLYNIKYSFLRKIWGLKSIISLSKNQDKKDAEIEEKILSALPKELKEYSTWNLSFIRVFNAWLLSGYGNKNVKICVIDSGIDKNHIDLANNIYTPKYSDRYEMTDELFDFMVKNP 742
Yoelii IKKPKKLYNIKYSFLRKMWGLESIFSLSKNRNQKNAGIEEKILNALPKELKEYSTWNLSFIRVFNAWLLSGYGNKNVKICVIDSGVDKNHIDLAKNIYTPKYSDRYEMTDDFFDFMVKNP 737
Falciparum TDASGHGTHVTGIIGGVANDLGVVGVAPNITLISLRFIDGKKYGGSFHAIKALNVCILNKAPIINASWGSSHFDVNLHLAVERLKYTLNGKGSVLIAASGNKSNDNDISPLYPATFTFPH 912
Knowlesi TDSSGHGTHVTGIVGGVANGLGMVGVAPDVTLISLRFIDGVKYGGSFHAIKAINVCILNKTPIINASWGSNKYDANIYLAVQRLKYTFNGKGTVLVTAAGNENKNNDEHPLYPSNFKLPH 1015
Vivax TDSSGHGTHVTGIVGGLANDLGMVGVAPNVTLISLRFIDGVKYGGSFHAIKAINVCILNKAPIINASWGSSKYDANIYLAVQRLKYTFNGKGTVLVTAAGNENKNNDEHP--------L- 1036
Chabaudi SDTSGHGTHVSGIAGASANSLGMVGVAPNIKLISLRFIDGDNYGGSFHVIKAINVCILNKSPIINASWGSRNYDTNMYLAIQRLKYTFKGKGTVVVAAAGNENKNNDLYPIYPASYKLQN 825
Berghei IDTSGHGTHVSGIAAASANSLGMVGVAPNINLISLRFIDGDNYGGSFHVIKAINICILNKSPIINASWGSRNYDTNMFLAIERLKYTFKGKGTVFIAAAGNENKNNDLYPIYPASYKLQN 862
Yoelii IDTSGHGTHVSGIAAASANSLGMVGVAPDVNLISLRFIDGDSYGGSFHVIKAINVCILNKSPIINASWGSRNYDTNMFLAIERLKYTFKGKGTVFIAAAGNENKNNDLYPIYPASYKLPN 857
Falciparum VYSVASISRNFEISPFSNYGHKSVHILAPGHHIYSTIPNNSYKIFTGTSMAAPHVCGVSALVYSVCYNQGFIPQAEEVLDILTRTSIKIISTKKRTINDSLVNAEGAVLTTLLGGLWMQM 1032
Knowlesi VYSVASISKNFEISPFSNYGVKSVHIMAPGHHIYSTTPNNSYKINTGTSMAAPHVCGVNALIYSVCYNQGFIPSAEEVLDILTRTAIKIISRRRRTINDSLVNAEAAVLTTLLGGLWMQM 1135
Vivax ---VASISKNFEISPFSNYGVNSVHIMAPGHHIYSTTPNNSYKINTGTSMAAPHVCGVNALIYSVCYNQGFIPPAEEVLDILTRTSIKVISRRRRTINDSLVNAEAAVLTTLLGGLWMQM 1153
Chabaudi VYSVGAINKFLQISPFSNYGAKSVHILAPGHHIYSTTPMNTYKTNTGTSMAAPHVSGVAALIYSVCHNQGFIPEAEEVLEIITRTSIKIVTREKKTMHNSLVNAEAAVLTTLLGGLWMQM 945
Berghei VYSVGSINKFLQISPFSNYGANSVHILAPGHHIYSTTPMNTYKMNTGTSMAAPHVSGVAGLIYSVCYKQGFIPDADEVLEIITRTSIKIVSKDKKTIHNSLINAEAAVLTTLLGGLWIQM 982
Yoelii VYSVGSINKFLQISPFSNYGANSVHILAPGHHIYSTTPMNTYKMNTGTSMAAPHVSGVAGLIYSVCHKQGFIPESDEVLDIITRTSIKIVSKDKKTIHNSLINAEAAVLTTLLGGLWMQM 977
TM domain
Falciparum DCYFVKFNLEKGKKKHIPVVFSAYKKGVYETDIVIAIIPIDGKSKIYGEIHIPIKIVTDVNIPNFQESPRRGKNYTIDSNEAQHDEVLSYICENALYNLYEYDSHYLLASVILFFLALLS 1152
Knowlesi DCHFVKFNLESGKKKHIPVVFSAYKKGIYETDIVIAVISTEENSNVYGEILIPIRIVTDPKVDNFKESPRTGKKMIIDENEASHDEVLSYICENALYNLYEMDSNFLVTSLVLFFVAFIL 1255
Vivax DCHFVKFNLEGGKEKHIPVVFSAYKKGIYETDIVIAVIPTEENSKVYGEILIPIRIVTDPKAENFKESPRNGKKMIIDENEASHDEVLSYICENALYNLYEMDSNFLVMSLVLFFVAFIL 1273
Chabaudi DCHFAKFYLNKDKQKSIPVVFSAYKDGMYETDIIIGIKPVDTNSKEYGEIVIPIKILTNPNLKDFSASPRIGKKIHIDANESIDDDILSYICENALYNLYEHDNTFLISSLILFFLGIIL 1065
Berghei DCHFAKFYLNENKQKSVPIVFSAYKDGVYESDIIIGIQPEDANSKEYGEIVIPIKILTNPKLKDFSLSPRVGKKIRIDENES-NDDILSYICENALYNLYEHDNSFLISSLILFFIGIIL 1101
Yoelii DCHFAKFYLNKDQQKNIPVVFSAYKDGMYESDIIIGIQPEDSNSKEYGEIVIPIKILTNPKLKNFNLSPRVGKKIHIDANES-NDDILSYICENALYNLYEHDNSFLISSLILFFIGIIL 1096

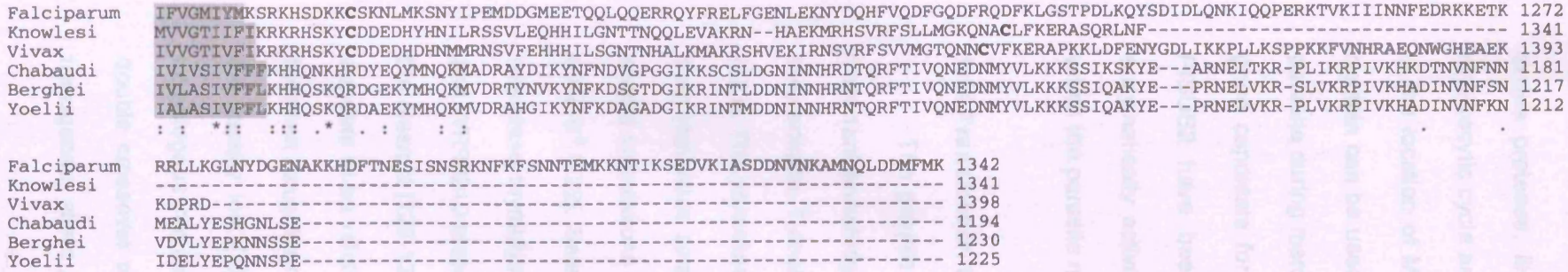
Falciparum IFVGMIYMKSRKHSDKKCSKNLMKSNYIPEMDDGMEETQQLQQERRQYFRELFGENLEKNYDQHFVQDFGQDFRQDFKLGSTPDLKQYSDIDLQNKIQQPERKTVKIIINNFEDRKKETK 1272
Knowlesi MVVGTIIFIKRKRHSKYCDDEDHYHNILRSSVLEQHHILGNTTNQQLEVAKRN--HAEKMRHSVRFSLLMGKQNACLFKERASQRLNF---------- 1341
Vivax IVVGTIVFIKRKRHSKYCDDEDHDHNMMRNSVFEHHHILSGNTNHALKMAKRSHVEKIRNSVRFSVVMGTQNNCVFKERAPKKLDFENYGDLIKKPLLKSPPKKFVNHRAEQNWGHEAEK 1393
Chabaudi IVIVSIVFFFKHHQNKHRDYEQYMNQKMADRAYDIKYNFNDVGPGGIKKSCSLDGNINNHRDTQRFTIVQNEDNMYVLKKKSSIKSKYE---ARNELTKR-PLIKRPIVKHKDTNVNFNN 1181
Berghei IVLASIVFFLKHHQSKQRDGEKYMHQKMVDRTYNVKYNFKDSGTDGIKRINTLDDNINNHRNTQRFTIVQNEDNMYVLKKKSSIQAKYE---PRNELVKR-SLVKRPIVKHADINVNFSN 1217
Yoelii IALASIVFFLKHHQSKQRDAEKYMHQKMVDRAHGIKYNFKDAGADGIKRINTMDDNINNHRNTQRFTIVQNEDNMYVLKKKSSIQAKYE---PRNELVKR-PLVKRPIVKHADINVNFKN 1212
: : *:: ::: .* . : : :
Falciparum RRLLKGLNYDGENAKKHDFTNESISNSRKNFKFSNNTEMKKNTIKSEDVKIASDDNVNKAMNQLDDMFMK 1342
Knowlesi ---------- 1341
Vivax KDPRD---------- 1398
Chabaudi MEALYESHGNLSE---------- 1194
Berghei VDVLYEPKNNSSE---------- 1230
Yoelii IDELYEPQNNSPE---------- 1225

surface. The protein is predicted to be a membrane-bound, calcium dependent serine protease, like MESH. PfSUB2 is expressed at the correct point in the erythrocytic cycle and may be located on the parasite surface during invasion which is the location of MSP1 and AMA1 shedding. Most convincingly the PfSUB2 pro-domain can be used to specifically inhibit both AMA1 and MSP1 shedding from the parasite during merozoite shedding assays [120]. If PfSUB2 is MESH it represents a good candidate for drug design and development. However, to date studies on PfSUB2 have been hampered by the inability to express the protein in an enzymatically active recombinant form. Also the low levels of the protein present within the parasite make detection of the protein difficult.

1.11 Transfection technology

The genetic manipulation of organisms has long enabled scientists to gain important knowledge of the expression of genes and the function of the proteins they encode. Transfection of *P. falciparum* has only been possible relatively recently [121]. The parasites are electroporated with a circular bacterial derived plasmid that then replicates episomally within the parasite. Transfection efficiency remains low; recent calculations by O'Donnell *et al.* put the Figure for transfection efficiency at $0.8x10^{-6}$ [122]. Selectable markers such as the *T. gondii* and human dihydrofolate reductase thymidylate synthase (*dhfr-ts*) genes confer resistance to pyrimethamine and WR99210 respectively and allow for the selection of parasites stably harbouring the plasmid [123-125]. Replication of episomally carried plasmids within the parasite appears to be relatively efficient but there is inefficient segregation of the plasmids between daughter merozoites, and in the absence of drug pressure these plasmids are rapidly lost [122, 126]. Where plasmids carry suitable targeting sequences, homologous recombination into the genome can take place by both single and double crossover events [123, 124, 127]. Targeted gene disruption, expression of transgenes, allelic exchange and promoter studies have all been described [123,

124, 127-131]. Attempts to use similar technology to over-express *P. falciparum* proteins within the parasite have been less successful. Healer *et al.* [132], for example, attempted to over-express AMA1 using the *ama1* gene encoded on an episomal plasmid. The total levels of AMA1 in transfected parasites were found to be equivalent to the levels found in untransfected parasites. Inducible control of individual gene expression is available in *T. gondii* and the system has recently been adapted for use in *P. falciparum* however, it has yet to used to conditionally knock out an endogenous *P. falciparum* gene [133, 134].

As recombinant, enzymatically active PfSUB2 has yet to be obtained, studies within the parasite using some of the techniques mentioned above will help to understand the role of PfSUB2 within the erythrocytic cycle.

1.12 Project Aims

The objective of this project was to elucidate the function of PfSUB2 in the asexual blood-stage life cycle of the parasite. Two related strategies were used, both involving genetic manipulation of the parasite. In the first of these the aim was to study the enzymatic activity of purified PfSUB2 obtained from the parasite. Purification was to be facilitated by the over-expression of modified PfSUB2 in the parasite. In the second approach the aim was to define the sub-cellular location and fate of the protease by 'tagging' the endogenous gene product with suitable epitope or fluorescent tags.

2. Materials and Methods

2.1 Molecular Biology: DNA preparation and manipulation

2.1.1 *E. coli* strains used

Plasmodium falciparum DNA is often unstable in *E. coli*, due in part to the high A+T content of coding sequences and intergenic regions. The *E. coli* PMC103 (Genotype: *mcrA Δ (mcrBC-hsdRMS-mrr)* 102 recD sbcC) and XL-10 Gold® Ultracompetent cells (Stratagene) are recommended for cloning *Plasmodium* DNA [135]. Vectors 2.2.1 to 2.2.4 were cloned initially into PMC103 cells; however the transformation efficiency and DNA yields from these cells were unsatisfactory, and further plasmids were cloned using XL-10 Gold® cells. As the stability problems found with *Plasmodium* DNA seem only to manifest themselves in cloning steps, vectors 2.2.1 to 2.2.4 were subsequently transformed into *E. coli* DH5α™ cells (Invitrogen) to increase DNA yields [135].

All pMOS*Blue* constructs were maintained in the MOS*blue* *E. coli* strain (Amersham Biosciences). Plasmids requiring digestion with *Cla* I, a restriction endonuclease unable to digest methylated DNA, were transformed into SCS110 *E. coli* cells (Stratagene) which are deficient in *dam* and *dcm* methylases. For protein expression *E. coli* strain BL21(DE3) (Stratagene) was used.

2.1.2 Preparation of PMC103 competent cells

A glycerol stock of PMC103 cells was streaked onto a Luria-agar (L-agar) plate and left to grow overnight at 37°C. A colony from this plate was picked and placed in a 5 mL Luria-broth (L-broth) culture and left to grow shaking overnight at 37°C. 40 mL SOB medium (with 10 mM $MgCl_2$ added just before use) was inoculated with 400 µL of the overnight culture and left shaking overnight at 18°C. The culture was then chilled on ice for 10 minutes before being transferred to a polypropylene centrifuge tube (Corning) and centrifuged at 3,000 g for 10 minutes at 4°C. The supernatant was discarded and the pellet re-suspended in 12.8 mL of ice-

cold TB buffer (10 mM PIPES, 15 mM $CaCl_2$, 250 mM KCl, pH 6.7, 55 mM $MnCl_2$). This suspension was held on ice for 10 minutes and then pelleted as before. The supernatant was discarded and the pellet re-suspended in 3.2 mL of ice-cold TB buffer. 240 µL of dimethyl sulphoxide (DMSO) was then added drop wise. The suspension was then held on ice for 10 minutes before dispensing into 100 µL aliquots and freezing in an ethanol bath. Aliquots were stored at -70°C.

2.1.3 Transformation of *E. coli*

Transformation of DH5α™, XL-10 Gold®, MOS*blue*, SCS110 and BL21(DE3) cells was according to manufacturers' instructions. PMC103 cells were transformed according to the following method. DNA was added to 100 µL of competent cells. The cells were then held on ice for 1 hour and then heat shocked in a water bath at 42°C for 45 seconds. The cells were then held on ice for 2 minutes before placing in an Eppendorf tube containing 50 µL L-broth and left shaking at 37°C for one hour. The cells were then plated on a selective LB agar plate.

2.1.4 DNA production

DNA for cloning steps and sequencing was prepared using the S.N.A.P kit (Invitrogen) according to manufacturers' instructions. DNA for transfections was prepared using the Qiagen® Plasmid Maxi kit according to manufacturers' instructions. *E. coli* were grown in Terrific broth to obtain maximal yields of bacteria. Plasmids pHHT-sub2, pHHT-sub2HA, pHHT-sub2w and pHHT-sub2wHA (see 2.2.1-2.2.4) were expressed poorly and were difficult to produce in the amounts needed for transfection. For these plasmids the Very Low-Copy Plasmid protocol was used, as described in the manufacturers' guide. DNA yields and purity were assessed by absorbance using a spectrophotometer (Unicam UV1). Samples were finally ethanol precipitated and re-dissolved in water to a final concentration of 3.3 µg/µL.

2.1.5 Genomic DNA preparation and plasmid recovery from *P. falciparum*

Plasmodium falciparum genomic DNA was extracted using the DNeasy® Tissue Kit (Qiagen). This kit was also used for the recovery of plasmid DNA from transfected parasite lines.

2.1.6 Polymerase Chain Reaction (PCR)

PCR for amplification of sequences used in the construction of plasmids was performed using *Pfu* Turbo® DNA polymerase (Stratagene) or Platinum® *Taq* High fidelity DNA polymerase (Invitrogen). Both enzymes were used according to the respective manufacturers' instructions. AmpliTaq® DNA polymerase (Roche) was used for PCR reactions where proofreading action was not required. The PCR reaction was performed according to the manufacturers' instructions. Oligonucleotide primers for use in PCR and sequencing were purchased from Oswel. PCR purification was performed using the QIAquick® PCR Purification Kit (Qiagen).

2.1.7 Site directed mutagenesis (SDM)

Site directed mutagenesis was performed using the QuikChange® XL Site-Directed Mutagenesis Kit (Stratagene) according to manufacturers instructions.

2.1.8 Automated sequencing

BigDye® Terminator v1.1 Cycle Sequencing Kit (Applied Biosystems) was used with reaction mix set up according to instructions. The reactions were placed in a PCR machine (ThermoHybaid Omn-E) and the following program applied: 96°C for 45 s, 50°C for 30 s and 60°C for 2 min, for a total of 25 cycles. Samples were then ethanol precipitated in 0.5 mL Eppendorf tubes by the addition of 50 µL 95% ethanol and 2 µL 3 M sodium acetate (pH 3.0) followed by incubation at room temperature for an hour before centrifugation at 13,200 rpm for 20 min. The ethanol

was then aspirated and the DNA pellet washed once in 0.5 mL 70% ethanol. The ethanol was removed and the pellet dried for 1 min in a heating block set at 95°C. The pellet was then re-suspended in 10 µL MegaBACE™ Loading Solution (Amersham Biosciences) and loaded on a MegaBACE™ sequencing machine (Amersham Biosciences).

2.1.9 DNA-Modifying Enzymes

Restriction endonucleases were purchased from Roche with the exception of *Bgl* II which was purchased from NEB. All restriction digests were carried out according to manufacturers' instructions. Clean up after restriction digests was performed using the QIAquick® PCR Purification Kit (Qiagen). Alkaline phosphatase and T4 polynucleotide kinase were purchased from Roche and used according to manufacturers' instructions.

2.1.10 DNA Ligation

Ligations were performed using the Rapid DNA Ligation Kit (Roche).

2.1.11 Gel extraction

Gel extractions were carried out using the QIAquick® Gel Extraction Kit (Qiagen) according to manufacturers' instructions.

2.2 Vector construction

2.2.1 Construction of pHHT-sub2

A 3.5 kb fragment encoding the predicted ectodomain of a synthetic *pfsub2* (*pfsub2*$_{synth}$) gene was constructed using the method of Withers-Martinez *et al.*, with codon usage optimised for *Trichoplusia ni* [136]. The synthetic gene was designed to facilitate cloning and expression of the *pfsub2* gene as the A+T content is lower than the authentic gene. Note that the parasite is known to be capable of

transcribing such genes as all reporter genes used in *P. falciparum* transfections derived from organisms with a lower A+T content. The *pfsub2*$_{synth}$ fragment was cloned into pMOS*Blue*, forming the plasmid FIM which was then linearised with *EcoR* I. A 20 bp linker, designed to contain terminal overhangs complimentary to those left following digestion by *EcoR* I, as well as an internal *BstE* II site (in bold), was produced by annealing together oligonucleotides sb2LNK1 (5'-AATT**GGTTACC**CGGGATCCG-3') and sb2LNK2 (5'-AATTCGGATCCCG**GGTAACC**-3'). The linker was ligated into the *EcoR* I site of FIM forming FIM-LNK. The PfSUB2 ectodomain coding sequence was then excised using *Pst* I and *BstE* II and gel purified. Plasmid pHHT was constructed by excision of the *tk* gene from pHHT-TK using *Xho* I [127]. Oligonucleotides pH-LNK1 (5'-TCGA*CTGCAG*ACCCG**GGTTACC**A-3') and pH-LNK2 (5'-TCGAT**GGTAACC**CGGGT*CTGCAG*-3') were annealed together to form a linker containing terminal overhangs complimentary to those left following digestion with *Xho* I, as well as an internal *Pst* I site (in italics) and an internal *BstE* II site (in bold). The linker was ligated into pHHT, forming plasmid pHHT-LNK. pHHT-LNK was digested with *Pst* I and *BstE* II and gel purified. The gel purified *pfsub2* ectodomain was ligated into pHHT-LNK forming pHHT-sub2. This entire procedure is shown schematically in Figure. 2.1

2.2.2 Construction of pHHT-sub2HA

To insert sequence encoding a single haemagglutinin (HA) epitope tag (YPYDVPDYA) within the coding sequence of the *pfsub2*$_{synth}$ gene, overlap extension PCR was performed using FIM-LNK as template and using primers C (5'-**TACCCCTACGACGTACCCGACTACGCC**CATCATCATCACC-3') and B (5'-**GGCGTAGTCGGGTACGTCGTAGGGGTA**GCTGTCGTATTCG -3') [137, 138]. Sequence encoding the HA tag is marked in bold. Primers A (5'-

Figure 2.1 Construction of pHHT-sub2

Schematic representation of the construction of pHHT-sub2. The construct places the region of the *pfsub2*$_{synth}$ gene encoding the putative PfSUB2 ectodomain under the control of the *hsp86* promoter.

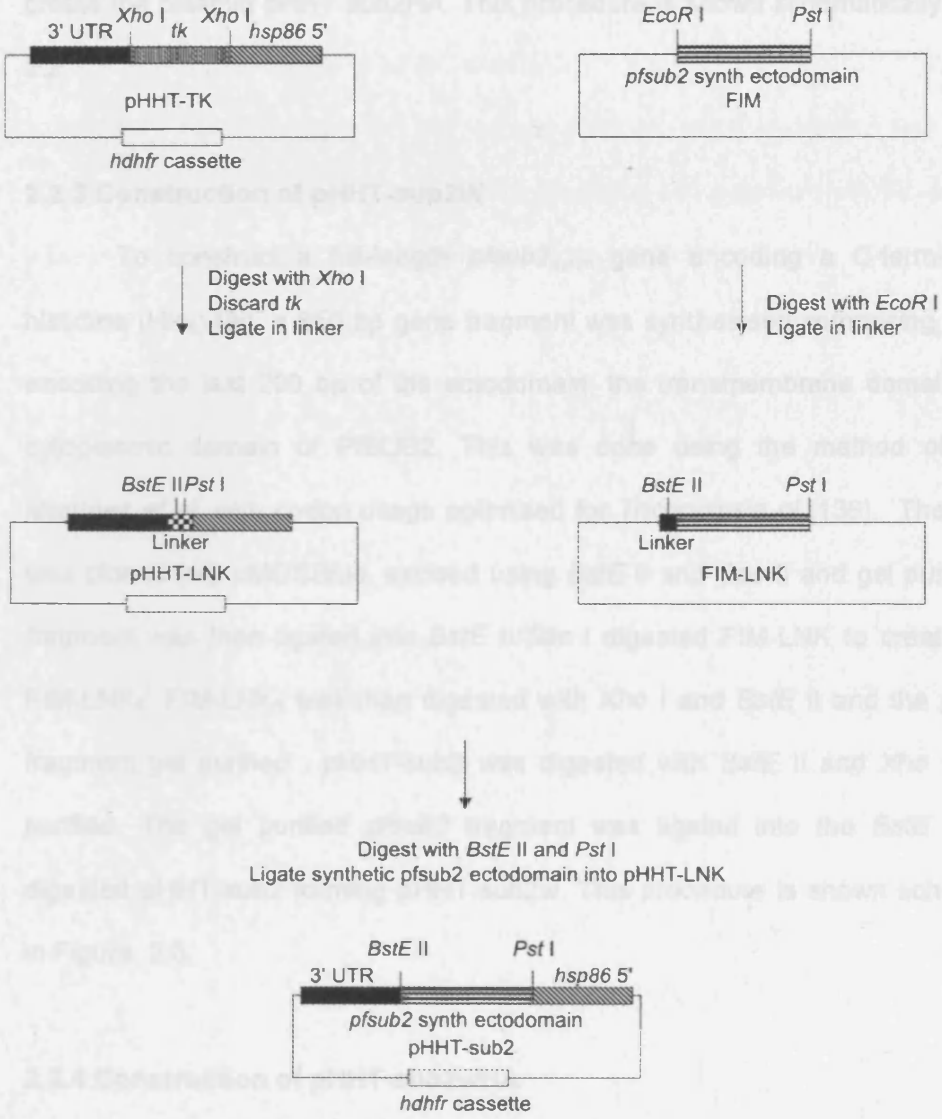
3' UTR
Xho I
tk
Xho I
hsp86 5'
pHHT-TK
hdhfr cassette
EcoR I
Pst I
pfsub2 synth ectodomain
FIM
Digest with Xho I
Discard tk
Ligate in linker
Digest with EcoR I
Ligate in linker
BstE II
Pst I
Linker
pHHT-LNK
BstE II
Pst I
Linker
FIM-LNK
Digest with BstE II and Pst I
Ligate synthetic pfsub2 ectodomain into pHHT-LNK
BstE II
Pst I
3' UTR
hsp86 5'
pfsub2 synth ectodomain
pHHT-sub2
hdhfr cassette

AAAGGTTGAAATACACCTTGAACGGAAAAGGCTCAGTGTT -3') and D (5'-GGGCGATCGGTGCGGGCCTCTTCGCTATTACGC-3') were then used to amplify the region flanking the tag. The amplified fragment was digested with *Xho* I and *BstE* II, gel purified, and ligated into *Xho* I/*BstE* II-digested FIM-LNK to create plasmid FIM-LNKHA. This plasmid was then digested with *Xho* I and *BstE* II and the fragment containing the HA tag ligated into *Xho* I/*BstE* II digested pHHT-sub2 to create the plasmid pHHT-sub2HA. This procedure is shown schematically in Figure. 2.2.

2.2.3 Construction of pHHT-sub2W

To construct a full-length $pfsub2_{synth}$ gene encoding a C-terminal hexa-histidine (His_6) tag, a 850 bp gene fragment was synthesised comprising sequence encoding the last 200 bp of the ectodomain, the transmembrane domain and the cytoplasmic domain of PfSUB2. This was done using the method of Withers-Martinez *et al.* with codon usage optimised for *Trichoplusia ni* [136]. The fragment was cloned into pMOS*Blue*, excised using *BstE* II and *Sac* II and gel purified. This fragment was then ligated into *BstE* II/*Sac* I digested FIM-LNK to create plasmid $FIM\text{-}LNK_{fl}$. $FIM\text{-}LNK_{fl}$ was then digested with *Xho* I and *BstE* II and the $pfsub2_{synth}$ fragment gel purified. pHHT-sub2 was digested with *BstE* II and *Xho* II and gel purified. The gel purified *pfsub2* fragment was ligated into the *BstE* II /*Sac* II digested pHHT-sub2 forming pHHT-sub2w. This procedure is shown schematically in Figure. 2.3.

2.2.4 Construction of pHHT-sub2wHA

To construct a full length $pfsub2_{synth}$ gene encoding a single HA epitope tag (YPYDVPDYA), followed by a C-terminal hexa-histidine (His_6) tag, a 900 bp gene fragment was synthesised comprising sequence encoding the last 200 bp of the ectodomain, the transmembrane domain and the cytoplasmic domain of PfSUB2

Figure 2.2 Construction of pHHT-sub2HA

Schematic representation of the construction of pHHT-sub2HA. The construct places the region of the *pfsub2*$_{synth}$ gene encoding the putative PfSUB2 ectodomain with a C-terminal HA tag under the control of the *hsp86* promoter.

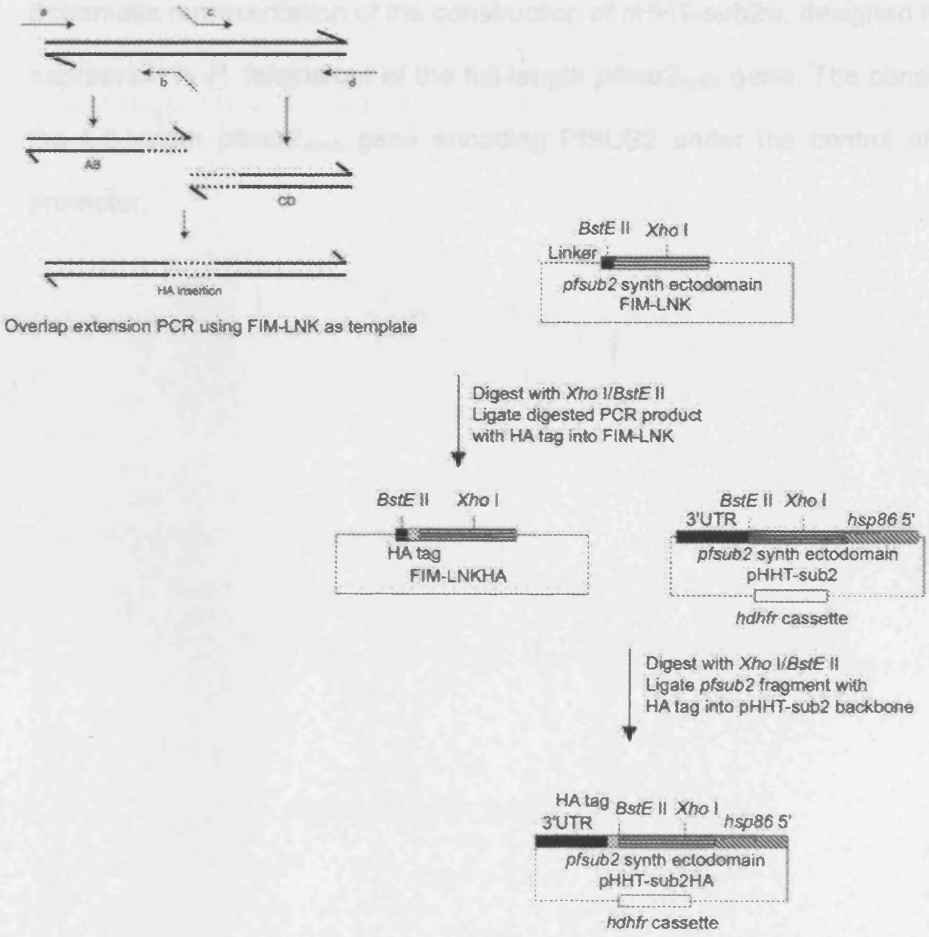
a
c
b
d
AB
CD
HA insertion
Overlap extension PCR using FIM-LNK as template
BstE II
Xho I
Linker
pfsub2 synth ectodomain
FIM-LNK
Digest with Xho I/BstE II
Ligate digested PCR product
with HA tag into FIM-LNK
BstE II
Xho I
HA tag
FIM-LNKHA
BstE II
Xho I
3'UTR
hsp86 5'
pfsub2 synth ectodomain
pHHT-sub2
hdhfr cassette
Digest with Xho I/BstE II
Ligate pfsub2 fragment with
HA tag into pHHT-sub2 backbone
HA tag
3'UTR
BstE II
Xho I
hsp86 5'
pfsub2 synth ectodomain
pHHT-sub2HA
hdhfr cassette

Figure 2.3 Construction of pHHT-sub2w

Schematic representation of the construction of pHHT-sub2w, designed for episomal expression in *P. falciparum* of the full-length *pfsub2*$_{synth}$ gene. The construct places the full-length *pfsub2*$_{synth}$ gene encoding PfSUB2 under the control of the *hsp86* promoter.

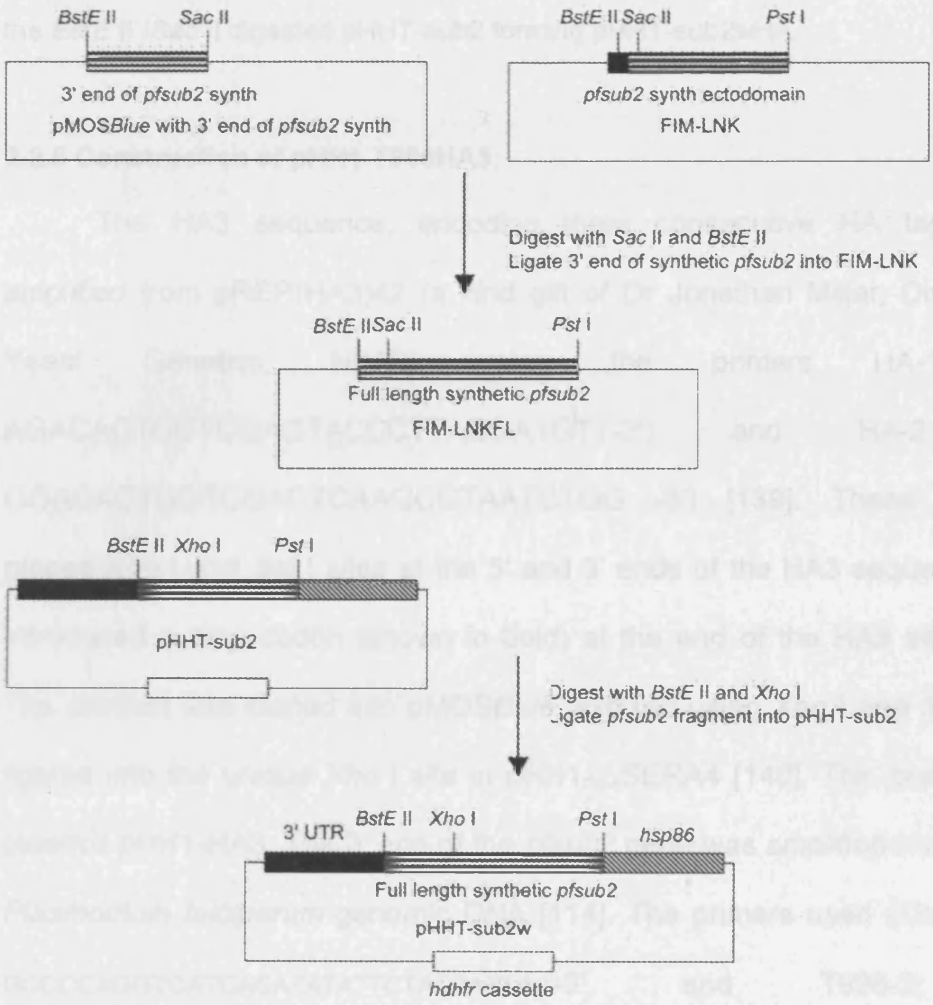
BstE II
Sac II
3' end of pfsub2 synth
pMOSBlue with 3' end of pfsub2 synth
BstE II Sac II
Pst I
pfsub2 synth ectodomain
FIM-LNK
Digest with Sac II and BstE II
Ligate 3' end of synthetic pfsub2 into FIM-LNK
BstE II Sac II
Pst I
Full length synthetic pfsub2
FIM-LNKFL
BstE II
Xho I
Pst I
pHHT-sub2
Digest with BstE II and Xho I
Ligate pfsub2 fragment into pHHT-sub2
3' UTR
BstE II
Xho I
Pst I
hsp86
Full length synthetic pfsub2
pHHT-sub2w
hdhfr cassette

with a HA and His_6 tag. This was also done using the method of Withers-Martinez *et al.*, with codon usage optimised for *Trichoplusia ni* [136]. The fragment was cloned into pMOS*Blue* then excised using *BstE* II and *Sac* II and gel purified. FIM-LNK was digested with *BstE* II and *Sac* II and the 900 bp fragment ligated in to create the plasmid FIM-LNK_{flHA}. pHHT-sub2 was digested with *BstE* II and *Xho* I and gel purified. FIM-LNK_{flHA} was then digested with *Xho* I and *BstE* II and the synthetic *pfsub-2* N-terminal fragment gel purified. The gel purified fragment was ligated into the *BstE* II /*Sac* II digested pHHT-sub2 forming pHHT-sub2wHA.

2.2.5 Construction of pHH1-T996HA3

The HA3 sequence, encoding three consecutive HA tags, was amplified from pREP(HA3)42 (a kind gift of Dr Jonathan Millar, Division of Yeast Genetics, NIMR) using the primers HA-1 (5′-AGACACTGCTCGAGTACCCTTACGATGTT-3′) and HA-2 (5′-GGACACTGGTCGAC**TCA**AGCGTAATCTGG -3′) [139]. These primers placed *Xho* I and *Sal* I sites at the 5′ and 3′ ends of the HA3 sequence and introduced a stop codon (shown in bold) at the end of the HA3 sequence. The product was cloned into pMOS*Blue*, excised using *Xho* I and *Sal* I and ligated into the unique *Xho* I site in pHH1-△SERA4 [140]. This creates the plasmid pHH1-HA3. The 3′ end of the *pfsub2* gene was amplified from T9/96 *Plasmodium falciparum* genomic DNA [114]. The primers used (T996-1; 5′-GCCCCAGGTCATCACATATATTCTACTATTCC-3′, and T996-2; 5′-GGACACTG**CTCGAG**TTTCATAAACATATCATC -3′) remove the stop codon from the end of the *pfsub2* coding sequence and form a continuous reading frame into the HA3 region at the end of which a new stop codon has been created. The amplified fragment includes a *Bgl* II site and the reverse primer

places a *Xho* I site (in bold) at the 3' end. The fragment was cloned into pMOS*Blue* and then excised using *Bgl* II and *Xho* I. The *sera4* gene fragment was excised from pHH1-HA3 using *Xho* I and *Bgl* II. The T9/96 DNA fragment was ligated into this position. This procedure is shown schematically in Figure. 2.4.

2.2.6 Construction of pHH1-T996w

Primers T9961 (5'-GCCCCAGGTCATCACATATATTCTACTATTC-3') and $T996_w$ (5'- **CTCGAG**TCATTTCATAAACATATCATCAAGTTGATTCATTGC-3') were used to amplify a 1.2 kb fragment of the 3' end of the *pfsub2* gene, including the stop codon, from T9/96 *Plasmodium falciparum* genomic DNA [114]. Primer $T996_w$ places an *Xho* I site (in bold) after the stop codon. There is an internal *Bgl* II site within the fragment. The fragment was cloned into pMOS*Blue* and excised using *Bgl* II and *Xho* I. The *sera4* gene fragment was excised from pHH1-△SERA4 [140] using *Bgl* II and *Xho* I and the *pfsub-2* fragment ligated in. This creates the plasmid pHH1-$T996_w$.

2.2.7 Construction of pHC1-CATprom plasmids

To characterise the *pfsub2* promoter a series of fragments of the region immediately 5' to the *pfsub2* gene were amplified from T9/96 *Plasmodium falciparum* genomic DNA. The reverse primer R1 (5'-**CTCGAG**TATACGGAAAGAGAAAAAAAAAATAAC-3') inserts an *Xho* I site (in bold) at a position which lies directly before the start of the *pfsub2* coding sequence. The forward primers used were F1 (5'-**GCTCAGC**CTACAATTTTAAATATATTCATATTATGG-3'), F2 (5'-**GCTCAGC**GGACCATATATAATGTTTTATGG-3'), F3 (5'-**GCTCAGC**ATATATATGTATATATATATATATGGG-3'), F4 (5'- **GCTCAGC**ATAATA

Figure 2.4 Construction of pHH1-T996HA3

Schematic representation of the construction of pHH1-T996HA3, designed to insert an HA3 epitope tag at the 3′ end of the endogenous *pfsub2* gene by single-crossover, targeted homologous recombination.

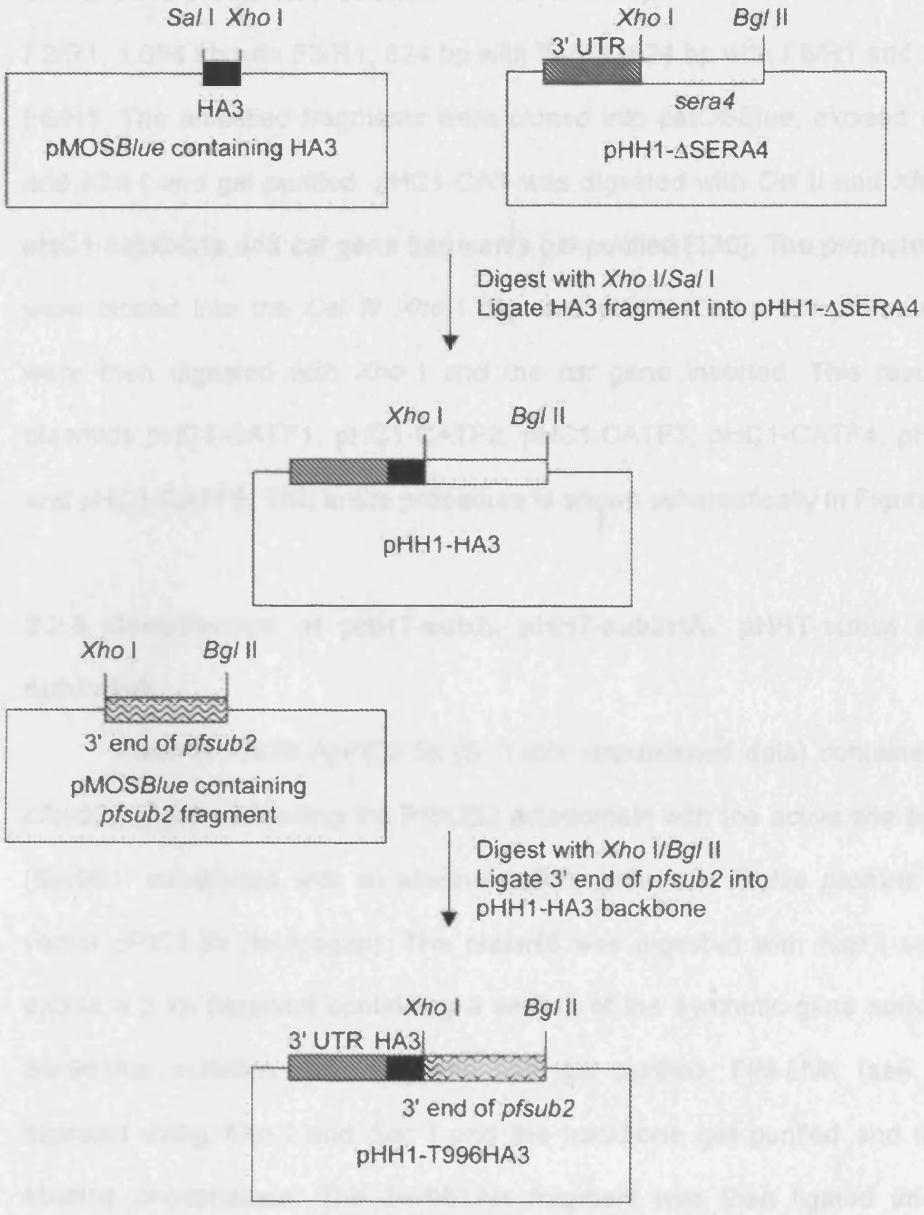
Sal I Xho I
HA3
pMOSBlue containing HA3
Xho I Bgl II
3' UTR
sera4
pHH1-ΔSERA4
Digest with Xho I/Sal I
Ligate HA3 fragment into pHH1-ΔSERA4
Xho I Bgl II
pHH1-HA3
Xho I Bgl II
3' end of pfsub2
pMOSBlue containing
pfsub2 fragment
Digest with Xho I/Bgl II
Ligate 3' end of pfsub2 into
pHH1-HA3 backbone
Xho I Bgl II
3' UTR HA3
3' end of pfsub2
pHH1-T996HA3

CACAACAAAGAAAACATTCC-3'), F5 (5'-**GCTCAGC**GGTTTTTTTTAATATATATAGATAAATGG-3') and F6 (5'-**GCTCAGC**TTCCTCTTTCATCATACACATGAGG-3').

A *Cel* II site is marked in bold in each forward primer. Amplification with the primer pairs produced products of 1.459 kb with primer pairs F1/R1, 1.267 kb with F2/R1, 1.054 kb with F3/R1, 824 bp with F4/R1, 624 bp with F5/R1 and 286 bp with F6/R1. The amplified fragments were cloned into pMOS*Blue*, excised using *Cel* II and *Xho* I and gel purified. pHC1-CAT was digested with *Cel* II and *Xho* I and the pHC1 backbone and *cat* gene fragments gel purified [130]. The promoter fragments were cloned into the *Cel* II/ *Xho* I digested pHC1. The pHC1-promoter plasmids were then digested with *Xho* I and the *cat* gene inserted. This resulted in the plasmids pHC1-CATF1, pHC1-CATF2, pHC1-CATF3, pHC1-CATF4, pHC1-CATF5 and pHC1-CATF6. This entire procedure is shown schematically in Figure. 2.5.

2.2.8 Construction of pHHT-sub2$_i$, pHHT-sub2HA$_i$, pHHT-subw$_i$ and pHHT-sub2wHA$_i$

Plasmid Pfs2S-ApPIC3.5k (S. Yeoh, unpublished data) contains part of the *pfsub2*$_{synth}$ gene encoding the PfSUB2 ectodomain with the active site serine codon (Ser961) substituted with an alanine codon, within the *Pichia pastoris* expression vector pPIC3.5k (Invitrogen). The plasmid was digested with *Ksp* I and *Sac* I to excise a 2 kb fragment containing a section of the synthetic gene surrounding the Ser961Ala mutation. This fragment was gel purified. FIM-LNK (see 2.2.1) was digested using *Ksp* I and *Sac* I and the backbone gel purified and treated with alkaline phosphatase. The Ser961Ala fragment was then ligated into FIM-LNK forming FIM-LNKS961A. This method was repeated for FIM-LNKHA, FIM-LNK$_{fl}$ and FIM-LNK$_{flHA}$, forming the vectors FIM-LNKHAS961A, FIM-LNK$_{fl}$S961A and FIM-LNK$_{flHA}$S961A respectively. pHHT-sub2 was digested with *Ava* I and *BstE* II and the

Figure 2.5 Construction of pHC1-CATprom plasmids

Schematic representation of the construction of pHC1-CATprom plasmids. The constructs place the *cat* gene under the control of fragments of the region 5' to the *pfsub2* gene.

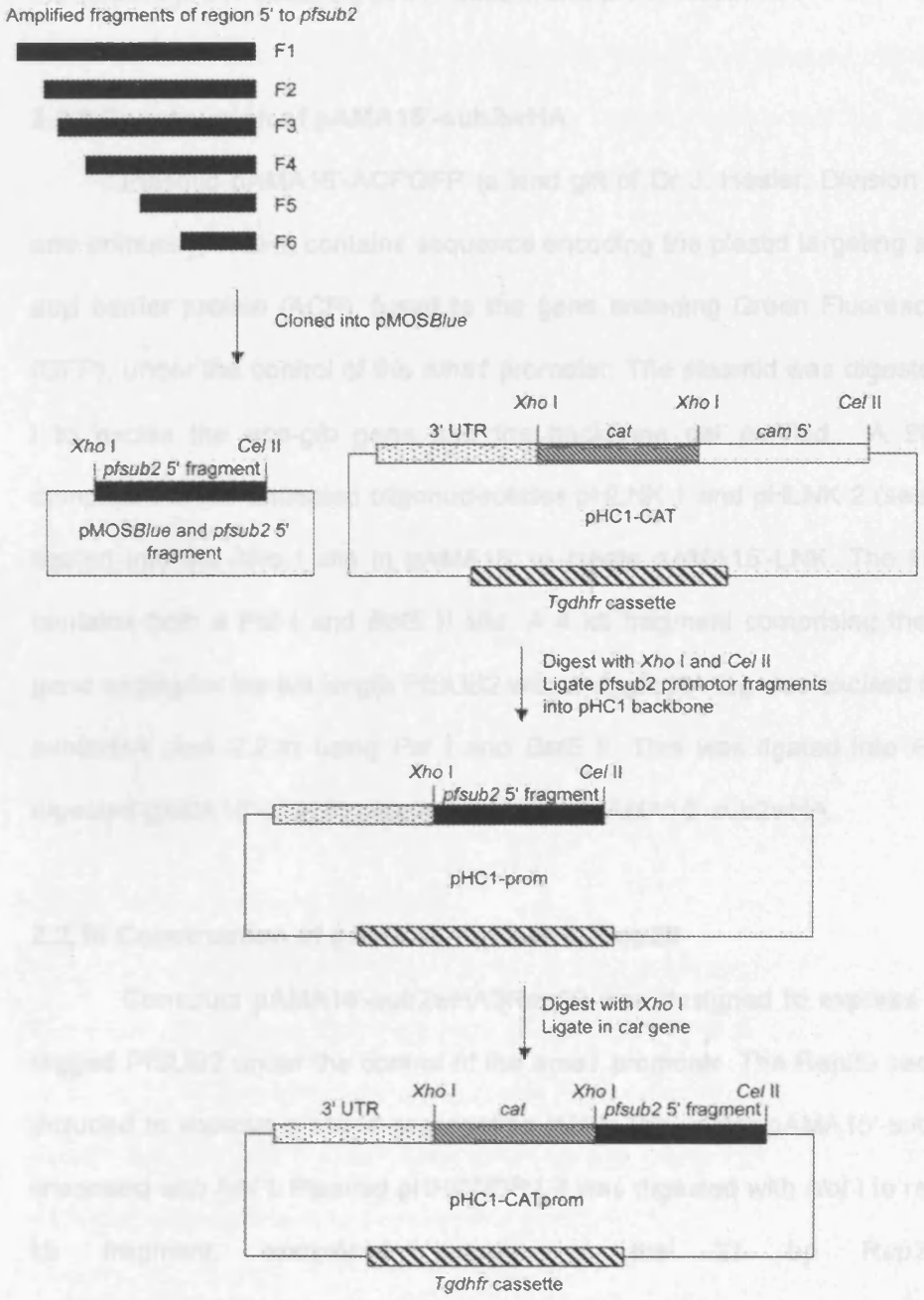
Amplified fragments of region 5' to pfsub2
F1
F2
F3
F4
F5
F6
Cloned into pMOSBlue
Xho I
Cel II
pfsub2 5' fragment
pMOSBlue and pfsub2 5' fragment
Xho I
Xho I
Cel II
3' UTR
cat
cam 5'
pHC1-CAT
Tgdhfr cassette
Digest with Xho I and Cel II
Ligate pfsub2 promotor fragments into pHC1 backbone
Xho I
Cel II
pfsub2 5' fragment
pHC1-prom
Digest with Xho I
Ligate in cat gene
Xho I
Xho I
Cel II
3' UTR
cat
pfsub2 5' fragment
pHC1-CATprom
Tgdhfr cassette

backbone gel purified and phosphatased. FIM-LNKS961A was digested with *Ava* I and *BstE* II and the 300 bp fragment gel purified. This fragment was then ligated into the pHHT-sub2 backbone forming pHHT-sub2$_i$. This modification was also performed on FIM-LNKHAS961A, FIM-LNK$_{fl}$S961A and FIM-LNK$_{flHA}$S961A to form the vectors pHHT-sub2HA$_i$, pHHT-sub2w$_i$ and pHHT-sub2wHA$_i$

2.2.9 Construction of pAMA15'-sub2wHA

Plasmid pAMA15'-ACPGFP (a kind gift of Dr J. Healer, Division of Infection and Immunity, WEHI) contains sequence encoding the plastid targeting sequence of acyl carrier protein (ACP), fused to the gene encoding Green Fluorescent Protein (GFP), under the control of the *ama1* promoter. The plasmid was digested with *Xho* I to excise the *acp-gfp* gene and the backbone gel purified. A 20 bp linker comprised of the annealed oligonucleotides pHLNK 1 and pHLNK 2 (see 2.2.1) was ligated into the *Xho* I site in pAMA15' to create pAMA15'-LNK. The linker region contains both a *Pst* I and *BstE* II site. A 4 kb fragment comprising the *pfsub2*$_{synth}$ gene coding for the full length PfSUB2 with a single HA tag was excised from pHHT-sub2wHA (see 2.2.4) using *Pst* I and *BstE* II. This was ligated into *Pst* I/*BstE* II digested pAMA15'-LNK to create the plasmid pAMA15'-sub2wHA.

2.2.10 Construction of pAMA15'-sub2wHA3Rep20

Construct pAMA15'-sub2wHA3Rep20 was designed to express a triple HA tagged PfSUB2 under the control of the *ama1* promoter. The Rep20 sequence was included to improve plasmid segregation [122]. The vector pAMA15'-sub2wHA was linearised with *Not* I. Plasmid pHHC*/DR1.4 was digested with *Not* I to release a 1.4 kb fragment, comprised entirely of the 21 bp Rep20 repeat (TAAGACCTA(T/A)(G/A)TTAGT(G/T)A(A/T)(A/C/G)(G/T)), which was gel purified [122]. The Rep20 sequence was ligated into the linearised pAMA15'-sub2wHA to create the vector pAMA15'-sub2wHARep20. The triple HA tag sequence, encoding

three consecutive HA tags, was amplified from pREP(HA3)42 using the primers HA3F (5'-ATCGATTACCCTTACGATGTTCCTGACTATGC-3') and HA3R3 (5'-*GGTAACC***TCA**AGCGTAATCTGGAACGTCGTAAGGG-3') [139]. This inserts a *Cla* I (shown underlined) site at the 5' end and a stop codon (shown in bold) directly followed by a *BstE* II (shown in italics) site at the 3' end of the triple HA tag sequence. The product was cloned into pMOS*Blue* and excised using *Cla* I and *BstE* II. A 850 bp gene fragment comprising sequence encoding the last 850 bp of the $pfsub2_{synth}$ cloned into pMOS*Blue* (see 2.2.3) was used as a template for site-directed mutagenesis (SDM). Primers SDMF (5'-CTGGACGACATGTTCATGAAG**ATCGAT**CACCACCATCACC-3') and SDMR (5'-GGTGATGGTGGTG**ATCGAT**CTTCATGAACATGTCGTCCAG-3') were used to insert a unique *Cla* I site (in bold) at the end of the synthetic gene directly before the stop codon. The modified end of the *pfsub2* synthetic gene was then excised from the pMOS*Blue* backbone using *BstE* II and *Sac* II. This fragment was gel purified and ligated into pAMA15'-sub2wHARep20 that had been digested with *BstE* II and *Sac* II. This construct was then digested with *Cla* I and *BstE* II and the triple HA tag sequence ligated into it to create pAMA15'-sub2wHA3Rep20. This procedure is shown schematically in Figure. 2.6.

2.2.11 Construction of pGEXHA3

Plasmid pGEXHA3 was designed to fuse three copies of the HA tag onto the 3' end of glutathione S transferase (GST). The commercially available plasmid pGEX-6P.1 (Amersham Biosciences) was linearised with *Xho* I. The triple HA tag in pMOS*Blue* (see 2.2.5) was excised using *Sal* I and *Xho* I and ligated into the pGEX6P.1 backbone to form the vector pGEXHA3.

Figure 2.6 Construction of pAMA15'-sub2wHA3Rep20

Schematic representation of the construction of pAMA15'-sub2wHA3Rep20. The construct places the full-length *pfsub2*$_{synth}$ gene encoding PfSUB2 with a C-terminal HA3 tag, under the control of the *ama1* promoter, and was designed for episomal expression of the tagged gene. The construct also contains a Rep20 sequence to improve plasmid segregation.

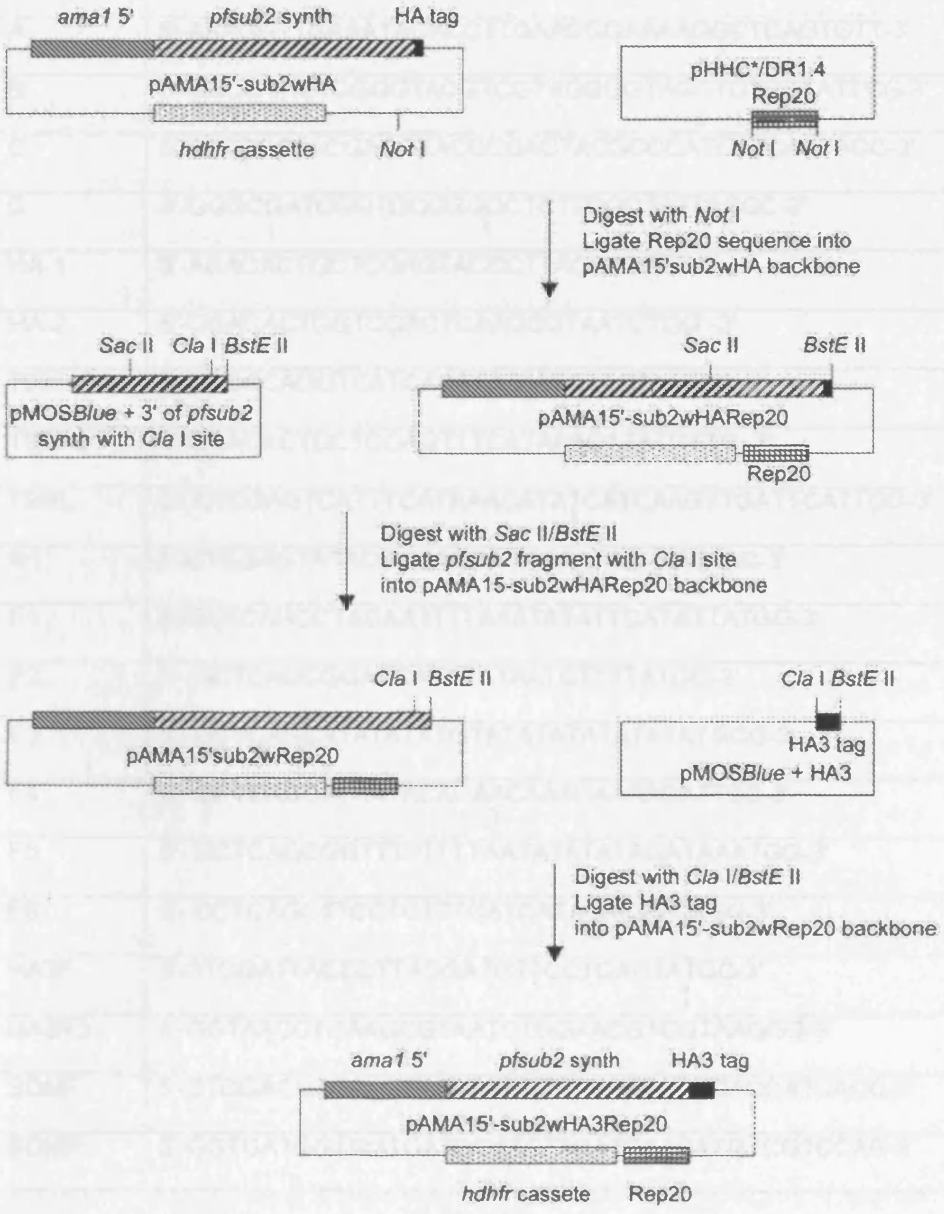
ama1 5'
pfsub2 synth
HA tag
pAMA15'-sub2wHA
hdhfr cassette
Not I
pHHC*/DR1.4
Rep20
Not I
Not I
Digest with Not I
Ligate Rep20 sequence into
pAMA15'sub2wHA backbone
Sac II
Cla I
BstE II
pMOSBlue + 3' of pfsub2
synth with Cla I site
Sac II
BstE II
pAMA15'-sub2wHARep20
Rep20
Digest with Sac II/BstE II
Ligate pfsub2 fragment with Cla I site
into pAMA15-sub2wHARep20 backbone
Cla I
BstE II
pAMA15'sub2wRep20
Cla I
BstE II
HA3 tag
pMOSBlue + HA3
Digest with Cla I/BstE II
Ligate HA3 tag
into pAMA15'-sub2wRep20 backbone
ama1 5'
pfsub2 synth
HA3 tag
pAMA15'-sub2wHA3Rep20
hdhfr cassete
Rep20

Name	Sequence	Vector
sb2LNK1	5'-AATTGGTTACCCGGGATCCG-3'	2.2.1
sb2LNK2	5'-AATTCGGATCCCGGGTAACC-3'	2.2.1
pH-LNK1	5'-TCGACTGCAGACCCGGGTTACCA-3'	2.2.1
pH-LNK2	5'-TCGATGGTAACCCGGGTCTGCAG-3'	2.2.1
A	5'-AAAGGTTGAAATACACCTTGAACGGAAAAGGCTCAGTGTT-3'	2.2.2
B	5'-GGCGTAGTCGGGTACGTCGTAGGGGTAGCTGTCGTATTCG-3'	2.2.2
C	5'-TACCCCTACGACGTACCCGACTACGCCCATCATCATCACC-3'	2.2.2
D	5'-GGGCGATCGGTGCGGGCCTCTTCGCTATTACGC-3'	2.2.2
HA-1	5'-AGACACTGCTCGAGTACCCTTACGATGTT-3'	2.2.5
HA-2	5'-GGACACTGGTCGACTCAAGCGTAATCTGG -3'	2.2.5
T996-1	5'-GCCCCAGGTCATCACATATATTCTACTATTCC-3'	2.2.5
T996-2	5'-GGACACTGCTCGAGTTTCATAAACATATCATC -3'	2.2.5
$T996_w$	5'- CTCGAGTCATTTCATAAACATATCATCAAGTTGATTCATTGC-3'	2.2.6
R1	5'-CTCGAGTATACGGAAAGAGAAAAAAAAAATAAC-3'	2.2.7
F1	5'-GCTCAGCCTACAATTTTAAATATATTCATATTATGG-3'	2.2.7
F2	5'- GCTCAGCGGACCATATATAATGTTTTATGG-3'	2.2.7
F3	5'- GCTCAGCATATATATGTATATATATATATATGGG-3'	2.2.7
F4	5'- GCTCAGCATAATACACAACAAAGAAAACATTCC-3'	2.2.7
F5	5'- GCTCAGCGGTTTTTTTTAATATATATAGATAAATGG-3'	2.2.7
F6	5'- GCTCAGCTTCCTCTTTCATCATACACATGAGG-3'	2.2.7
HA3F	5'-ATCGATTACCCTTACGATGTTCCTGACTATGC-3'	2.2.10
HA3R3	5'-GGTAACCTCAAGCGTAATCTGGAACGTCGTAAGGG-3'	2.2.10
SDMF	5'-CTGGACGACATGTTCATGAAGATCGATCACCACCATCACC-3'	2.2.10
SDMR	5'-GGTGATGGTGGTGATCGATCTTCATGAACATGTCGTCCAG-3'	2.2.10

Table 2.1 Oligonucleotides used in vector construction.

2.3 Parasite culture and analysis

2.3.1 Drug stocks

Pyrimethamine (Sigma) was first made up at 10 mM concentration in 1% glacial acetic acid before dilution in PBS to a concentration of 200 µM. This was then filter sterilised and stored at 4°C before addition to culture medium. A 20 mM solution of WR99210 (Jacobus Pharmaceuticals) was made up in DMSO. This was then diluted to 20 µM in RPMI-1640 (GIBCO), filter sterilised, and stored at 4°C before addition to culture medium.

2.3.2 *P. falciparum* culture and transfection

Plasmodium falciparum line D10 (a laboratory clone of FC27 from Papua New Guinea, supplied by M. Grainger, NIMR) was cultivated and synchronised using standard procedures [141, 142]. Ring stage parasites were transfected with 100 µg of purified plasmid DNA for stable transfection as described previously [125]. In brief, a culture at approximately 5% parasitemia was pelleted by centrifugation and washed in incomplete cytomix (120 mM KCl, 0.15 mM $CaCl_2$, 2 mM EDTA, 5 mM $MgCl_2$, 10 mM K_2HPO_4/KH_2PO_4, 25 mM HEPES, pH 7.6). The culture was then pelleted again and the cytomix removed. 200 µL of the pelleted cells were added to 200 µL incomplete cytomix containing 100 µg plasmid DNA and placed in a 0.2 cm cuvette (Bio-Rad). The sample was then electroporated using a Gene Pulser Xcell™ electroporator (Bio-Rad) with settings of 0.31 kV and 960 µF. The sample was then removed from the cuvette and placed in a flask containing 25 mL medium (RPMI-1640 supplemented with 25 mM HEPES, 200 µL hypoxanthine, 20 µg/mL gentamicin, 0.25% (w/v) Albumax II, 0.2% $NaHCO_3$, pH 6.72, 2 mM L-glutamine, 5% human serum) pre-warmed to 37°C. The flask was then supplemented with a further 200 µL fresh RBCs. Parasites were cultured for 48 hours post-transfection prior to addition of drug. Parasite cultures transfected with plasmids containing the human

dhfr gene were supplemented with 10 nM WR99120, and this concentration of drug was maintained until parasite establishment. Parasites transfected with plasmids containing the pyrimethamine-resistant *Toxoplasma gondii dhfr* gene were treated for 48 hours with 0.2 nM pyrimethamine before this was reduced to 0.1 nM. Medium was replaced every 4 days until parasite establishment. At day 14 half of each culture was added to 12.5 mL medium plus 200 µL fresh RBCs. Parasites were generally detectable in blood smears after approximately 3 weeks. Parasites containing integrated forms of plasmids were selected by drug cycling as follows. The parasites were cultured without drug selection for 3 weeks before re-addition of drug. Once parasites were again detectable the process was repeated until an integration line had been established as determined by Southern blot analysis (see 2.3.6).

2.3.3 Plasmid recovery

Once parasites could be seen in blood smears, and had reached a parasitemia of approximately 5%, plasmid DNA was recovered (see Materials and Methods 2.1.5). DNA was subjected to *Dpn* I digestion to remove any residual input DNA, then cleaned using a PCR purification kit (Section 2.1.8). Transformation of competent *E. coli* (strain DH5α) were then transformed with the recovered DNA. Colonies were picked and plasmid DNA recovered. These clones were then analysed by restriction digest and compared on agarose gel electrophoresis to similar digests of the original plasmid used for transfection to confirm the absence of rearrangements.

2.3.4 Five-day growth rate assay

Transfected parasites were cultured in the absence of drug for a week prior to start of the growth assay. Schizont stage parasites of both transfected and parental untransfected lines were purified from culture using 70% (v/v) Percoll

(Amersham Pharmacia) [143]. The schizonts were then added to fresh media containing RBCs and allowed to invade for 2 hours before sorbitol treatment [142]. The parasitemia of all the cultures was adjusted to 0.5% parasitemia at a 4% haematocrit. Every 48 hours the cultures were diluted 1:5 with fresh medium containing fresh red blood cells at a 4% haematocrit. Thin films were made every 24 hours, stained with Giemsa and the parasitemia assessed by microscopic examination.

2.3.5 Time course

Schizont stage parasites were purified from parasite culture using 70% Percoll. The parasites were cultured in fresh medium containing no added RBCs for a further 3 hours to ensure the schizonts were fully mature. Fresh blood was then added and the parasites allowed to invade for 2 hours. Parasites were then treated with sorbitol leaving a culture of 2 hour old ring stage parasites. Thin films were taken immediately and then at 6-7 hour intervals for 48 hours. Samples were stained with Giemsa for microscopic analysis as well as being processed for indirect immunofluorescence assays (IFA) (see 2.4.5).

2.3.6 Southern blot

DNA recovered from transgenic lines was digested with various restriction enzymes to provide fragment sizes suitable for Southern blotting. Digested samples were electrophoresed on a 0.7% agarose (Bio-Rad Laboratories) gel overnight at 40 V. Following staining with ethidium bromide the gel was visualised on a UV transilluminater next to a ruler and left for 5 minutes for the UV light to nick the DNA. The gel was then incubated for 1 hour in denaturing solution (0.5 M NaOH, 0.75 M NaCl). The gel was rinsed in double-distilled water (ddH_20) and incubated for a further 1 hour in neutralising solution (0.5 M Tris-HCl, pH 7.4, 0.75 M NaCl). The DNA was transferred to a Hybond N+ membrane by capillary transfer overnight. A

DNA probe was radiolabelled with α-^{32}P adenine triphosphate (dATP) (Amersham Biosciences) using the Prime-It® II Random Primer Labelling kit (Stratagene) according to the manufacturers' instructions. The probe was hybridised overnight with the membrane in hybridisation buffer (6 x SSC, 5 x Denhardts, 0.5% SDS, 0.01 mg/mL salmon sperm DNA) at 62°C. The next day the probe was removed and the membrane washed for 20 minutes at 62°C in 2 x SSC. This wash step was repeated a further 2 times. The membrane was then wrapped in Saran wrap and exposed to X-ray film at -70°C to visualise bound probe.

2.3.7 Chloramphenicol Acetyl Transferase (CAT) Assay

A parasite culture containing approximately 200 µL 5% parasitised blood was centrifuged at 1500 rpm for 5 minutes. The supernatant was discarded and the pellet re-suspended in 1.5 volumes of 0.15% (w/v) saponin and left on ice for 10 minutes. The sample was then centrifuged for 10 minutes at 2800 rpm. The supernatant was discarded and the pellet re-suspended in 500 µL TEN buffer (40 mM Tris-HCl pH 7.6, 1 mM EDTA pH 8.0, 150 mM NaCl). The sample was then centrifuged at 14000 rpm for 1-2 minutes and the supernatant removed. This step was repeated once. The pellet was then re-suspended in 220 µL 0.25 M Tris-HCl (pH 7.6) and freeze/thawed 3 times in a dry ice/ ethanol bath to lyse the parasites. The sample was then heated for 65°C and then centrifuged for 1 minute at 14000 rpm. 200 µL of the resulting supernatant was transferred to a fresh tube. To 100 µL of each sample a substrate mix of 20 µL acetyl CoA (40 mM) and 1 µL ^{14}C-chloramphenicol was added. A negative control of substrate mix added to 100 µL 0.25 M Tris-HCl (pH 7.6) was prepared. The positive control was as for the negative control but with the addition of 0.5 µL (5 units) bacterial CAT enzyme (Promega) pre-diluted 1/500 in 0.25 M Tris-HCl (pH 7.6). The reactions were incubated overnight at 37°C. Each tube was then supplemented with 500 µL ethyl acetate and vortexed for 1 minute. The sample was then centrifuged at 14000 rpm for 2 minutes

and the top phase collected into a fresh tube. The sample was then evaporated overnight in a fume hood. 10 µL of ethyl acetate was added to each tube and the samples spotted onto a thin layer chromatography (TLC) plate (Silica gel, 250 µM layer, 20 x 20 cm, Whatman®). Ascending chromatography was performed in a TLC chamber equilibrated with 97% (v/v) chloroform 3% (v/v) methanol. Once the samples had resolved the plate was removed from the chamber and allowed to dry in the fume food. The TLC plate was then exposed to X-ray film to detect positions of migration of radiolabelled species.

2.3.8 Inhibitor studies

PfSUB2HA parasites were synchronised using standard procedures [142]. Approximately 46 hr later, mature schizont stage parasites were isolated using 70% Percoll [143]. The purified schizonts were divided equally between Eppendorfs each containing 0.5 mL media and an appropriate concentration of drug added (see table 2.2) or 0.5% DMSO as a control. The tubes were then incubated at 37°C for 4 hours to allow schizont rupture and release of merozoites into the medium. After 4 hrs thin blood films smears were made and stored with desiccant at -70°C. The effect of the various inhibitors on the trafficking of PfSUB2 on the free merozoite surface was then analysed by IFA.

Alternatively, to assess the affect of the drugs on RBC invasion by the parasite, RBCs were added to the Eppendorf alongside the mature schizonts (to create a haematocrit of 2%) and the tube then incubated for 4 hours at 37°C. After this time smears were made and Giemsa stained to assess invasion.

2.4 Immunochemical methods

2.4.1 Antibodies and associated reagents.

A number of antibodies and associated reagents were used in this work (see Table 2.3). For detection of proteins on Western blots either a horseradish

Chemical	Mode of action	Conc.	Supplier	Reference
BAPTA-AM	Inhibition of microneme secretion	25 µM	Molecular Probes	[34]
BDM	Inhibitor of myosin ATPase	5mM	Sigma	[15]
Colchicine	Inhibition of microtubule polymerisation	1 mM	Sigma	[144]
Cytochalasin B	Inhibition of actin polymerisation	4 µM	Sigma	[12]
Cytochalasin D	Inhibition of actin polymerisation	4 µM	Sigma	[60]
EGTA	Calcium chelator	10 mM	Sigma	[145]
JAS	Stabilisation of actin polymerisation	5 µM	Molecular Probes	[21]
Latrunculin A	Inhibition of actin polymerisation	5 µM	Sigma	[146]
Staurosporine	Inhibition of microneme secretion	5 µM	Sigma	[15]

Table 2.2 Drugs used to study PfSUB2 movement

Antibody name	Type	Target	Conc. (IFA)	Conc. (Western blot)	Reference/ Supplier
3F10	mAb	HA epitope	1/500	1/1000	[147], Roche
12CA5	mAb	HA epitope	1/200	Culture supernatant	[148], in house
H5	mAb	RAP2	N/A	Culture supernatant	[149], in house
58F8	mAb	AMA1 N-terminus	1/100	N/A	[56], in house
HIS-1	mAb	Polyhistidine tag	N/A	1/1000	Sigma
X509	mAb	MSP1	1/1,600	N/A	[150], in house
Alexa Fluor® 594 4G2	mAb	AMA1	1/50	N/A	[151], in house
Alexa Fluor® 594 61.3	mAb	RhopH2	1/50	N/A	[152], in house
Alexa Fluor® 594 H5	mAb	RAP2	1/50	N/A	[149], in house
Alexa Fluor® 594 anti-human	Polyclonal	Human IgG	1/500	N/A	Molecular probes
Anti-rat biotinylated	Polyclonal	Rat IgG	1/500	1/8000	Chemicon
Anti- mouse biotinylated	Polyclonal	Mouse IgG	N/A	1/1000	Jackson Immunological Research
Fluorescein streptavidin	N/A	Biotin	1/500	N/A	Vector Laboratories
HRP-streptavidin	N/A	Biotin	N/A	1/8000	Bio-Rad

Table 2.3 Antibodies and associated reagents used in this work.

peroxidase (HRP)-conjugated secondary antibody or a combination of biotin-labelled secondary and HRP-labelled streptavidin was used. For IFA a biotin-labelled secondary antibody followed by fluorescein (FITC)-labelled streptavidin was used to label target proteins with fluorescein. All other antibodies used in IFA were either directly labelled with Alexa Fluor® 594 or were used in combination with an Alexa Fluor® 594-labelled secondary antibody.

2.4.2 Purification of monoclonal antibodies (mAbs) 12CA5, H5 and 58F8

Hybridoma supernatant was passed over a Protein G Sepharose column (Amersham Pharmacia) overnight and the column washed in PBS. Bound antibody was eluted with 0.2 M glycine-HCl, 0.15 M NaCl, pH 2.7 containing 0.02% NaN_3. Eluted protein was collected into 1 M Tris-HCl (pH 8.2) to neutralise it. The collected antibody was then concentrated by ultrafiltration using an XM50 membrane (Amicon) and then run on a PD-10 desalting column according to the manufacturers' instructions (Amersham Pharmacia). 12CA5 was eluted in PBS before addition of 0.02% sodium azide and storage at 4°C. H5 and 58F8 were eluted in 0.1M sodium bicarbonate buffer (pH 9.0) before conjugation to a fluorophore (see 2.4.3).

2.4.3 Alexa Fluor® 594 labelling of antibodies

Monoclonal antibodies 4G2 (anti-AMA1, [151]), 61.3 (anti-RhopH2, [152]), X509 (anti-MSP1, [150]) and H5 (anti-Rap2, [149]) were labelled with Alexa Fluor® 594 carboxylic acid, succinimidyl ester (Molecular Probes) according to the manufacturers instructions. The labelled mAb was separated from unreacted labelling reagent by the use of PD-10 desalting columns (Amersham Pharmacia) according to the manufacturers' instructions. The labelled mAb was eluted from the column using 300 µL fractions of PBS with 1% BSA. For all the directly labelled antibodies fraction 8 was used in IFAs at a dilution of 1/50.

2.4.4 Western blots

Parasite cultures were centrifuged (3 minutes at 2000 rpm) and the supernatant removed. The RBCs were saponin-lysed and the culture centrifuged as before to pellet the parasites. The sample was then re-suspended in an equal volume of 2 x sodium dodecyl sulphate (SDS) sample buffer (95 mM Tris-HCl, 20% glycerol, 4.6% (w/v) SDS and 0.01% Bromophenol blue) and boiled for 5 min. Alternatively parasitised RBCs were re-suspended in 4 volumes of Triton X-100 (TX-100) buffer (1% TX-100, 50 mM Tris HCl pH 8.0, 2 mM EDTA, 2 mM EGTA) and incubated on ice for 30 min. These samples were then centrifuged for 20 min at 13,000 rpm at 4°C and the TX-100 soluble supernatant re-suspended in an equal volume of 2 x SDS sample buffer and boiled. For samples that needed reducing 100 mM DTT was added to the SDS sample buffer before addition to the sample. Samples were electrophoresed on a 10% SDS polyacrylamide gel (SDS-PAGE) and transferred onto nitrocellulose membrane (Hybond-C extra, Amersham Life Science) electrophoretically overnight. The membranes were then blocked for one hour in 5% (w/v) milk powder in PBS with 0.05% Tween 20 (PBST) containing 0.1% sodium azide. The membrane was then washed once for 5 minutes in PBST before being incubated with the primary antibody for 1 hour. The membrane was then washed 3 times for 5 minutes each in PBST. The secondary antibody was added and incubated with the membrane for 1 hour. For HRP-conjugated antibodies the membrane was then washed 3 times (twice for 5 minutes and once for 30 minutes) in PBST. 2 mL of Enhanced Chemiluminescent solution (ECL, Pierce) was added per membrane and incubated for 5 minutes. The ECL solution was removed and the membrane exposed to X-ray film (Biomax MR film, Kodak®) to visualise bound antibody. For biotin-conjugated secondary antibodies the membrane was washed 3 times for 5 minutes in PBST and then incubated for an hour with the HRP-conjugated streptavidin. The membrane was then washed 3 times (twice for 5 minutes and once for 30 minutes) before ECL addition and visualisation as before.

2.4.5 Immunofluorescence assay (IFA)

Air-dried thin blood films from parasite cultures were fixed by plunging into ice-cold acetone for about 30 seconds, dried again, and circles drawn on the sample using an Immunopen™ (Calbiochem®). 50 µL of primary antibody (diluted in 1% BSA in PBST) was added to each circle with the exception of a negative control which comprised 50 µL of 1% BSA in PBST. The slide was incubated in the dark at room temperature for 30 minutes before being washed in PBS. If required 50 µL of secondary antibody (diluted as before) was added to each circle and the slide incubated in the dark at room temperature for 30 min before washing in PBS. For IFAs using the biotin-streptavidin system the tertiary FITC-labelled streptavidin antibody (diluted in PBST with 1% BSA) was added to each circle and the slide incubated in the dark at room temperature for 30 minutes. The slide was washed in PBS and dipped in a solution (1 µg mL^{-1}) of 4,6-diamidino-2-phenylindole (DAPI) in PBS to visualise parasite nuclei. The slide was re-washed in PBS and a drop of Citifluor (Citifluor Ltd) added to each circle. A coverslip was then placed over the slide and the sample viewed using a Zeiss Axioplan 2 imaging system. For dual labelling the method used was as above but with the addition of extra antibody steps and washes before the DAPI staining.

2.4.6 Affinity purification of parasite-derived PfSUB2HA

Schizonts of the PfSUB2HA line or clones thereof were purified by density centrifugation with 70% Percoll as described above [143]. 5 x volume of TX-100 buffer supplemented with protease inhibitors (1% TX-100 in 50 mM Tris-HCl pH 8.2 containing 10 µM E-64 and 1 µM pepstatin) was added to the schizont pellet and the solution incubated on ice with occasional vortexing for 30 minutes. The solution was then centrifuged for 20 min at 13,000 rpm at 4°C. The supernatant was removed precleared by being added to $1/10^{th}$ volume of 'dry' Protein G Sepharose™ 4 Fast

Flow (Amersham Biosciences) and left shaking at 4°C for 30 min. The sample was centrifuged through a Spin-X® column (Costar) to remove the Protein G Sepharose™ beads. A 1/50th volume of purified mAb 12CA5 (7.8 mg mL-1) was then added to the sample which was then incubated overnight at 4°C. The sample was then added to 1/10th volume of 'dry' Protein G Sepharose beads and left shaking for 30 min at 4°C. The beads were then washed 2 x 1 mL with wash buffer 1 (50 mM Tris HCl pH 8.2, 0.5% TX-100, 1 mg/mL BSA, 0.5 M NaCl), followed by 4 x 1 mL washes with wash buffer 2 (50 mM Tris HCl pH 8.2, 0.5% TX-100). Once the washes were complete the beads were re-suspended in 2.5 bead volume of digestion buffer (0.05% TX-100, 50 mM Tris-HCl pH 8.2, 5 mM $CaCl_2$), divided into 50 µL aliquots, snap frozen and stored at –70°C. These are referred to as PfSUB2HA beads. The process was repeated with extracts of PfSUB2w parasites and the beads (referred to as PfSUB2w beads) used as a negative control in subsequent manipulations.

As an alternative to working with protein immobilised on beads, attempts were made to elute bound protein eluted from the beads by addition of a synthetic HA peptide corresponding to the HA3 sequence (YPYDVPDYAGGGYPYDVPDYAGGGYPYDVPDYA; made in house by P. Fletcher). Prior to the wash steps described above, 200 µL of TX-100 buffer, containing a final concentration of 1 mg mL^{-1} HA peptide, was incubated with the beads at 4°C with shaking for 30 minutes. The solution was then centrifuged and the supernatants removed and analysed for the presence of eluted PfSUB2. The beads were then washed as before and analysed.

2.5 Protein expression and purification methods

2.5.1 Expression of GST-HA3

A starter culture of *E. coli* cells BL21(DE3) cells transformed with pGEXHA3 was grown overnight in Terrific broth containing 50 μg mL^{-1} ampicillin (Amp). The following day this culture was diluted 1/50 into fresh Terrific broth with Amp. The culture was grown for approximately 2 hrs at 37°C until an optical density (OD) at 600 nm of 0.6-1.0 had been reached. 1mM isopropyl beta D thiogalactopyranoside (IPTG) was then added to the culture and the cells grown for a further 4 hours. Cells were then pelleted and stored at –70°C.

2.5.2 Purification of GST-HA3

The bacterial pellet (see 2.5.1) was re-suspended in PBS containing 10 mM EDTA, 1 mM PMSF and 10 μM E-64 and run twice through a Cell Disrupter (Constant Systems). The lysate was then centrifuged at 18,000 rpm for 20 min at 4°C and the supernatant removed and clarified by filtration. The filtered supernatant was then chromatographed on a Glutathione Sepharose 4B (Amersham Pharmacia) column, which was then washed with PBS and eluted with 4 mL fractions of 10 mM reduced glutathione in 50 mM Tris-HCl pH 8.2. Eluate fractions were analysed by SDS-PAGE and Coomassie staining. Fraction 2 was shown to contain the most protein. This fraction was concentrated down to a volume of 1 mL using a Vivaspin 500 tube (Vivascience) and loaded onto a HiLoad™ 26/60 Superdex™ 200 prep grade column (Amersham Pharmacia) equilibrated in PBS, and 5 mL samples taken. Fractions 40-54 were analysed and fraction 47 shown to contain GST-HA3 and what are presumably two breakdown products (as all reacted with 3F10 on Western blot). Attempts to further purify the individual species by HPLC failed and were abandoned.

2.5.3 Estimation of the amount of purified PfSUB2

Various dilutions of the purified GST-HA3 (the full-length intact protein presumed to be the slowest migrating band of the three seen on SDS PAGE of purified samples; see 2.5.2) were electrophoresed under reducing conditions alongside known amounts of bovine serum albumin (BSA) (Sigma). Following Coomassie staining the intensity of the bands used to estimate the amount of GST-HA3 present. Further gels were then run of varying amounts of GST-HA3 alongside PfSUB2HA and the intensity of the bands seen by Western blot used to estimate the amount of PfSUB2HA present in affinity-purified samples.

2.5.4 Construction of a fluorogenic peptide

The N-acetylated synthetic peptide Ac-CQDMLNISQHQC, designed to mimic the MSP1 secondary cleavage site was synthesised by P. Fletcher (NIMR) [76]. The peptide was then coupled to tetramethylrhodamine to produce a fluorogenic peptide substrate, essentially using the approach described by Blackman *et al.* [153]. A 10 mM solution of Ac-CQDMLNISQHQC in dimethylformamide (DMF) was added to 50 mM Tris-HCl, pH 8.0 to a final concentration of 1.0 mM. Tris(carboxyethyl)phosphine (TCEP), from a freshly prepared 40 mM aqueous solution, was added to the peptide solution to a final concentration of 2.0 mM. The mixture was incubated at room temperature overnight. The reduced peptide was then purified by reversed-phase high-performance liquid chromatography (RP-HPLC) on a Vydac 10 mm x 25 cm semipreparative C18 column that was eluted at 1 mL min^{-1} with a 10-65% (v/v) gradient of acetonitrile in 0.1% TFA over 60 min. The purified reduced peptide was freeze-dried overnight and then taken up in 410 µL DMF and added to an equal volume of 6-iodoacetamidotetramethylrhodamine (6-IATR) in DMF (21.3 mM). This was added to 3.28 mL degassed 50 mM Tris-HCl pH 7.6 containing 0.2 mM EDTA with continuous stirring. This was left incubating overnight in the dark at room temperature. The reaction was then quenched by

addition of sodium 2-mercaptoethanesulphonate (MESNA) to a final concentration of 64 mM. After a further 2 hour incubation at room temperature the crude reaction mixture was applied to a 1.6 x 65 cm G10 Sephadex column (Amersham Pharmacia) equilibrated in 30% (v/v) aqueous acetic acid and eluted at 4 mL h^{-1} with the same solvent. 2 mL fractions were collected and 20 µL aliquots of these were analysed on a Vydac 4.6 mm x 25 cm C18 reversed phase column and eluted at 1 mL min-1 with a 25–35% (v/v) gradient of acetonitrile in 0.1% TFA over 30 min. HPLC analysis detected two peaks which were collected manually (in 33 % (v/v) acetonitrile plus 0.1% TFA) and analysed by mass spectrometry (performed by P. Fletcher). The mass spectrometry showed the two peaks to posses the same mass, and to correspond to the peptide labelled with a tetramethylrhodamine group at each cysteine side-chain. The peptide peaks were dried and re-suspended in 20 µL DMSO, then stored at -20°C. To measure the concentration of the peaks a 1/400 solution of the peptide in 0.05% NP-40 was made and the absorbance measured using an Unicam UV1 spectrophotometer from 300-650 nm. To confirm the labelled peptide could be cleaved 1 mg mL^{-1} Pronase (Roche) was added to the cuvette and the absorbance re-measured. The labelled peptide was named $MSP1_{rho}$.

2.5. 5 Detection of PfSUB2 activity using a fluorogenic substrate

The fluorogenic substrate described above ($MSP1_{rho}$) was diluted to 0.2 µM in digestion buffer (50 mM Tris HCl pH 8.2, 12 mM $CaCl_2$, 0.05% NP-40). 100 µL of this was added to wells of a white microtitre plate (Scientific Lab Supplies). Wells contained either 50 µL of PfSUB2w beads, 50 µL of PfSUB2HA beads (see 2.4.6), 50 µl of chymotrypsin (Sigma, at a final concentration of 1 µM) or 50 µL of buffer (0.05% TX-100, 50 mM Tris-HCl pH 8.2, 5 mM $CaCl_2$) added. The level of fluorescence of each well was measured using a fluorescence spectrophotometer (Varian) with measurements taken every 5 min over 400 min.

2.5.6 Detection of PfSUB2 activity – recombinant PfSUB2 ectodomain

The *pfsub2*$_{synth}$ gene encoding the putative PfSUB2 ectodomain was expressed in *Pichia pastoris* where it was found to be unfolded and inactive (M. Blackman and S. Yeoh, unpublished). 4 µL of the unfolded PfSUB2 ectodomain was added to 100 µL of PfSUB2HA or PfSUB2w beads (see 2.4.6) in an Eppendorf. The beads were then immediately pelleted and 5 µL of the supernatant removed, added to SDS sample buffer and boiled for 5 min. The beads were then re-suspended and incubated at 37°C. Further samples of the supernatant were taken after 30, 90, 150, 210, 270, 310 and 340 min. Western blots were then performed on the samples (see 2.4.4) to detect cleavage of the PfSUB2 ectodomain into smaller fragments.

2.5.7 Detection of PfSUB2 activity – MSP1$_{Clip}$ peptide

Synthetic peptide MSP1$_{Clip}$ (LQGMLNISQH) was designed to mimic the MSP1 secondary cleavage site and was synthesised by P. Fletcher (NIMR). The peptide was suspended in DMSO at 40 mg mL^{-1}. 5 µL of the stock peptide was added to 100 µL of PfSUB2HA or PfSUB2w beads (see 2.4.6) and the mixture immediately spun down and a 20 µL sample of the supernatant taken. The mixture was then re-suspended and incubated at 37°C for 2.5 hr. After this time a 20 µL sample of the supernatant was taken as before. The samples were analysed for cleavage of the peptide on a Vydac 4.6 mm x 25 cm C18 reversed phase column, eluted at 1 mL min^{-1} with a 10–40% (v/v) gradient of acetonitrile in 0.1% TFA over 15 min.

Chapter 3: Epitope tagging and localisation of PfSUB2 within the parasite

Introduction

PfSUB2 is found as a very small proportion of the total protein content of the merozoite and as a result has proved difficult to detect using standard immunochemical approaches such as IFA [114]. This means there are still many unanswered questions concerning the trafficking and sub-cellular location of the protease. PfSUB2 has previously been localised to the dense granules of the schizont which, alongside the micronemes and rhoptries, are one of three sets of secretory organelles found within the apical domain of the merozoite [116]. However, this location is inconsistent with the belief that PfSUB2 is responsible for shedding of AMA1 and MSP1 as the contents of apicomplexan dense granules are thought to be secreted predominantly after the parasite has invaded the RBC [10, 11]. The cleavage of both AMA1 and MSP1 from the parasite surface occurs prior to or during parasite entry into the RBC and, as described in the Introduction, may be essential for invasion to proceed [74, 154].

Advances in the transfection technology of *P. falciparum* have allowed the integration of sequences into the parasite genome [123, 124]. This has enabled the fusion of the reporter protein GFP to parasite proteins to allow detailed study of trafficking [155]. In *T. gondii,* sequence encoding short peptide epitope tags such as c-myc and triple haemagglutinin tags (HA3) are commonly integrated onto proteins to aid detection by immunochemical methods [156-159]. The *P. berghei* SUB2 (PbSUB2) has previously been successfully tagged at the C-terminus with an TrimycDuoXpress (TmDX) epitope tag [115]. In anticipation that an epitope tagged form of PfSUB2 might prove easier to detect within the parasite and allow detailed

investigation of the sub-cellular location of the protein, attempts were made to modify the C-terminus of the protein by the addition of an epitope tag.

3.1 Modification of PfSUB2 to integrate 3 copies of the HA tag

There are a number of anti-HA mAbs available for sensitive detection of proteins modified with this tag [157-159]. The HA3 tag therefore appeared suitable for the epitope tagging of PfSUB2. However, it was considered important to ensure that the tag was placed within PfSUB2 such that it did not interfere with the function of the protein and have detrimental effects on the parasite. The C-terminus of SUB2 is not highly conserved amongst *Plasmodium* species suggesting that the precise sequence of this region of the protease is not functionally critical (Figure 3.1). The successful C-terminus tagging of PbSUB2 referred to above also suggested that this region could be modified without detrimental effects [115]. It was therefore decided to attempt to incorporate an HA3 tag within the C-terminus of the protein.

Two plasmids were designed for this work; pHH1-T996HA3 and pHH1-T996w. pHH1-T996HA3 was designed to modify the *pfsub2* gene by the integration of sequence coding for a HA3 tag onto the 3' end of *pfsub2* gene [160]. The construct contains approximately 1 kb of targeting sequence derived from the 3' end of the *pfsub2* gene fused in frame with sequence encoding the HA3 tags and followed by a stop codon. This was placed upstream of the *P. berghei hsp86* 3' UTR sequence to ensure correct transcription termination and polyadenylation of the targeted gene. pHH1-T996w was designed as a control vector to simply ensure that integration could be achieved at the *pfsub2* locus. The construct contained the same *pfsub2* targeting sequence and stop codon but lacked the sequence encoding the HA3 tag. Integration of pHH1-T996w was therefore predicted to resurrect the wild-type *pfsub2* coding sequence but result in the replacement of the *pfsub2* 3'UTR (see Figure 3.2).

Figure 3.1 Multiple alignment of predicted 3' end of SUB2 sequences from *P. falciparum*, *P. knowlesi*, *P. vivax*, *P. chabaudi*, *P. berghei* and *P. yoelii*

The predicted cytoplasmic domain, which exhibits low conservation across SUB2 orthologues, is highlighted in yellow. : and . denote conserved or similar residues, * denotes identical residues. This alignment was produced by S. Yeoh using the ClustalX program.

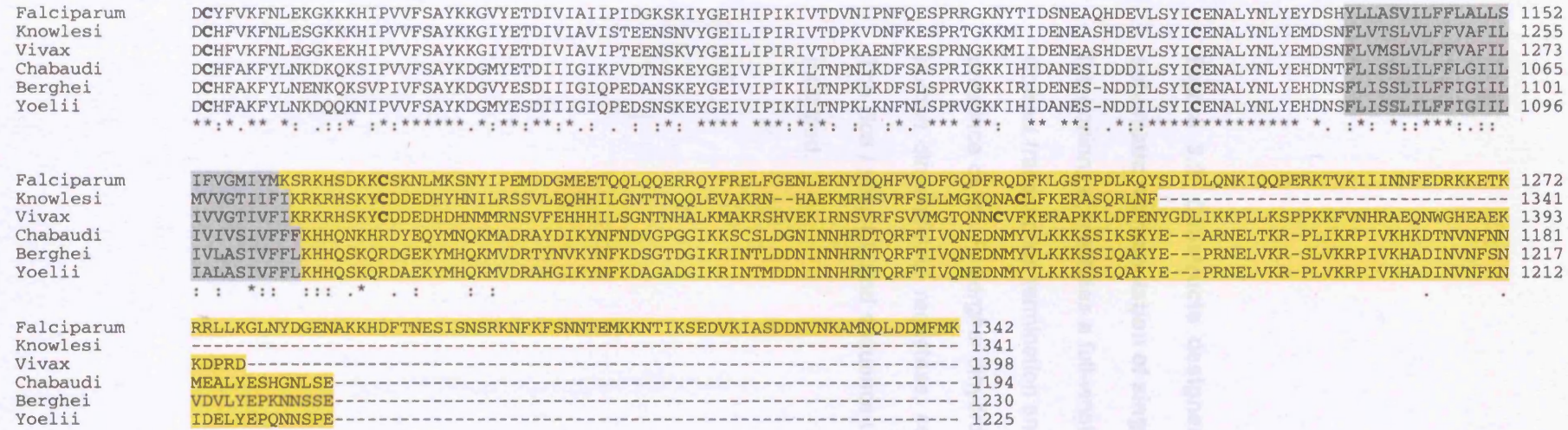
Falciparum DCYFVKFNLEKGKKKHIPVVFSAYKKGVYETDIVIAIIPIDGKSKIYGEIHIPIKIVTDVNIPNFQESPRRGKNYTIDSNEAQHDEVLSYICENALYNLYEYDSHYLLASVILFFLALLS 1152
Knowlesi DCHFVKFNLESGKKKHIPVVFSAYKKGIYETDIVIAVISTEENSNVYGEILIPIRIVTDPKVDNFKESPRTGKKMIIDENEASHDEVLSYICENALYNLYEMDSNFLVTSLVLFFVAFIL 1255
Vivax DCHFVKFNLEGGKEKHIPVVFSAYKKGIYETDIVIAVIPTEENSKVYGEILIPIRIVTDPKAENFKESPRNGKKMIIDENEASHDEVLSYICENALYNLYEMDSNFLVMSLVLFFVAFIL 1273
Chabaudi DCHFAKFYLNKDKQKSIPVVFSAYKDGMYETDIIIGIKPVDTNSKEYGEIVIPIKILTNPNLKDFSASPRIGKKIHIDANESIDDDILSYICENALYNLYEHDNTFLISSLILFFLGIIL 1065
Berghei DCHFAKFYLNENKQKSVPIVFSAYKDGVYESDIIIGIQPEDANSKEYGEIVIPIKILTNPKLKDFSLSPRVGKKIRIDENES-NDDILSYICENALYNLYEHDNSFLISSLILFFIGIIL 1101
Yoelii DCHFAKFYLNKDQQKNIPVVFSAYKDGMYESDIIIGIQPEDSNSKEYGEIVIPIKILTNPKLKNFNLSPRVGKKIHIDANES-NDDILSYICENALYNLYEHDNSFLISSLILFFIGIIL 1096
Falciparum IFVGMIYMKSRKHSDKKCSKNLMKSNYIPEMDDGMEETQQLQQERRQYFRELFGENLEKNYDQHFVQDFGQDFRQDFKLGSTPDLKQYSDIDLQNKIQQPERKTVKIIINNFEDRKKETK 1272
Knowlesi MVVGTIIFIKRKRHSKYCDDEDHYHNILRSSVLEQHHILGNTTNQQLEVAKRN--HAEKMRHSVRFSLLMGKQNACLFKERASQRLNF---------- 1341
Vivax IVVGTIVFIKRKRHSKYCDDEDHDHNMMRNSVFEHHHILSGNTNHALKMAKRSHVEKIRNSVRFSVVMGTQNNCVFKERAPKKLDFENYGDLIKKPLLKSPPKKFVNHRAEQNWGHEAEK 1393
Chabaudi IVIVSIVFFFKHHQNKHRDYEQYMNQKMADRAYDIKYNFNDVGPGGIKKSCSLDGNINNHRDTQRFTIVQNEDNMYVLKKKSSIKSKYE---ARNELTKR-PLIKRPIVKHKDTNVNFNN 1181
Berghei IVLASIVFFLKHHQSKQRDGEKYMHQKMVDRTYNVKYNFKDSGTDGIKRINTLDDNINNHRNTQRFTIVQNEDNMYVLKKKSSIQAKYE---PRNELVKR-SLVKRPIVKHADINVNFSN 1217
Yoelii IALASIVFFLKHHQSKQRDAEKYMHQKMVDRAHGIKYNFKDAGADGIKRINTMDDNINNHRNTQRFTIVQNEDNMYVLKKKSSIQAKYE---PRNELVKR-PLVKRPIVKHADINVNFKN 1212
Falciparum RRLLKGLNYDGENAKKHDFTNESISNSRKNFKFSNNTEMKKNTIKSEDVKIASDDNVNKAMNQLDDMFMK 1342
Knowlesi ---------- 1341
Vivax KDPRD---------- 1398
Chabaudi MEALYESHGNLSE---------- 1194
Berghei VDVLYEPKNNSSE---------- 1230
Yoelii IDELYEPQNNSPE---------- 1225

Figure 3.2: Constructs designed for modification of the *pfsub2* locus and schematic representation of single crossover integration of pHH1-T996HA3. Integration reconstitutes a full-length *pfsub2* gene with a triple HA tag at the 3' end. Correct transcription termination and polyadenylation of this gene is regulated by the presence of the *P. berghei* dihydrofolate reductase 3' UTR (Pb DT 3' UTR). *hdhfr*, human dihydrofolate reductase, conferring resistance to the antifolate WR99210. The *Sca* I sites (S) and sequence used for a probe (P) in Southern blot analysis are indicated.

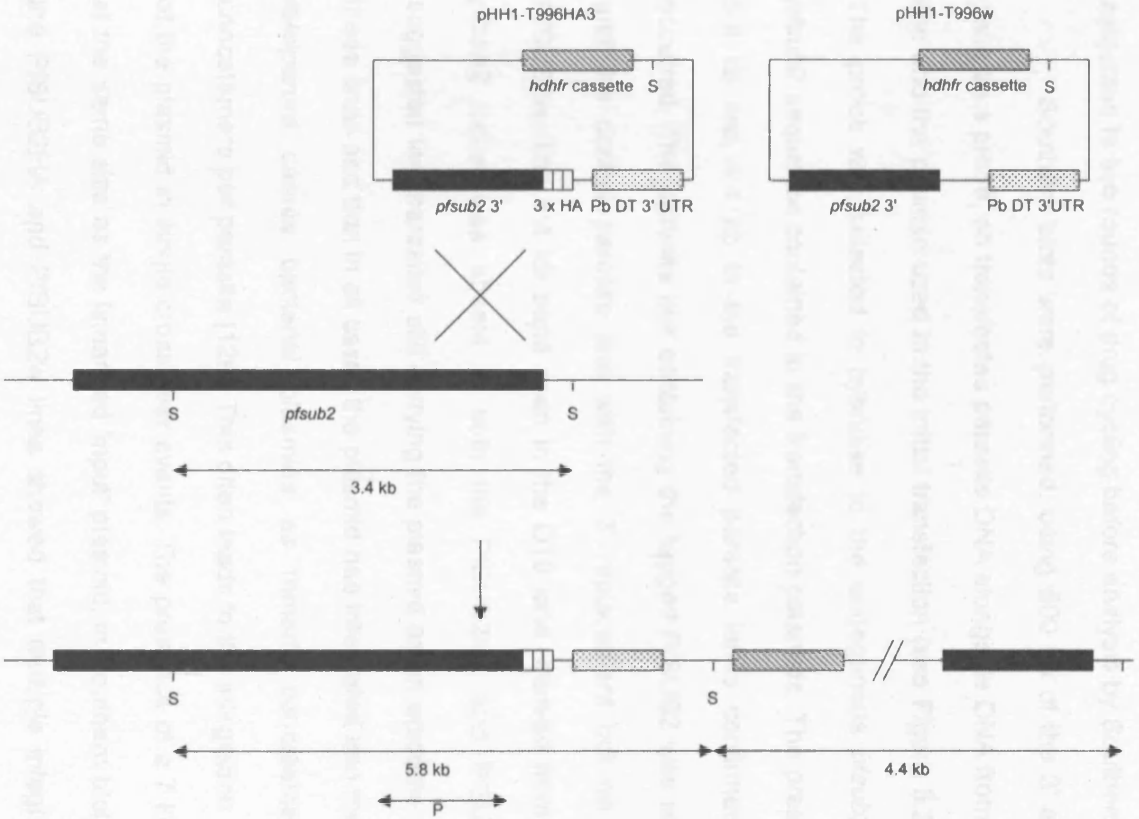
pHH1-T996HA3
hdhfr cassette
S
pfsub2 3'
3 x HA
Pb DT 3' UTR
pHH1-T996w
hdhfr cassette
S
pfsub2 3'
Pb DT 3'UTR
S
pfsub2
S
3.4 kb
S
S
5.8 kb
4.4 kb
P

D10 parasites were transfected with both pHH1-T996HA3 and pHH1-T996w and parasites detected in thin films after 24 days of selection with the antifolate WR99210. Plasmid was rescued from both lines by transformation into *E. coli* and three clones of each selected for restriction digest analysis alongside the 'original' plasmids used in the initial transfections. No rearrangements of the plasmids were detected in any of the clones selected (data not shown). The parasites were then subjected to two rounds of drug cycling before analysis by Southern blot.

Southern blots were performed, using 500 bp of the 3' end of the *pfsub2* gene as a probe, on transfected parasite DNA alongside DNA from the parental D10 line and the plasmid used in the initial transfection (see Figure 3.2 and Figure 3.3). The probe was selected to hybridise to the endogenous *pfsub2* as well as the *pfsub2* sequence contained in the transfection plasmids. The presence of bands of 5.8 kb and 4.4 kb in the transfected parasite lanes confirmed integration had occurred. The parasite line containing the tagged PfSUB2 was named PfSUB2HA and the control parasite line with the 3' replacement but no tag was named PfSUB2w. The 3.4 kb band seen in the D10 lane, derived from the endogenous *pfsub2* locus, was absent in both the PfSUB2HA and PfSUB2w lines. This suggested that parasites still carrying the plasmid as an episome were absent from these lines and that in all cases the plasmid had integrated into the *pfsub2* locus. *P. falciparum* carries bacterial plasmids as trimeric concatamers with multiple concatamers per parasite [126]. This often leads to the integration of multiple copies of the plasmid in single cross-over events. The presence of a 7 kb band, migrating at the same size as the linearised 'input' plasmid, in Southern blot analyses of both the PfSUB2HA and PfSUB2w lines showed that multiple integration events had occurred. However as neither plasmid contains a functional *pfsub2* cassette the integration of multiple copies of the plasmid should not result in additional copies of the complete gene and is therefore considered unlikely to result in increased PfSUB2 levels. Importantly, no additional DNA species were detected in the

Figure 3.3: Southern blot analysis of PfSUB2HA and PfSUB2w genomic DNA shows targeted integration.

Genomic DNA was prepared from parasite lines PfSUB2HA, PfSUB2w and untransfected (wild type) D10 parasites. DNA was digested with *Sca* I, alongside the input plasmid pHH1-T996HA3, and transferred to nylon membranes. Blots were probed with a 500 bp fragment (see Fig. 3.2) corresponding to a region within the 3' end of the *pfsub2* gene. The 4.4 kb and 5.8 kb bands correspond to the fragments produced upon *Sca* I digestion of genomic DNA if pHH1-T996HA3 or pHH1-T996w have integrated (see Figure 3.2).

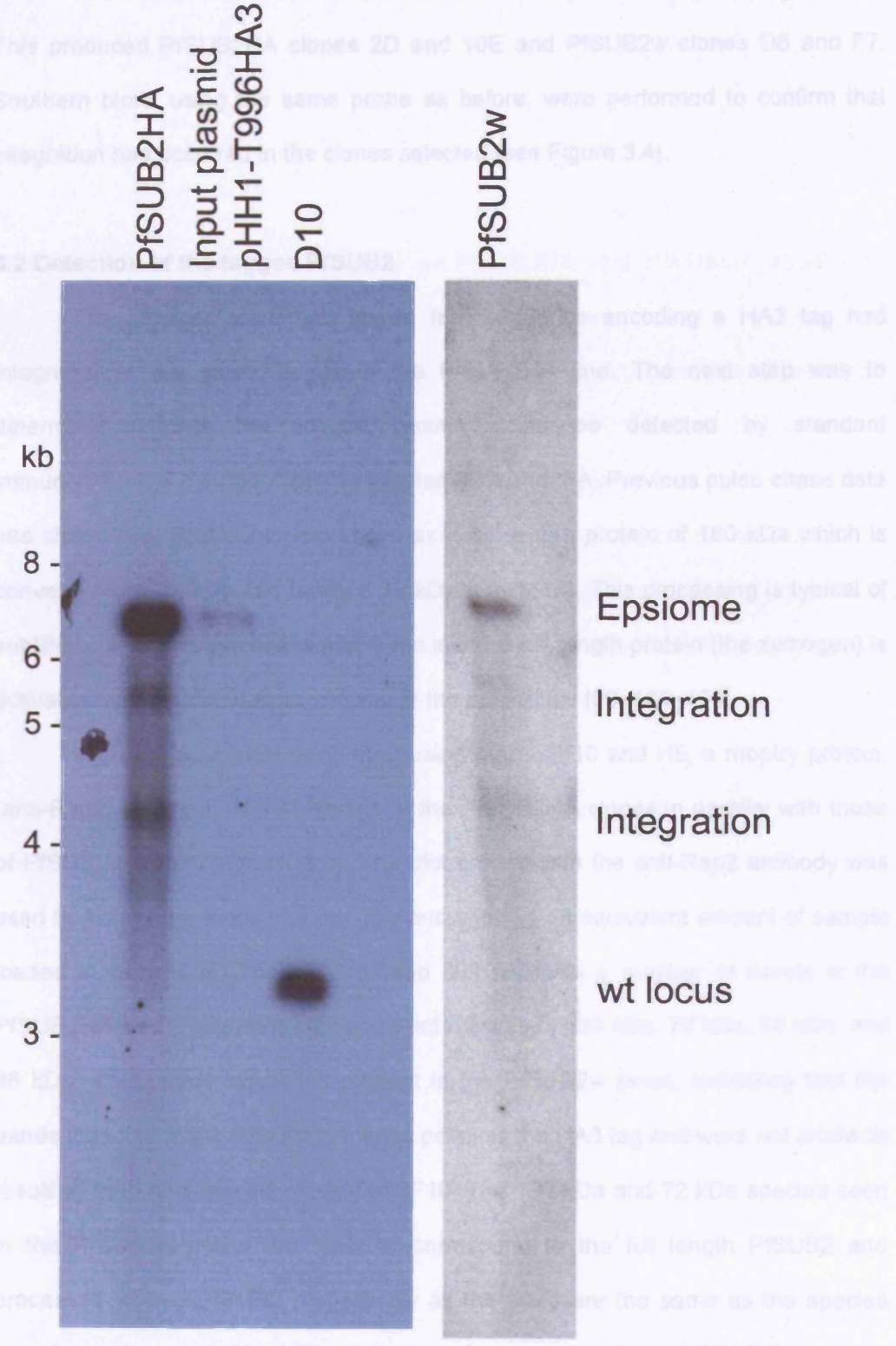
PfSUB2HA
Input plasmid
pHH1-T996HA3
D10
PfSUB2w
kb
8 -
6 -
5 -
4 -
3 -
Epsiome
Integration
Integration
wt locus

Southern blots, indicating that the plasmids did not integrate at any other sites within the parasite genome.

The PfSUB2HA and PfSUB2w lines were then cloned by limiting dilution. This produced PfSUB2HA clones 2D and 10E and PfSUB2w clones D8 and F7. Southern blots, using the same probe as before, were performed to confirm that integration had occurred in the clones selected (see Figure 3.4).

3.2 Detection of the tagged PfSUB2

The previous work had shown that sequence encoding a HA3 tag had integrated at the *pfsub2* locus in the PfSUB2HA line. The next step was to determine whether the tagged protein could be detected by standard immunochemical methods such as Western blot and IFA. Previous pulse chase data has shown that PfSUB2 is expressed as a full length protein of 160 kDa which is converted to a 74 kDa and finally a 72 kDa form [114]. This processing is typical of subtilisin-like serine proteases where the inactive full-length protein (the zymogen) is activated by the autocatalytic removal of the propeptide [99, 100, 161].

Western blots were performed using mAbs 3F10 and H5, a rhoptry protein, (anti-Rap2) to probe TX-100 lysates of the PfSUB2HA clones in parallel with those of PfSUB2w clones (Figure. 3.5). The blot probed with the anti-Rap2 antibody was used to assess the loading of the gels and showed an equivalent amount of sample loaded in each lane. The 3F10 probed blot revealed a number of bands in the PfSUB2HA lanes, migrating with apparent masses of 150 kDa, 72 kDa, 55 kDa, and 36 kDa. There were no bands present in the PfSUB2w lanes, indicating that the bands detected in the PfSUB2HA lanes possess the HA3 tag and were not artefacts resulting from non-specific binding of 3F10. The 150 kDa and 72 kDa species seen in the PfSUB2HA lane are likely to correspond to the full length PfSUB2 and processed 'active' PfSUB2 respectively as the sizes are the same as the species seen in previous work [114]. The detection of a processed form of PfSUB2

Figure 3.4: Southern blot analysis of PfSUB2HA and PfSUB2w transgenic clones shows targeted integration at the *pfsub2* locus.

Genomic DNA was prepared from PfSUB2HA clones 2D, 10E and PfSUB2w clones D8 and F7 and untransfected (wild type) D10 parasites. The DNA was digested with *Sca* I. was and electrophoresed alongside *Sca* I digested input plasmid pHH1-T996HA3. All samples were then transferred to nylon membranes. Blots were probed with a 500 bp fragment (see Figure 3.2) corresponding to a region within the 3' end of the *pfsub2* gene. The 4.4 kb and 5.8 kb bands correspond to the fragments produced upon *Sca* I digestion of genomic DNA if pHH1-T996HA3 or pHH1-T996w have integrated (see Figure 3.2).

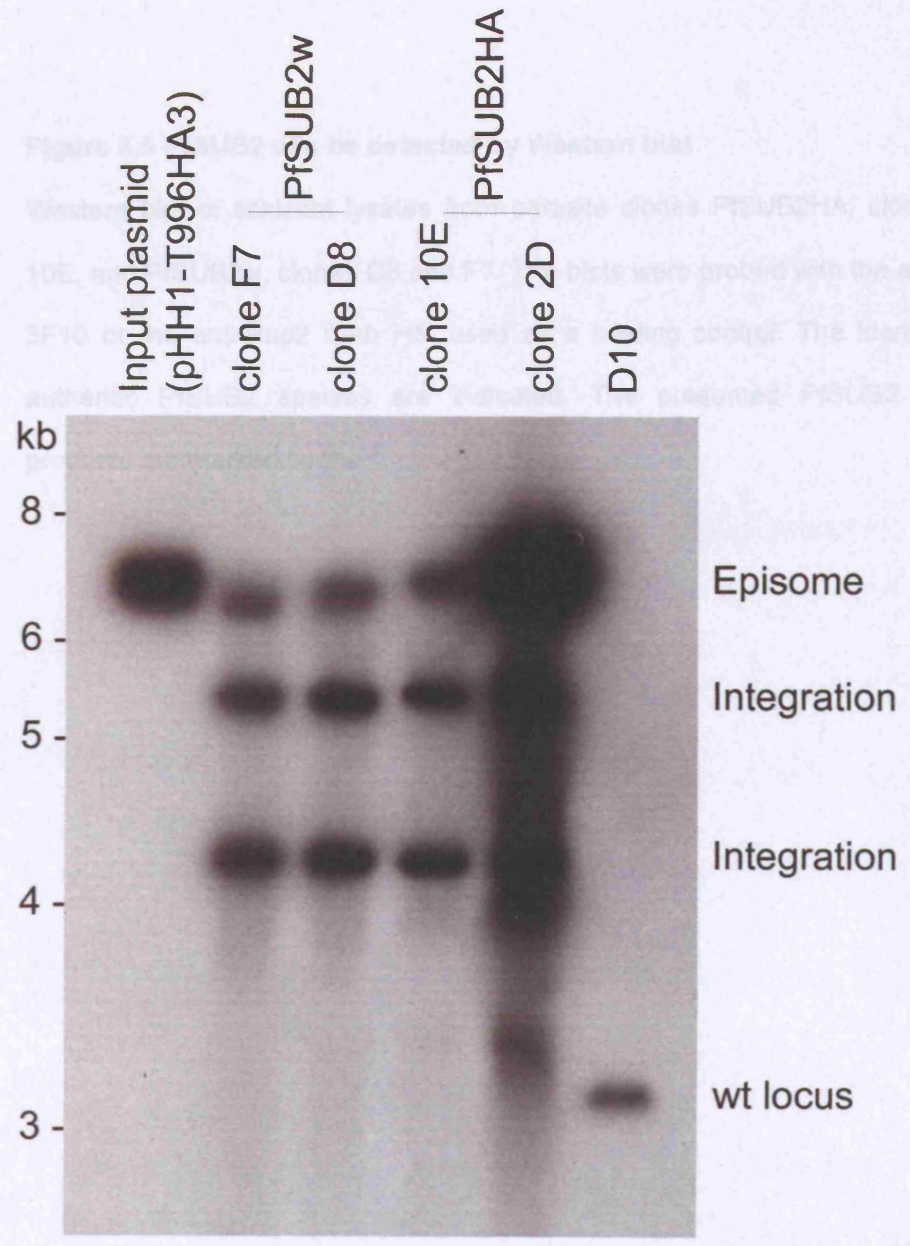
Input plasmid (pHH1-T996HA3)
clone F7
clone D8
PfSUB2w
clone 10E
clone 2D
D10
PfSUB2HA
kb
8
6
5
4
3
Episome
Integration
Integration
wt locus

Figure 3.5 PfSUB2 can be detected by Western blot

Western blot of schizont lysates from parasite clones PfSUB2HA, clones 2D and 10E, and PfSUB2w, clones D8 and F7. The blots were probed with the anti-HA mAb 3F10 or the anti-Rap2 mAb H5, used as a loading control. The identities of the authentic PfSUB2 species are indicated. The presumed PfSUB2 breakdown products are marked by the *.

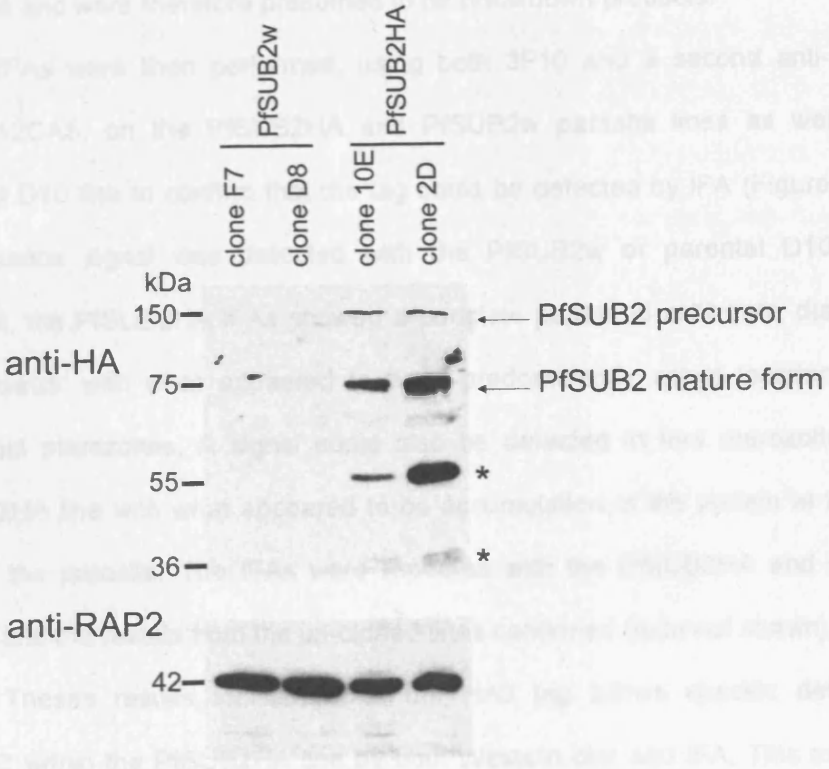
PfSUB2w
PfSUB2HA
clone F7
clone D8
clone 10E
clone 2D
kDa
150
anti-HA
75
55
36
anti-RAP2
42
PfSUB2 precursor
PfSUB2 mature form
*
*

suggested that the modified protease retained autocatalytic processing activity. In order for a PfSUB2 fragment to contain the catalytic triad, necessary for protease activity, as well as the transmembrane domain and C-terminal HA3 tag necessary for detection with 3F10, it would be predicted to have a mass of at least 67 kDa. This means that all fragments detected with a molecular mass below 67 kDa and detected by 3F10 are unlikely to contain a functional catalytic domain. As the two further species detected in the PfSUB2HA lanes of the 3F10 blot migrate with apparent masses of 55 kDa and 36 kDa they are unlikely to correspond to active protease and were therefore presumed to be breakdown products.

IFAs were then performed, using both 3F10 and a second anti-HA mAb called 12CA5, on the PfSUB2HA and PfSUB2w parasite lines as well as the parental D10 line to confirm that the tag could be detected by IFA (Figure 3.6). No fluorescence signal was detected with the PfSUB2w or parental D10 line. In contrast, the PfSUB2HA IFAs showed a punctate pattern in schizonts, distant from the nucleus, with what appeared to be a predominantly apical location seen in individual merozoites. A signal could also be detected in free merozoites of the PfSUB2HA line with what appeared to be accumulation of the protein at the apical end of the parasite. The IFAs were repeated with the PfSUB2HA and PfSUB2w clones and the results from the un-cloned lines confirmed (data not shown).

Theses results indicated that the HA3 tag allows specific detection of PfSUB2 within the PfSUB2HA line by both Western blot and IFA. This means that studies into the sub-cellular location of PfSUB2 could now be undertaken as well as investigation of the time of expression of the protein.

3.3 Tagging PfSUB2 does not affect parasite growth

Previous attempts to knock-out SUB2 within both *P. falciparum* and *P. berghei* have been unsuccessful suggesting an essential role for the protein in the RBC cycle [115, 117]. This important role for PfSUB2 means that any alterations to

Figure 3.6 Detection of epitope-tagged PfSUB2 by IFA using anti-HA monoclonal antibodies

IFA images of schizonts and free merozoites from uncloned parasite lines PfSUB2HA and PfSUB2w. Samples were probed with either mAb 3F10 or 12CA5 (both of which are specific for HA). Parasite nuclei are stained throughout with DAPI (blue). The anti-HA mAb reacts with the PfSUB2HA parasite line but not the PfSUB2w parasite line. Magnification 100x.

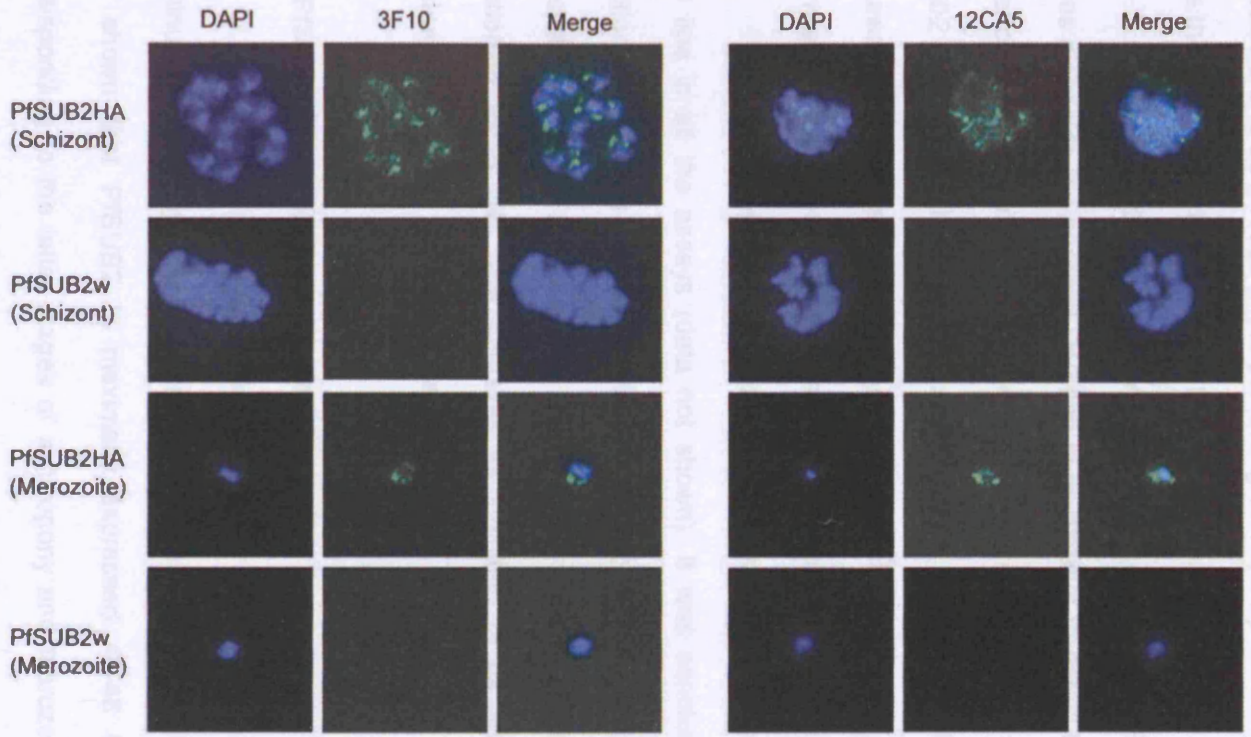
DAPI
3F10
Merge
DAPI
12CA5
Merge
PfSUB2HA (Schizont)
PfSUB2w (Schizont)
PfSUB2HA (Merozoite)
PfSUB2w (Merozoite)

the function of the protein may prove detrimental to the growth of the parasite. The HA3 tag was placed at the C-terminus of PfSUB2 in a bid to prevent the tag affecting the activity of the protease and affecting the growth of the parasite. Certain *Plasmodium* 3' UTR elements have been shown to enhance expression of parasite proteins, and it was therefore considered a possibility that the replacement of the endogenous *pfsub2* 3'UTR with the *P. berghei hsp86* 3' UTR might affect expression of PfSUB2 and as a result affect parasite growth [162]. The next set of experiments were therefore designed to explore this possibility.

Multiple growth assays were performed on the PfSUB2HA and PfSUB2w clones alongside the parental D10 line in an attempt to detect any growth defect or enhancement caused by either the addition of a HA3 tag or replacement of the *pfsub2* 3' UTR. Tightly synchronised cultures with identical parasitemias were cultured over five days and every 24 hours thin films were made, stained with Giemsa and the parasitemia assessed by microscopic examination.

The PfSUB2HA and PfSUB2w clones grew at the same rate as the parental D10 line in all the assays (data not shown). It was concluded that neither the addition of a HA3 tag at the C-terminal of PfSUB2 nor the replacement of the 3' UTR affected growth of the parasite. This implied that the modified PfSUB2 was functioning as in wild type parasites as inhibition of its activity is likely to be deleterious to growth of the parasite.

3.4 PfSUB2 is expressed during schizogony

The previous work had shown that the addition of a HA3 tag to the C-terminus of PfSUB2 greatly facilitated detection of the protein by IFA. Previous work has shown that PfSUB2 is maximally expressed 40-48 hour post invasion, corresponding to the latter stages of schizogony and merozoite release from the RBC [19, 114, 116]. The microarray data of Le Roch *et al.* places PfSUB2 in a cluster of genes that are all highly transcribed at the schizont stage and many of

which code for proteins thought to have a role in cell invasion [19]. In order to confirm these results by IFA a time course was performed to pinpoint the time of PfSUB2 expression.

Thin films of a culture tightly synchronised parasites were made every 6-8 hours over the period of an entire blood-stage cycle, and then analysed by IFA using the anti-HA mAb 3F10 (see Figure 3.7). A signal could first be detected in early ring stage parasites (2 hours post invasion) and appeared 'ring' shaped which may indicate a parasite plasma membrane location for the protein. The signal had disappeared by the next slide taken at 8 hours post invasion and was not detected in the trophozoite stage slides. PfSUB2 was next detected at 37 hours post invasion at the early schizont stage where the 3F10 signal appeared diffuse. In the next slide, at 44 hours post invasion, the signal was apical and typical of that seen with previous late schizont smears.

These experiments indicate that PfSUB2 appears in the schizont stage and is present throughout invasion as well as during the early ring stage. This is consistent with the previous microarray data, and the timing of expression of PfSUB2 is consistent with it playing a role in invasion [19]. The results also imply that neither the addition of a HA3 tag to the C-terminus nor the replacement of the *pfsub2* 3'UTR altered the time of expression of PfSUB2.

3.5 Localisation of PfSUB2 within the blood-stage parasite

PfSUB2 had previously been detected by IFA in the schizont, free merozoite and early ring stages of the *P. falciparum* RBC cycle (see 3.6 and 3.7). The protein appeared to concentrate at the apical end of the merozoite, both in the segmented schizont and free merozoite, before re-localisation across the entire surface of the parasite in the ring stage parasites. Further work focused on the use of mAbs against other parasite proteins to perform a more detailed study of the location of the protease within the parasite.

Figure 3.7 Time course experiment showing that PfSUB2 is expressed during schizogony and detectable immediately following erythrocyte invasion

Giemsa stained or IFA images of intraerythrocytic stages of the transgenic PfSUB2HA parasite line at various points during the asexual blood-stage cycle. For IFA, samples were probed with the anti-HA mAb 3F10 and parasite nuclei are stained with DAPI. Time (in hours) since invasion is indicated below each pair of images. Magnification 100x.

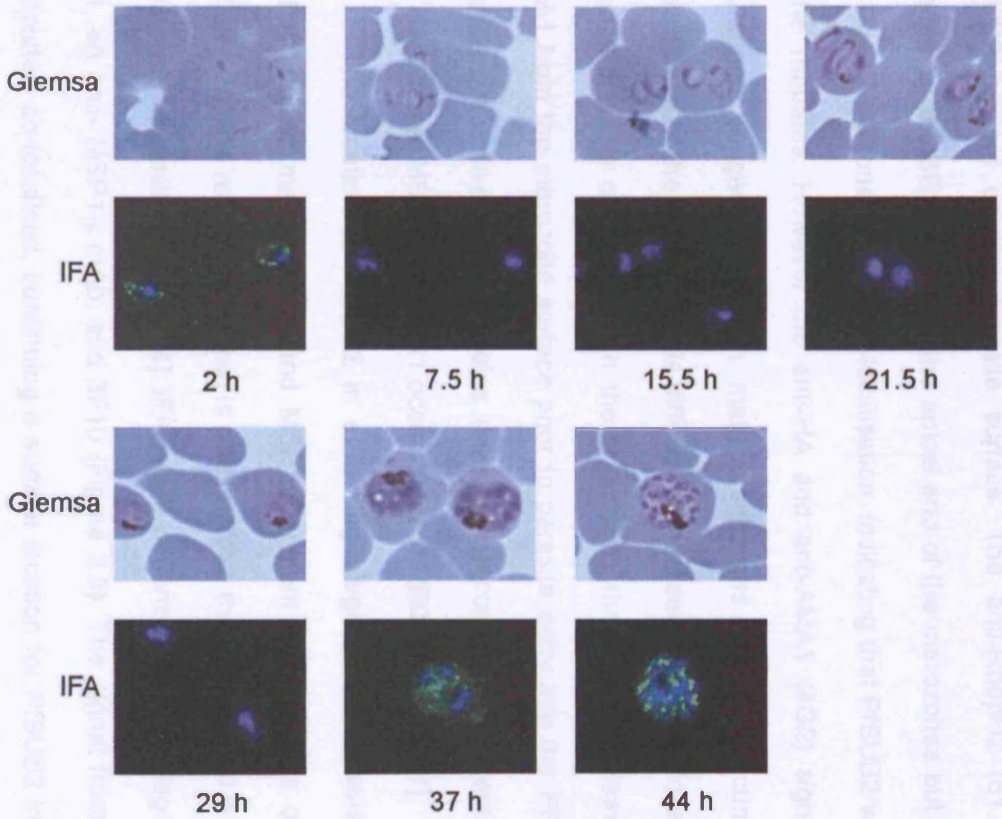
Giemsa
IFA
2 h
7.5 h
15.5 h
21.5 h
Giemsa
IFA
29 h
37 h
44 h

Micronemes and rhoptries are both found at the apical prominence of the merozoite while dense granules are found within the apical cytoplasm [7]. A number of proteins have been localised to the *Plasmodium* micronemes or the rhoptries, including RhopH2, a rhoptry protein, and AMA1, a microneme component [58, 59, 152]. MSP1 is found on the merozoite surface [68]. Antibodies against RhopH2, AMA1 and MSP1 were used in dual labelling of PfSUB2HA clone 2D schizonts with 3F10 (anti-HA), and the results of these analyses are shown in Figure 3.8. The anti-MSP1 signal did not overlap with the 3F10 signal indicating that there was no PfSUB2 present on the parasite surface. The anti-RhopH2 (61.3) signal was adjacent to the 3F10 signal at the apical end of the merozoites but again merging the signals demonstrated no co-localisation, indicating that PfSUB2 was not present in the rhoptries. However the anti-HA and anti-AMA1 (4G2) signals completely overlapped suggesting that in mature schizonts PfSUB2 accumulates in the micronemes of the parasite. This differs from the dense granule location previously described but is consistent with the hypothesis that PfSUB2 cleaves MSP1 and AMA1 from the merozoite surface prior to parasite entry into the RBC [116], since micronemes, unlike dense granules, release their contents at or during invasion and the cleavage of MSP1 and AMA1 occurs prior to RBC entry [10, 11].

The location of PfSUB2 in early ring stage parasites was then studied. $MSP1_{19}$ is the membrane bound MSP1 fragment that remains on the parasite surface after the rest of the protein is cleaved from the surface and is carried into the RBC on the parasite surface [74]. IFAs were performed on ring stage parasites with 1E1, an anti- $MSP1_{19}$ mAb, and 3F10 (Figure 3.9). The signal from the two mAbs completely co-localised, confirming a surface location for PfSUB2 in the ring stage parasites. AMA1 and MSP1 are both cleaved from the parasite surface and therefore the protease responsible is expected to be located here. The surface location of PfSUB2 in ring stage parasites indicates that during invasion PfSUB2

Figure 3.8 PfSUB2 localises to the micronemes of the schizont

IFA images of schizonts of PfSUB2HA clone 2D dual-labelled with mAb 3F10 (anti-HA) and either mAb X509 (anti-MSP1), mAb 61.3 (anti-RhopH2), or mAb 4G2 (anti-AMA1). Parasite nuclei are stained throughout with DAPI (blue). Magnification 100x.

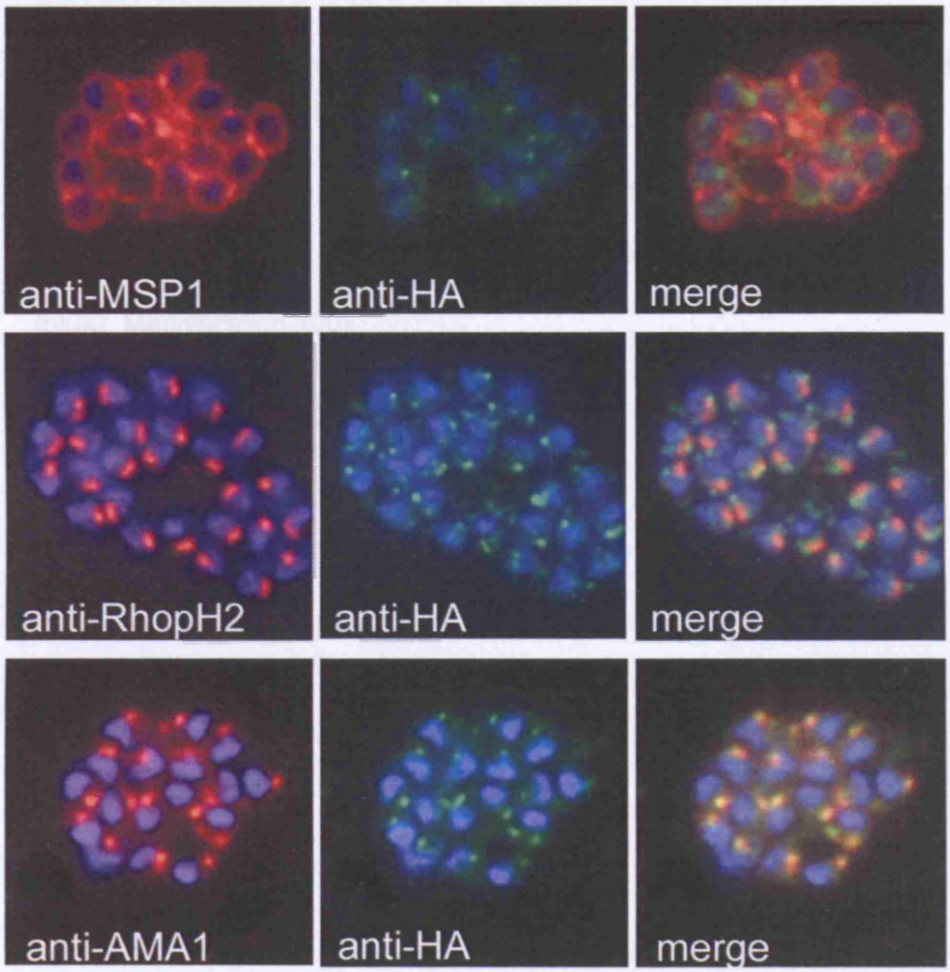
anti-MSP1
anti-HA
merge
anti-RhopH2
anti-HA
merge
anti-AMA1
anti-HA
merge

Figure 3.9 PfSUB2 remains at the plasma membrane of the newly invaded parasite

Ring stages of PfSUB2HA clone 2D (≤2 h post-invasion) probed with anti-$MSP1_{19}$ mAb 1E1 and anti-HA mAb 3F10. Parasite nuclei are stained throughout with DAPI (blue). Magnification 100x.

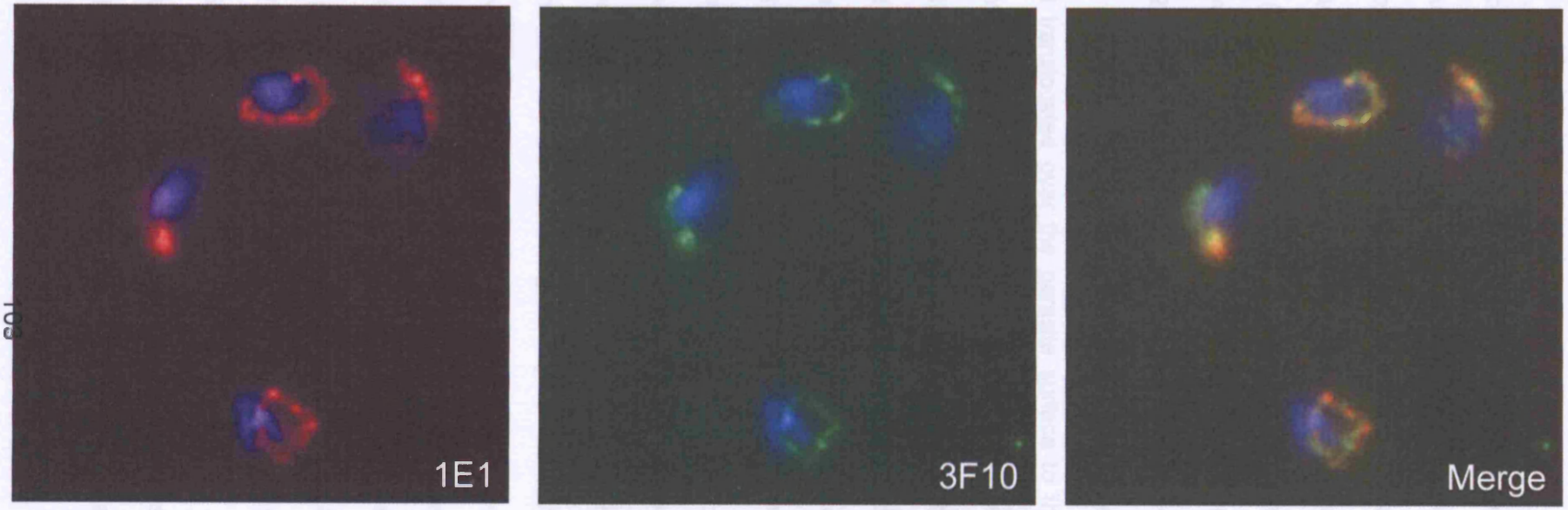
1E1
3F10
Merge

moves onto the parasite surface and is therefore in a position to cleave AMA1 and MSP1.

The location of PfSUB2 on free merozoites was then analysed (Figure 3.10). Previous IFAs of free merozoites had shown the 3F10 signal as a tight dot at the end of the parasite with a faint signal detected around the merozoite surface and it had been presumed that this corresponded to protease still resident in the micronemes (Figure 3.6). However on closer inspection some intriguing results were obtained. IFAs were performed on the free merozoites with both 3F10 and 61.3 (anti-RhopH2) (Figure 3.10). Remarkably, the 3F10 signal was found to localise at the opposite end of the parasite to the RhopH2 signal indicating that one of the proteins had translocated over the parasite surface to the posterior end of the parasite. A mAb against a second rhoptry protein Rap2 was then used alongside 3F10 to confirm this unexpected result and once again the rhoptry protein was at the opposite end of the parasite to the PfSUB2. However it remained to be determined whether it was PfSUB2 or the rhoptry proteins that were translocated to the posterior of the cell. The mAb 58F8 recognises the N-terminal of AMA1 which is cleaved from the rest of the protein within the micronemes of the parasite [56]. The mAb therefore only reacts with the intact protein found in the micronemes and can be used to determine the apical end of the parasite. IFAs of PfSUB2HA free merozoites with both 58F8 and 61.3 showed the two signals adjacent to each other. This implies that the RhopH2 was still located in the rhoptries at the apical end of the free merozoites, in turn indicating that it was the PfSUB2 that had re-localised to the posterior of the parasite. Further study of the PfSUB2HA merozoites on these slides revealed that in a very small proportion of cases (< 5%) the PfSUB2 signal appeared as twin foci on either side of the merozoite implying the PfSUB2 was circling the parasite on its way to the posterior.

These experiments used an HA3 tag to enable study of the location of PfSUB2 within the parasite. PfSUB2 was shown to accumulate in the micronemes of

Figure 3.10 PfSUB2 translocates to the posterior of the merozoite upon release from the schizont

IFA images of free merozoites of the PfSUB2HA clone labelled with mAb 3F10 (anti-HA) and either mAb 4G2 (anti-AMA1), mAb X509 (anti-MSP1) or mAb 61.3 (anti-RhopH2). Nuclei are stained throughout with DAPI (blue). The PfSUB2 signal in (A) is located at the posterior of the cell. The PfSUB2 signal in (B) appears to form twin foci on either side of the merozoite, consistent with it representing PfSUB2 'captured' *en route* to the merozoite posterior. Magnification 100x.

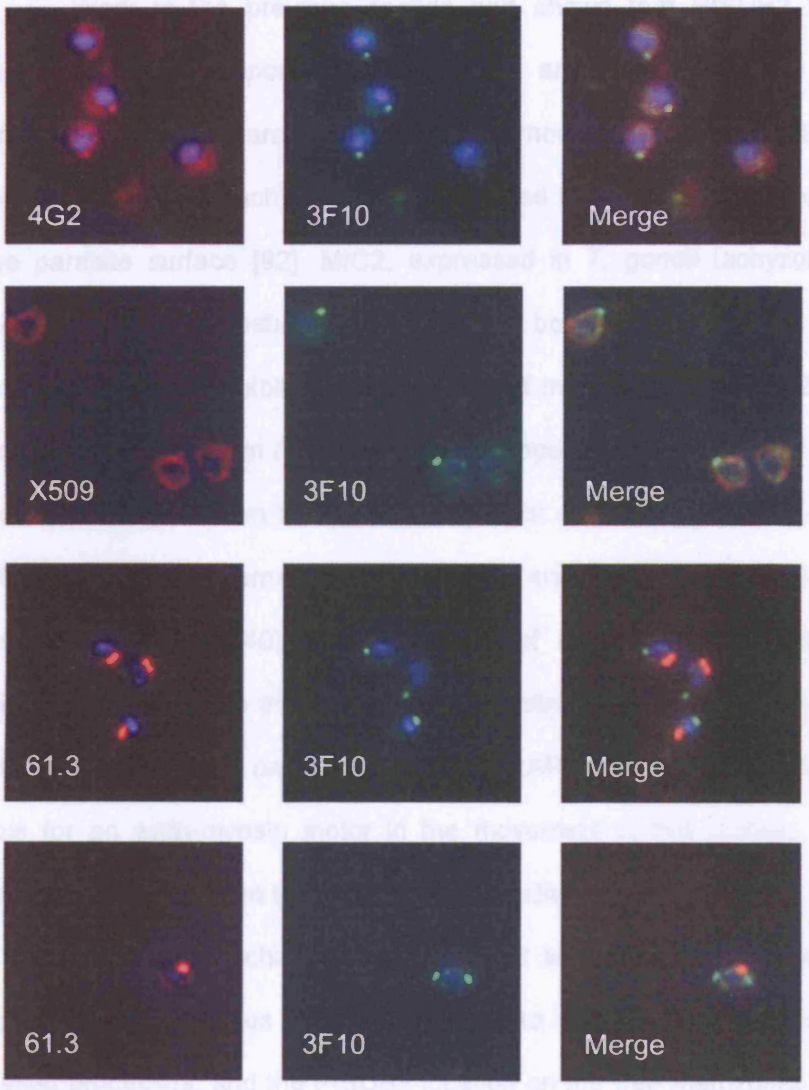
4G2
3F10
Merge
X509
3F10
Merge
61.3
3F10
Merge
A
61.3
3F10
Merge
B

the schizont until merozoite release upon which the protein was observed to translocate over the parasite surface to the posterior of the parasite. During or after invasion the protein then re-localises over the membrane of ring stage parasite surface.

3.6 Translocation of PfSUB2 is dependent on the actinomyosin motor

Work in the previous section had shown that PfSUB2 moves onto the merozoite surface upon schizont rupture and is subsequently capped to the posterior end of the parasite. The *T. gondii* rhomboid protease TgROM5 localises to the posterior of the tachyzoite and is believed to be involved in cleaving MIC2 from the parasite surface [92]. MIC2, expressed in *T. gondii* tachyzoites, and TRAP, expressed in *Plasmodium* sporozoites are both members of the TRAP family of proteins and also exhibit a similar pattern of movement to PfSUB2. These proteins are both released from micronemes and capped to the posterior of the parasite and both have been shown to be involved in host cell invasion [10, 27-29, 34, 35]. The TRAP and MIC2 C-termini bind to aldolase and this in turn mediates an interaction with actin [28, 39, 40]. The movement of MIC2 has been also shown to be dependent on myosin through the use of inhibitors of this protein [15]. The similarity of the capping on the parasite surface of TRAP and MIC2 with PfSUB2 suggested a role for an actin-myosin motor in the movement of this protein. The next set of experiments attempted to explore this possibility.

PfSUB2HA schizonts were cultured and allowed to release merozoites in the presence of various compounds known to inhibit actin polymerisation or myosin-based processes, and the PfSUB2 location on the free merozoites analysed by IFA (see Figure 3.11). The results were also summarised in Table 3.1.

The first compound tested was colchicine which destabilises microtubules and has been shown to inhibit merozoite invasion of RBC [144]. The *P. falciparum* merozoite has several microtubules which are responsible for the translocation of

Figure 3.11 PfSUB2 translocation to the posterior of the cell is dependent on actin polymerisation

IFA images of free PfSUB2HA merozoites stained with mAb 3F10 (anti-HA) and mAb 61.3 (anti-RhopH2). Parasite nuclei are stained throughout with DAPI (blue). Merozoites were released from schizonts in the presence of 1% (v/v) DMSO only, 5 µM latrunculin A (Latrunc) or 4 µM cytochalasin D (CytD). Latrunculin but not cytochalasin D appeared to interfere with posterior accumulation of PfSUB2. Magnification 100x.

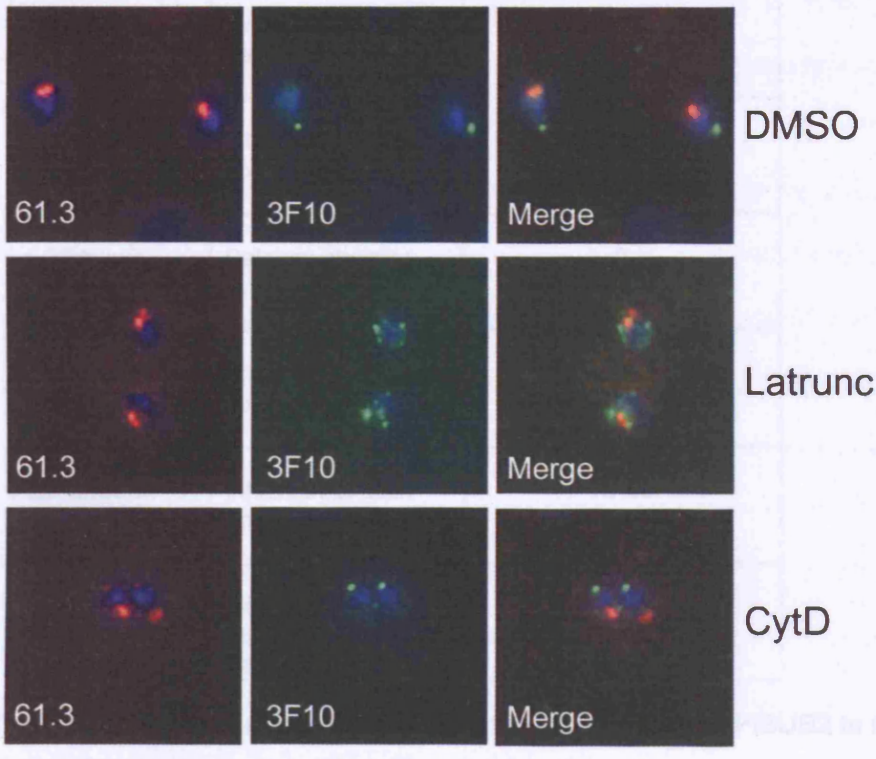
61.3
3F10
Merge
DMSO
61.3
3F10
Merge
Latrunc
61.3
3F10
Merge
CytD

Chemical	Mode of action	Inhibition of PfSUB2 movement (%)
BAPTA-AM (25 µM)	Inhibition of microneme secretion	40
BDM (5 mM)	Inhibitor of myosin ATPase	50
Colchicine (1 mM)	Inhibition of microtubule polymerisation	0
Cytochalasin B (4 µM)	Inhibition of actin polymerisation	0
Cytochalasin D (4 µM)	Inhibition of actin polymerisation	0
EGTA (10 mM)	Calcium chelator	0
JAS (5 µM)	Stabilisation of actin polymerisation	0
Latrunculin A (5 µM)	Inhibition of actin polymerisation	70-90
Staurosporine (5 µM)	Inhibition of microneme secretion	N/A

Table 3.1 Effect of various chemicals on the translocation of PfSUB2 to the posterior of the merozoite

micronemes to the apical end of the parasite [58]. Merozoites released in the presence of colchicine displayed no inhibition of PfSUB2 movement when compared to the DMSO control (data not shown). It was concluded that microtubules do not play a role in the capping of merozoite surface PfSUB2. Since PfSUB2 is a microneme protein, compounds that inhibit the release of the contents of these organelles, such as staurosporine and BAPTA-AM, would be expected to restrict the movement of PfSUB2 on the merozoite surface by preventing secretion of the protein [15, 34]. Unfortunately schizonts cultured in the presence of staurosporine were unable to rupture and appeared phenotypically abnormal (data not shown). This was unexpected as a previous report with *P. knowlesi* merozoites reported no toxicity at concentrations of staurosporine higher than those used in these experiments [163]. However BAPTA-AM did not inhibit the rupture of schizonts and release of merozoites and therefore the effects of this compound could be studied. In free merozoites released in the presence of BAPTA-AM only 60% of merozoites showed PfSUB2 at the posterior of the cell in comparison with the DMSO control. The PfSUB2, instead of appearing as a tight signal at the posterior of the parasite, was detected in many of the parasites as a diffuse signal spread over the parasite surface or else still adjacent to the rhoptries. The BAPTA-AM did not effect AMA1 localisation over the parasite surface, as determined by IFAs with the anti-AMA1 mAb 4G2. This suggests that the BAPTA-AM may be inhibiting PfSUB2 capping by a mechanism other than inhibition of microneme release as this would also be expected to prevent relocalisation of AMA1 over the parasite surface.

EGTA is a calcium chelator that inhibits merozoite invasion of RBC and the release of AMA1 and MSP1 from the surface of the RBC [60, 75, 145]. Subtilisin-like serine proteases often require calcium for stability, e.g. PfSUB1 has been shown to require calcium to cleave its substrates [112, 164]. PfSUB2 may also be a calcium dependent protease. IFA analysis of merozoites released into EGTA indicated that this compound had no effect on PfSUB2 movement (data not shown). If PfSUB2 is a

calcium dependent serine protease, as the inhibition of MSP1 and AMA1 processing by EGTA would imply, then it is possible that the protease does not need to be active to be trafficked to the posterior of the cell [60].

The next compounds tested were cytochalasin B and D and latrunculin A, both of which inhibit actin polymerisation although through different mechanisms. Cytochalasins bind to the barbed end of F-actin filaments and block all association and dissociation reactions at the end while latrunculins bind G- actin noncovalently and prevent actin assembly [165, 166]. Interestingly, merozoites released in the presence of latrunculin A showed clear inhibition of PfSUB2 capping. In these parasites the PfSUB2 had moved to the posterior of the parasite in only 10-30% of parasites as compared to the DMSO control parasites. The PfSUB2 pattern on the majority of the free merozoites appeared as a diffuse signal over the parasite surface or adjacent to the RhopH2 signal in the rhoptries. This suggested that the capping of PfSUB2 is actin dependent. IFA analysis of these merozoites using the anti-AMA1 mAb 4G2 showed the AMA1 in a circumferential pattern over the parasite surface as with the control merozoites, suggesting latrunculin does not inhibit microneme release *per se*. Cytochalasin B and D both inhibit merozoite invasion of RBCs, an observation long known to indicate that *Plasmodium* actin is susceptible to these compounds [12, 60]. However, neither of these drugs had any affect on the capping of PfSUB2. The protein was detected as a tight dot at the posterior of the parasite, not discernibly different from control parasites released in the presence of DMSO solvent only. Although this result was unexpected there are numerous accounts of differences in the effects of latrunculin and cytochalasin, presumably due to their differing modes of action on actin polymerisation [167-169]. *P. falciparum* has unusually short actin filaments [23]. Latrunculin which prevents the assembly of actin filaments rather than the cytochalasin which binds to the filaments and prevents lengthening may therefore have a greater effect. Cytochalasins can

inhibit invasion of the cell and this may reflect a need for longer filaments for invasion as opposed to shorter filaments capable of capping PfSUB2.

Jasplakinolide is a compound which stabilises actin filaments and in *T. gondii* increases the rate of gliding motility while decreasing the rate of invasion [21]. This compound was found to have no effect on the movement of PfSUB2 when merozoites were released in its presence. As actin polymerisation appears necessary for capping of PfSUB2 it is not surprising that compounds which stabilise actin in this state do not inhibit the movement. It is possible that jasplakinolide might increase the rate of PfSUB2 capping though at present it would be technically very difficult to study this.

BDM inhibits the ATPase activity of myosin and has previously been shown to inhibit invasion in many Apicomplexa [13, 15, 16, 170]. The affect of this compound on capping of PfSUB2 was therefore tested. In initial experiments PfSUB2HA merozoites were released in the presence of 50 mM BDM, but this proved to be toxic to the parasite. IFAs showed 'shrivelled' schizonts with no merozoite release (data not shown). A lower concentration of 5 mM BDM was then used, and this did not appear toxic to the parasites. In the merozoites released under these conditions there was a marked inhibition of PfSUB2 movement to the posterior of the parasite. Compared to the control parasites released in DMSO, PfSUB2 was capped in only 50% of BDM-treated parasites. The pattern of PfSUB2 expression in parasites where the capping was inhibited was the same as previously seen, with either a diffuse pattern over the parasite surface or the protein still adjacent to the rhoptries. The inhibition of PfSUB2 movement on the merozoite surface by both myosin inhibitors as well as inhibitors of actin polymerisation suggests that the action of both these proteins is necessary for the capping of the protein.

The ability of *P. falciparum* to invade RBC in the presence of a number of these compounds was then tested. EGTA has previously been shown to inhibit RBC

invasion and was used as a positive control [145]. The presence of EGTA inhibited invasion by 90% in comparison with the DMSO control. Cytochalasin D has previously been shown to block RBC invasion but to confirm the active state of the drug used in these experiments the stocks were tested to confirm that lack of inhibition of PfSUB2 capping was not due to the use of inactive cytochalasin D [60]. At the concentrations used, cytochalasin D blocked 100% of parasite invasion. It was concluded that the compound was active. Latrunculin A was tested and shown to inhibit invasion by 90%, as compared to the DMSO control. At a concentration of 5 mM, BDM reduced parasite invasion by 75%, approximately consistent with previous studies of others that noted a 50% invasion at this concentration [13].

Translocation of AMA1 and TRAP on the sporozoite surface is not affected by cytochalasin D despite this compound inducing total blockage of invasion [50].

Although the compounds that were found to inhibit capping of PfSUB2 also inhibited erythrocyte invasion by the parasite it is unlikely that the lack of PfSUB2 capping is the sole reason for the reduced ability to invade. Cytochalasin D blocks *P. falciparum* RBC invasion but appeared to have no affect on the capping of PfSUB2. This indicates that the actin cytoskeleton plays a further role in invasion than capping PfSUB2 to the posterior of the parasite.

The region of PfSUB2 that may be interacting with the actinomyosin complex is unknown. The C-termini of both TRAP and MIC2 have been shown to be necessary for this interaction [28]. However this region of PfSUB2 is not highly conserved and this study shows that it can clearly be modified without phenotypic affect by the addition of an HA3 tag. This suggests that another region of the molecule is responsible for interaction with the actin-myosin motor, either directly or via another protein.

Discussion

PfSUB2 is a minor parasite component and as a result had proved difficult to localise accurately within the parasite. In this study, the successful tagging of PfSUB2 with a HA3 tag has enabled a detailed study of the localisation of the protein within various stages of the RBC cycle. The presence of the HA3 tag at the PfSUB2 C-terminus does not appear to affect either the processing of the protein or the growth of the parasite. PfSUB2 has been localised to the micronemes of the schizont and upon merozoite release re-localises over the parasite surface where it is capped to the posterior of the merozoite. The capping of PfSUB2, like that of MIC2 on the surface of *T. gondii* tachyzoites, appears to be linked to both the actin cytoskeleton and the myosin motor [15, 40]. Both MIC2 and TRAP, expressed in *Plasmodium* sporozoites, have both been shown to interact via their C-terminus to aldolase and in turn to the actin cytoskeleton [39, 40]. The residues necessary for this interaction are conserved within the TRAP family C-terminus and include a tryptophan residue and a number of acidic residues [28]. These features are absent in the PfSUB2 cytoplasmic tail and as this region is unconserved amongst *Plasmodium* species and can be modified by the addition of a tag it seems unlikely that it is this region of the protein that is responsible for interactions with the actin cytoskeleton.

Unlike MIC2 capping, which takes place explosively at the point of interaction with a host cell, the movement of PfSUB2 to the posterior of the parasite can clearly occur efficiently in the absence of attachment to erythrocytes [10]. This fact could explain the limited shedding of MSP1 and AMA1 from the surface of free merozoites [60, 75].

The invasive half-life of *P. falciparum* merozoites is extremely short and shedding of MSP1 is known to go to completion during the brief (~30 seconds) time course of erythrocyte invasion [6]. The free merozoites studied by IFA in this work are therefore unlikely to still be invasive and the observed capping of PfSUB2 may

not reflect what occurs during invasion. As invading *P. falciparum* merozoites are so difficult to visualise, due in part to both the speed of invasion and the small size of the cell, studies of this stage were not undertaken [7, 9]. On the invading parasite, PfSUB2 capping may occur simultaneously with entry into the parasitophorous vacuole with the protease concentrating at the moving junction and sweeping back around the parasite cleaving the AMA1 and MSP1 as it moves.

In the absence of invasion both AMA1 and MSP1 are shed inefficiently from the parasite surface [60]. However PfSUB2 is considered to be present on the parasite surface and in a position to cleave both proteins. AMA1 and MSP1 are both thought to bind to the RBC and in this way mediate attachment of the merozoite to the RBC surface [64, 65, 68, 69]. It is possible that binding to the host cell surface causes a conformational change in the proteins leading to the cleavage sites becoming sterically available and allowing more efficient cleavage of the proteins from the surface by PfSUB2.

Chapter 4: Purification of PfSUB2 and activity studies

Introduction

AMA1 and MSP1 are both shed from the parasite surface by the action of a serine protease prior to or during *P. falciparum* merozoite entry into the RBC [60, 74, 154]. AMA1 is cleaved 29 residues upstream of the start of the predicted transmembrane sequence at a threonine residue (Thr517) within the sequence RAEVT↓SNNEV [60]. MSP1 is cleaved 96 residues upstream of the GPI anchoring sequence between a leucine (Leu1606) and an asparagine (Asn1607) residue within the sequence QDML↓NISQHQ [76]. Despite the difference in the number of residues above the membrane at which these cleavage sites occur, the structure of the $MSP1_{19}$ fragment means that the cleavage site probably lies in close proximity to the GPI anchor and at a similar distance from the membrane as does the AMA1 cleavage site [6, 77]. Also, despite the lack of sequence similarity flanking the sites of AMA1 and MSP1 cleavage earlier evidence has indicated that the enzyme responsible is the same [60]. As explained in the Introduction sheddases are a group of enzymes that cleave ectodomains of integral membrane proteins and, rather than recognising a particular amino acid sequence, appear only to require an exposed or unhindered sequence of minimum length between the transmembrane domain and cleavage site [79-82]. The enzyme responsible for the shedding of AMA1 and MSP1 is therefore considered to be a sheddase and has been named MESH (merozoite surface sheddase) [60, 95]. The best candidate for MESH, as discussed in the Introduction, is PfSUB2 [95].

The sequence of PfSUB2 indicates that it is a secreted subtilisin-like type I integral membrane protein possessing all the primary structural requirements for protease activity [114, 116]. PfSUB2 is first synthesised as a 160 kDa protein which undergoes processing to form a 74 kDa and finally a 72 kDa protein, presumed to be the active form of the enzyme [114]. This processing is reminiscent of that of PfSUB1 and is typical of subtilisins which are synthesised as inactive zymogens

before autocatalytic cleavage to remove the propeptide and reveal an active protease [99-101]. Subtilisin propeptides are involved in the folding of the protein, which is critical for the formation of an active protease, and can also act as specific potent inhibitors of their respective enzyme [102-108]. As an example of this, the PfSUB1 propeptide has been used as a specific inhibitor of the enzyme [171]. The PfSUB2 propeptide can also be used *in vitro* to specifically inhibit both AMA1 and MSP1 shedding from the parasite surface, further supporting the hypothesis that PfSUB2 is MESH [120].

Attempts at expressing correctly folded and active PfSUB2 in heterologous expression systems have proved unsuccessful [172]. As PfSUB2 is present as a relatively small proportion of the total protein content of the parasite there have been no previous attempts to purify the protein directly from the parasite [114]. However it was considered that the successful HA3 tagging of PfSUB2 in Chapter 3 might enable purification of active PfSUB2 from the parasite, allowing studies of the function of the protein. The aim of the work described in this chapter was to purify active PfSUB2 from the PfSUB2HA line.

4.1 Affinity purification of HA-tagged PfSUB2 from the parasite

The work in this chapter focused on purifying active PfSUB2 from the parasite and these attempts utilised the HA3 tag present at the C-terminus of PfSUB2 in the *P. falciparum* line PfSUB2HA (see Chapter 3). The work in Chapter 3 had also created the control line PfSUB2w in which the PfSUB2 had no tag present and so this line was used as a control in purification experiments.

PfSUB2 had previously been shown to be maximally expressed in the erythrocytic cycle during late schizogony and merozoite release and these results were confirmed with the PfSUB2HA line [19, 114, 116] (Chapter 3). Schizont stage parasites can be purified from culture and this enabled the purification to be carried out only on parasites that would be expressing PfSUB2 [143].

In order to purify PfSUB2 from the parasite a protocol that comprised a number of steps was developed. Firstly a TX-100 lysate of PfSUB2HA or PfSUB2w schizonts was incubated with Protein G Sepharose beads. This was designed as a preclearing step to remove any proteins that bound non-specifically to the beads. The beads were then removed and the anti-HA mAb 12CA5 added. The 12CA5 was expected to bind to the HA3 tag present at the C-terminus of the tagged PfSUB2 in the PfSUB2HA line. The lack of a HA3 tag in the PfSUB2w line meant that the 12CA5 was not expected to bind to any proteins in this lysate. After incubation overnight to ensure antibody binding had gone to completion the lysates were incubated with a second batch of Protein G Sepharose beads to bind the antibody-antigen complex. The beads were then pelleted by centrifugation, the supernatant removed and discarded, and the beads washed several times to remove any unbound proteins. The 12CA5 bound to the PfSUB2 in the PfSUB2HA line was expected to bind to the Protein G Sepharose beads and this would result in PfSUB2 bound to the beads via the antibody. As the PfSUB2w lysate was not predicted to contain any proteins that would bind to the 12ACA5 it was expected that the Protein G Sepharose beads would have only the antibody bound to them. The Protein G Sepharose beads from the PfSUB2HA line purification were named PfSUB2HA beads and those from the purification involving the PfSUB2w line were named PfSUB2w beads.

Western blots were then performed using the anti-HA mAb 3F10 to probe the samples taken during the PfSUB2HA purification in parallel with samples from the control PfSUB2w purification. These are shown in Figure. 4.1. Lanes 1 and 2 contain samples of the initial PfSUB2HA TX-100 lysate. Four bands were detected in these lanes, migrating with apparent masses of 150 kDa, 72 kDa, 55 kDa, and 36 kDa. These bands were identical to those previously detected with the PfSUB2HA line (Chapter 3) and were presumed to correspond to the full-length protein (150 kDa), processed active forms of PfSUB2 (72 kDa) and two breakdown products (55

Figure 4.1 PfSUB2 can be affinity-purified purified from parasites expressing epitope-tagged protease

Western blot of samples taken from various steps in the affinity-purification of HA-tagged PfSUB2, probed with the anti-HA mAb 3F10.

Lanes 1 and 2, TX-100 lysates of PfSUB2HA schizonts;

Lane 3, TX-100 lysate of PfSUB2w schizonts;

Lanes 4 and 5, PfSUB2HA lysates after preclearing;

Lane 6, PfSUB2w lysate after preclearing;

Lanes 7 and 8, PfSUB2HA lysates after addition of the anti-HA mAb 12CA5;

Lane 9, PfSUB2w lysate after the addition of 12CA5;

Lanes 10 and 11, PfSUB2HA lysates after depletion of the mAb 12CA5/PfSUB2HA complexes by incubation with Protein G Sepharose beads;

Lane 12, PfSUB2w lysate after depletion of mAb 12CA5 by incubation with Protein G Sepharose beads;

Lanes 13 and 14, PfSUB2HA beads;

Lane 15 PfSUB2w beads.

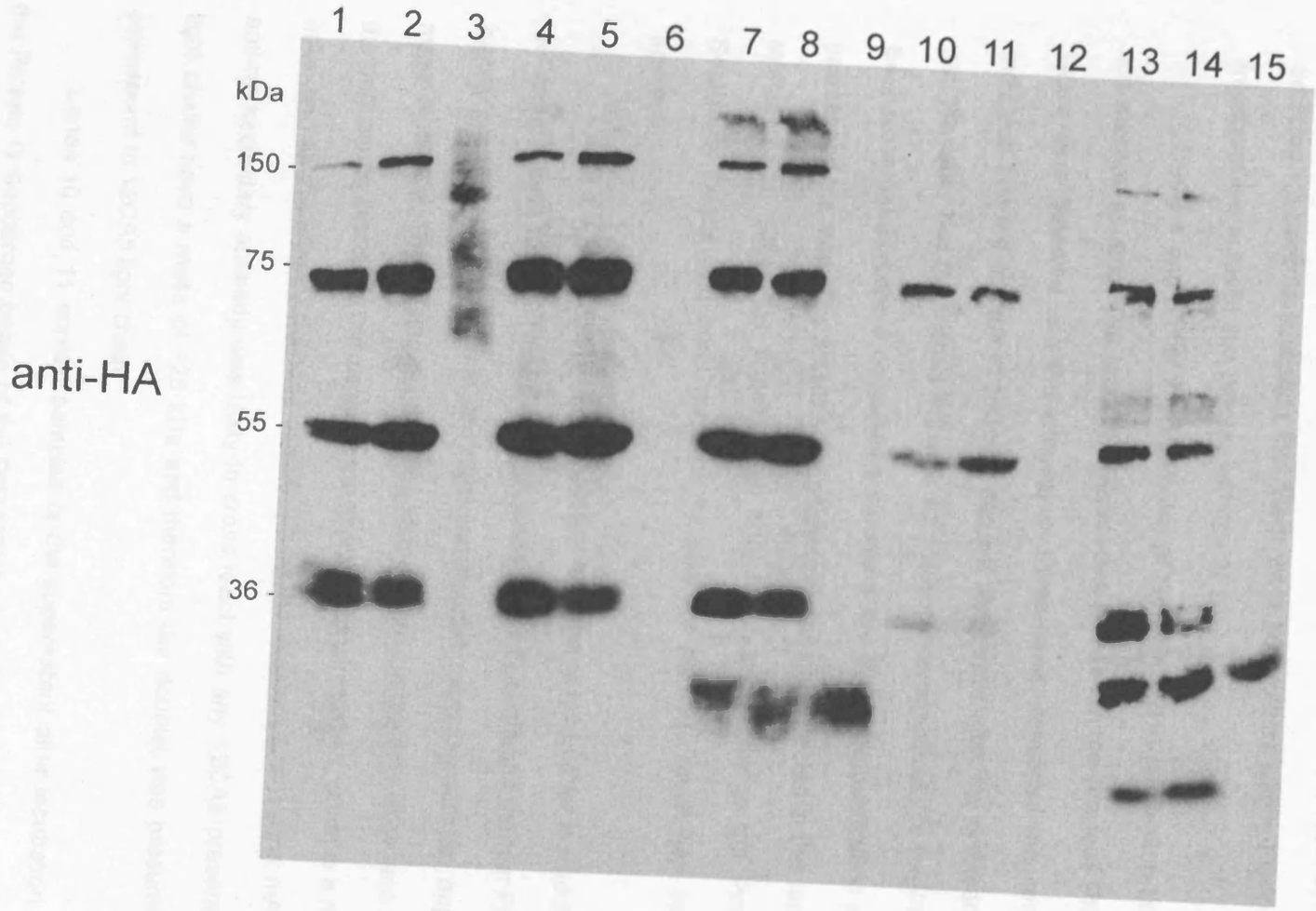
1 2 3 4 5 6 7 8 9 10 11 12 13 14 15
kDa
150
75
55
36
anti-HA

kDa and 36 kDa). Lane 3 contained the PfSUB2w TX-100 lysate and here there was a slight smear detected around 150 kDa to 70 kDa. This is likely to be due to unspecific binding of the antibody or an error made during production of the Western blot. Previous Western blots performed on the PfSUB2w line (Chapter 3) with 3F10 detected no species indicating that there were no proteins within TX-100 soluble fraction of the parasite that reacted with the 3F10.

Lanes 4 and 5 contained samples of the PfSUB2HA purification taken after the preclearing step. The four PfSUB2 species as seen in the previous PfSUB2HA lanes were detected and the intensity of these bands remained the same. This indicated that the amount of PfSUB2 had not decreased after the preclearing step and therefore that the tagged PfSUB2 did not bind non-specifically to the Protein G Sepharose beads. Lane 6 contained a sample of the PfSUB2w purification after the preclearing the step. The smear seen previously was not detected in this lane. This indicated that either the proteins had bound non-specifically to the Protein G Sepharose beads and been removed or that the previous result had been an artefact.

Lanes 7,8 and 9 contained samples of the lysates taken after the addition of the anti-HA mAb 12CA5. The PfSUB2HA lanes (7 and 8) contained the four PfSUB2 bands previously detected and an additional doublet migrating with an apparent mass of 25 kDa. The 25 kDa doublet was also detected in the PfSUB2w lane (9) as the only bands detected. The samples are likely to contain 12CA5, which is a mouse mAb, and as the primary antibody used to probe the Western blot is a rat mAb the anti-rat secondary antibody was likely to cross react with any 12CA5 present. IgG light chains have a mass of ~25 kDa and therefore the doublet was presumed to correspond to 12CA5 light chain.

Lanes 10 and 11 contain samples of the supernatant after incubation with the Protein G Sepharose beads of the PfSUB2HA purification. The intensity of the 74 kDa, 55 kDa and 36 kDa bands previously detected had decreased and the 150

kDa species, presumed to be the full length PfSUB2, and the 25 kDa doublet, presumed to be the 12CA5 light chains, were no longer detected. This indicated that the 12CA5 and a proportion of the PfSUB2 had been removed from the supernatant and was presumably bound to the Protein G Sepharose beads. Lane 12 contained a sample of the supernatant after incubation with the Protein G Sepharose beads of the PfSUB2w purification. There were no bands detected in this lane. The disappearance of the 25 kDa doublet previously detected indicated that the 12CA5 had been bound to the Protein G Sepharose beads.

The final three lanes 13,14 and 15 contained samples of the Protein G Sepharose beads after the wash steps. Lanes 13 and 14 contained samples from the PfSUB2HA purification. These lanes contained the four PfSUB2 species, the 25 kDa doublet and an additional doublet migrating with an apparent mass of 58 kDa. The heavy chains of IgG have a mass of around 50 kDa and it was therefore likely that the 58 kDa doublet represented the heavy chains of the 12CA5. The presence of the 12CA5 bands indicated that the antibody had bound to the Protein G Sepharose and the presence of the PfSUB2 bands indicated that the protein had bound to the Protein G Sepharose via the 12CA5. Taken together, these results indicated that the purification of PfSUB2 from the PfSUB2HA parasite had been successful. The presence of a HA3 tag on the four species of PfSUB2 meant that all had been purified. Unfortunately the 150 kDa protein, presumed to be the full length PfSUB2, is unlikely to be active as it contains the propeptide which is likely to be an inhibitor of the enzyme. Similarly, the 55 kDa and 36 kDa species are also unlikely to be active they are likely too small to contain the catalytic triad needed for protease activity as well as the C-terminal HA3 tag, and are therefore presumed to be breakdown products. The 72 kDa species is presumed to represent the active terminal processing product and is probably the only active form of the enzyme that had been purified. This means that only a proportion of the purified PfSUB2 bound

to PfSUB2HA beads is likely to exhibit activity and that detecting this activity may be challenging.

Lane 15 contained a sample of the PfSUB2w beads from the PfSUB2w purification. The only bands detected in this lane were the 25 kDa doublet. This indicated that the 12CA5 had bound to the beads but that there were no other proteins present. These beads could then be used as a negative control to ensure any activity detected with the PfSUB2HA was specifically due to the PfSUB2 present.

The previous work had resulted in the purification of PfSUB2 onto Protein G Sepharose beads. The next step was to attempt to remove the PfSUB2 from the PfSUB2HA beads. Protein can be removed from the Protein G Sepharose beads by lowering the pH to 3.0-2.5; however, this pH was considered likely to inactivate the protease. Attempts were therefore made to remove the purified PfSUB2 from the Protein G Sepharose beads by competitive elution using a peptide based on the HA3 tag sequence (YPYDVPDYAGGGYPYDVPDYAGGGYPYDVPDYA; synthesised in house by P. Fletcher). It was hoped that this peptide would compete with the PfSUB2 for binding to the 12CA5 and in turn release the protein into the supernatant.

A 1 mg mL^{-1} solution of the peptide was incubated with the PfSUB2HA beads and resulting supernatants analysed by western blots, probing with the anti-HA mAb 3F10 (data not shown). Unfortunately it was impossible to detect whether the PfSUB2 had been released or not as the lanes containing the peptide produced a strong signal consisting of a smear down the length of the blot. This was likely to be due to the 3F10 reacting with the high concentration of the HA3 peptide present in these samples. This made detection of any other bands in this lane impossible and it could not be determined if the PfSUB2 had been released from the beads or not. As a result further attempts to remove the PfSUB2 from the beads using this approach were abandoned.

PfSUB2 is predicted to be a type I integral membrane protein, anchored to the parasite membrane by its C-terminal transmembrane domain. It was therefore considered that the purified protein may remain active attached to the Protein G Sepharose beads via the 12CA5. It was decided that further attempts to detect protease activity mediated by the purified PfSUB2 would be carried out without removal of the protein from the beads. The PfSUB2HA and PfSUB2w beads were aliquoted and stored at -70°C in peptide digestion buffer (50 mM Tris-HCl pH 8.2, 12 mM $CaCl_2$). These were the same storage conditions as used previously for purified recombinant PfSUB1 [112]. PfSUB2 shows the closest homology to the prokaryotic subtilases which are almost all predicted to contain calcium binding sites and therefore PfSUB2 may require calcium to exhibit enzyme activity [98, 114, 116]. This is further indicated by the buffer conditions used for MSP1 shedding assays where supplementation with calcium is required for the enzyme to cleave the protein [75]. PfSUB2 appeared to have been purified from the parasite and appropriate conditions for activity chosen. It could now be determined if the purified PfSUB2 exhibited activity.

4.2 Construction of a fluorogenic peptide

Peptides labelled with a rhodamine group at each end are commonly used as substrates in studies of enzymatic function [153, 173, 174]. The high local concentration of rhodamine on the peptide causes intramolecular dimerisation of the dye and this results in the fluorescence of the rhodamine being quenched [173, 174]. Incubation of the peptide with an appropriate enzyme results in its cleavage and the local high concentration of rhodamine is lost. The dye molecules dissociate and this results in a corresponding rise in fluorescence that can be detected and measured. As an example of the use of such a substrate, the pH and cation dependence, inhibitor profile, and affect of the propeptide on PfSUB1 have all been studied through the use of a rhodamine labelled peptide [112, 153, 171].

As previously mentioned, cleavage of MSP1 occurs between the leucine and asparagine residues within the sequence QDML↓NISQHQ [76]. It was therefore hypothesised that a rhodamine labelled peptide based on the MSP1 secondary cleavage site might therefore be used as a potential substrate for detecting purified PfSUB2 activity.

To prepare this substrate the peptide Ac-CQDMLNISQHQC, based on the MSP1 secondary cleavage site, was first synthesised in house by P. Fletcher. The method of Blackman *et al.* was used to attach rhodamine groups to the two cysteine residues on the peptide forming the peptide $MSP1_{rho}$ [153]. The final product was analysed by RP-HPLC and resolved under the conditions used into two separate peaks indicating the presence of two separate species (Figure 4.2). However when these peaks were collected and analysed by mass spectroscopy (performed by P. Fletcher) they exhibited identical *m/z* values, suggesting that they were chemically identical and both corresponded to the same product, namely the peptide labelled with a tetramethylrhodamine group at each cysteine side-chain (Figure 4.3). In the following work both species were used to assess the activity of PfSUB2.

4.3 Evaluation of the experimental PfSUB2 fluorogenic substrate

The fluorogenic peptide $MSP1_{rho}$ had been constructed but it remained to be seen if it could be cleaved and a rise in fluorescence detected. The absorption spectrum of dimeric tetramethylrhodamine has its peak at 520 nm with a shoulder at 554 nm. When the dye dissociates to form monomers there is a shift in the absorption profile with the peak now at 554 nm with the shoulder at 520 nm [153, 173, 174]. When overlaid the two spectra cross at the isosbestic point, 528 nm [175]. This phenomenon can be exploited to determine whether cleavage of the modified peptide results in monomerisation of the dye.

Pronase, a non-specific protease, was first used to determine the effects of cleavage of $MSP1_{rho}$. The visible absorption spectrum of $MSP1_{rho}$ was measured

Figure 4.2 RP-HPLC analysis of $MSP1_{rho}$ produces two peaks

Reversed phase HPLC fractionation of crude $MSP1_{rho}$ preparations. The two peaks corresponding to the tetramethylrhodamine-labelled peptide are indicated with asterisks (*).

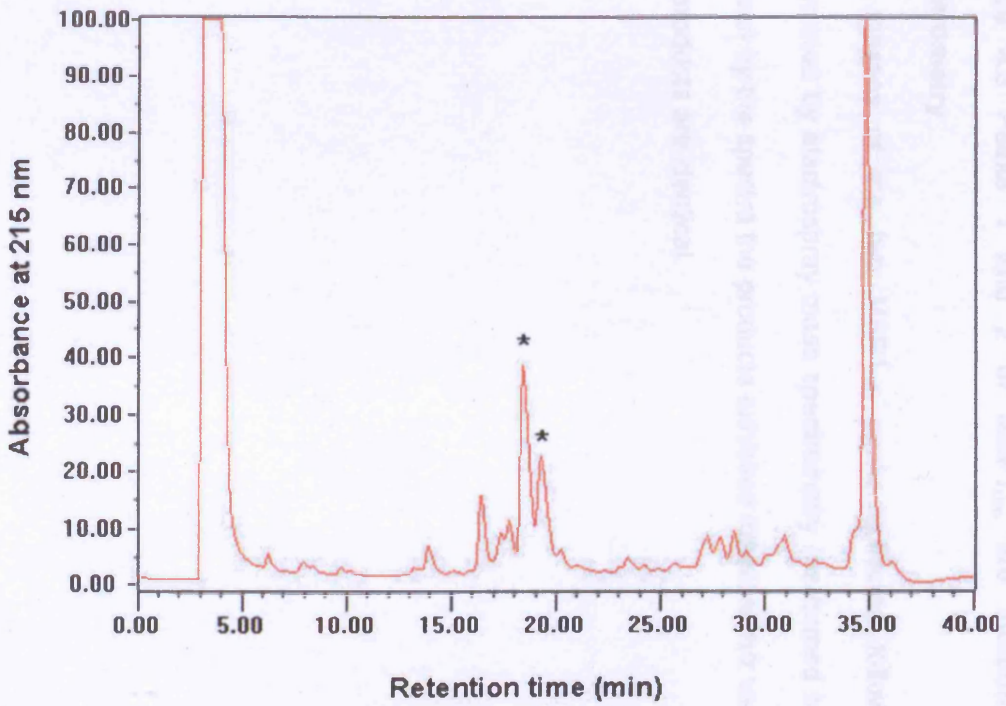
Absorbance at 215 nm
100.00
90.00
80.00
70.00
60.00
50.00
40.00
30.00
20.00
10.00
0.00
0.00
5.00
10.00
15.00
20.00
25.00
30.00
35.00
40.00
Retention time (min)

Figure 4.3 Peaks 1 and 2 of $MSP1_{rho}$ are indistinguishable by mass spectrometry

The masses of the two $MSP1_{rho}$ peaks collected following RP-HPLC, were determined by electrospray mass spectrometry (performed by P. Fletcher). As can be seen by the spectra the products exhibited identical *m/z* values indicating that the two products are identical.

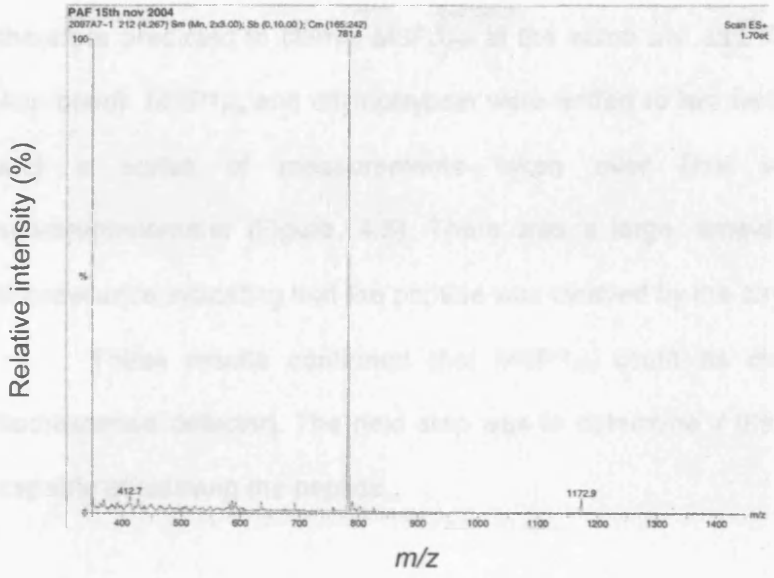
PAF 15th nov 2004
781.8
412.7
1172.9
Relative intensity (%)
m/z
1

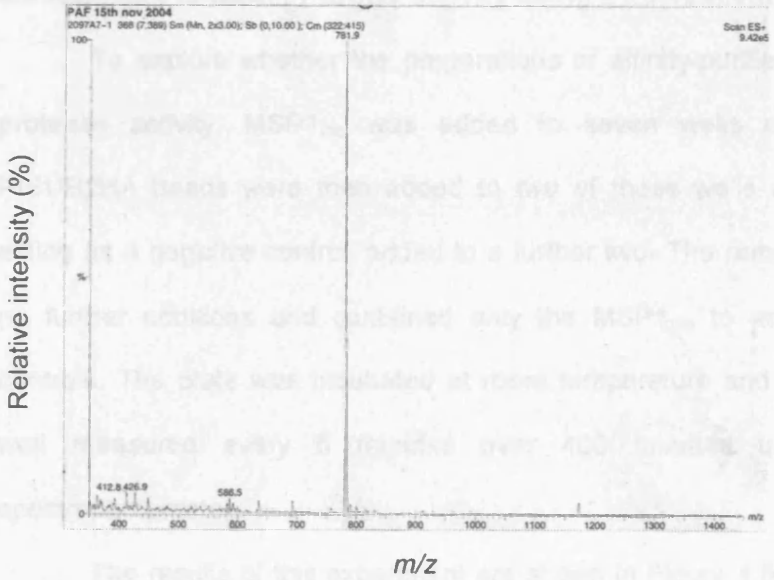
PAF 15th nov 2004
781.9
412.8,426.9
586.5
Relative intensity (%)
m/z
2

using a spectrophotometer before and after the addition of Pronase (Figure 4.4). There was a clearly visible shift in the spectrum, with the peak moving from 520 nm to 554 nm, after the Pronase addition indicating that the peptide had been cleaved.

The next step was to determine if cleavage of the peptide resulted in a detectable rise in fluorescence. Chymotrypsin is a serine protease that cleaves substrates on the C-terminal side of aromatic and leucine residues and was therefore predicted to cleave $MSP1_{rho}$ at the same site as PfSUB2 (i.e. at the Leu-Asn bond). $MSP1_{rho}$ and chymotrypsin were added to two wells of a microtitre plate and a series of measurements taken over time with a fluorescence spectrophotometer (Figure. 4.5). There was a large, time-dependent increase in fluorescence indicating that the peptide was cleaved by the chymotrypsin.

These results confirmed that $MSP1_{rho}$ could be cleaved and a rise in fluorescence detected. The next step was to determine if the purified PfSUB2 was capable of cleaving the peptide.

4.4 Attempts to detect PfSUB2 activity using a fluorescent peptide

To explore whether the preparations of affinity-purified PfSUB2 possessed protease activity, $MSP1_{rho}$ was added to seven wells of a microtitre plate, PfSUB2HA beads were then added to two of these wells and PfSUB2w beads, acting as a negative control, added to a further two. The remaining three wells had no further additions and contained only the $MSP1_{rho}$ to act as further negative controls. The plate was incubated at room temperature and fluorescence of each well measured every 5 minutes over 400 minutes using a fluorescence spectrophotometer.

The results of this experiment are shown in Figure 4.6. Wells that contained $MSP1_{rho}$ alone showed no rise in fluorescence indicating that the peptide was stable during this period of time at room temperature. In contrast, the wells that additionally

Figure 4.4 Cleavage of $MSP1_{rho}$ causes a shift in absorption spectrum

Absorption spectra of $MSP1_{rho}$ (A) before and (B) after addition of Pronase. The absorption spectrum peak of $MSP1_{rho}$ before addition of 1 mg mL^{-1} Pronase is 520 nm indicating that the rhodamine has formed dimers. Upon addition of Pronase the peak shifts to 554 nm indicating that the peptide has been cleaved and that the dye has formed monomers.

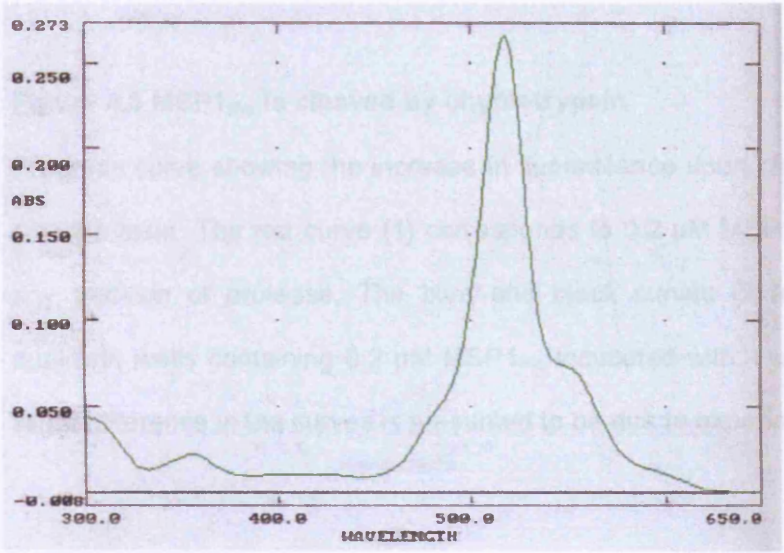
0.273
0.250
0.200
ABS
0.150
0.100
0.050
-0.000
300.0
400.0
500.0
650.0
WAVELENGTH

A

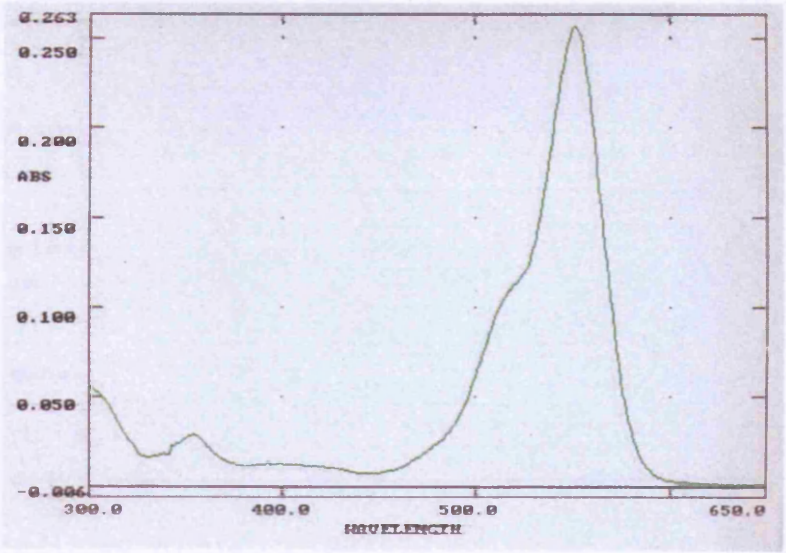
0.263
0.250
0.200
ABS
0.150
0.100
0.050
-0.006
300.0
400.0
500.0
650.0
WAVELENGTH

B

Figure 4.5 $MSP1_{rho}$ is cleaved by chymotrypsin

Progress curve showing the increase in fluorescence upon cleavage of $MSP1_{rho}$ by chymotrypsin. The red curve (1) corresponds to 0.2 μM $MSP1_{rho}$ incubated without any addition of protease. The blue and black curves (2 and 3) correspond to duplicate wells containing 0.2 μM $MSP1_{rho}$ incubated with 1 μM chymotrypsin. The slight difference in the curves is presumed to be due to experimental error.

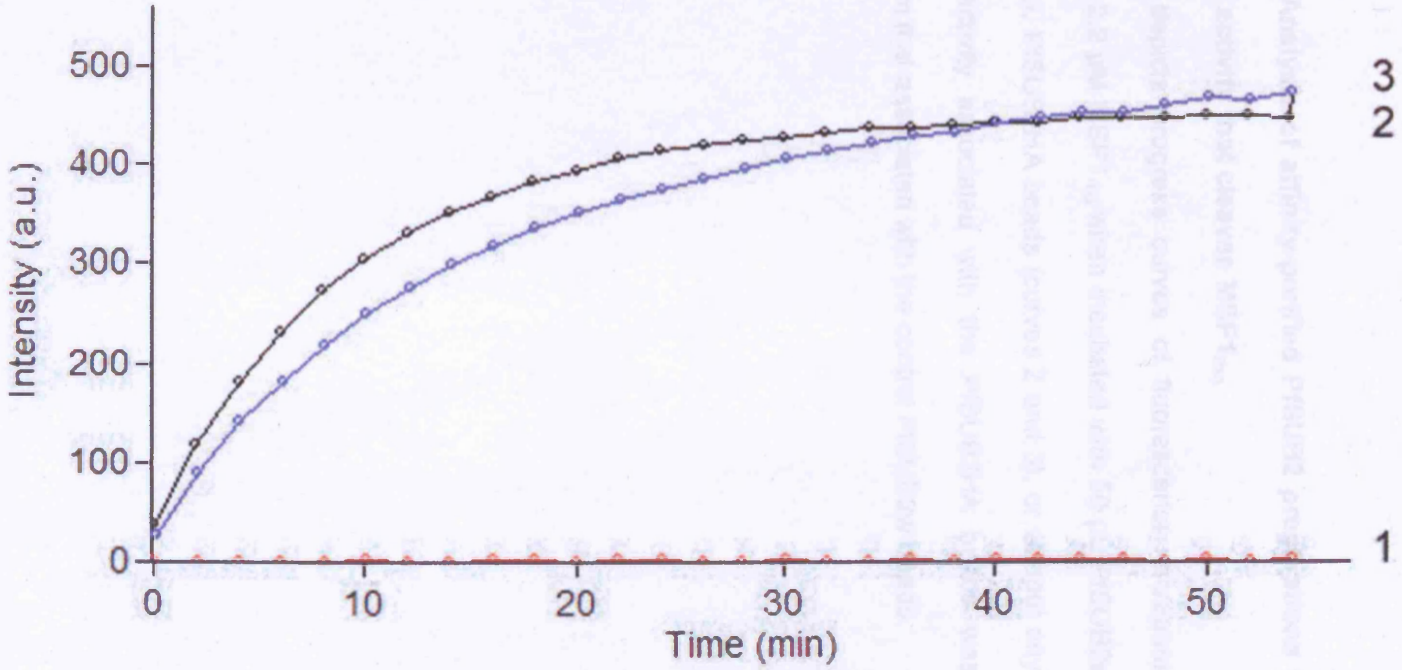
Intensity (a.u.)
500
400
300
200
100
0
0
10
20
30
40
50
Time (min)
3
2
1

Figure 4.6 Analysis of affinity-purified PfSUB2 preparations for the presence of protease activity that cleaves $MSP1_{rho}$

The graph depicts progress curves of fluorescence increases associated with cleavage of 0.2 µM $MSP1_{rho}$ when incubated with 50 µL PfSUB2w beads (curves 1 and 4), 50 µL PfSUB2HA beads (curves 2 and 3), or without any additions (curves 5-7). The activity associated with the PfSUB2HA beads was not significantly different from that associated with the control PfSUB2w beads.

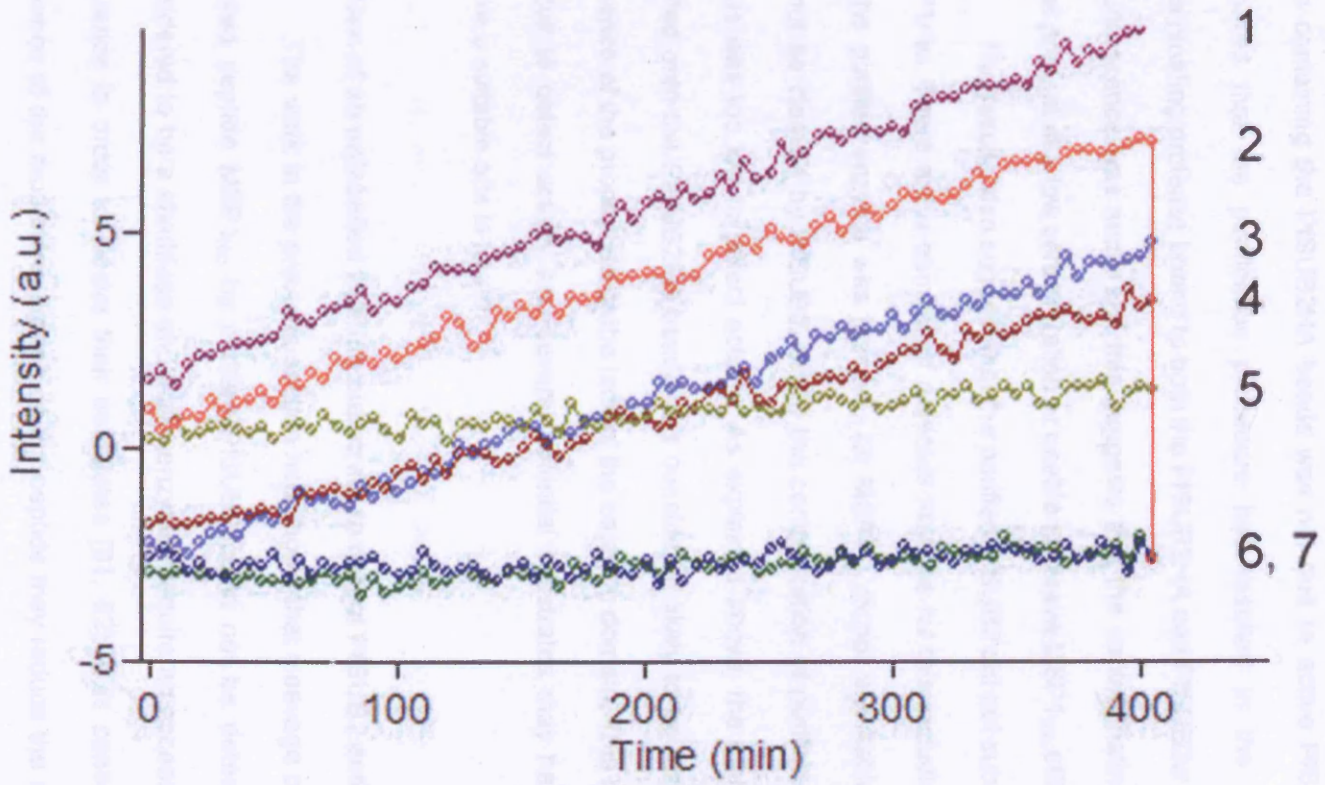
Intensity (a.u.)
5
0
-5
0
100
200
300
400
Time (min)
1
2
3
4
5
6, 7

contained PfSUB2HA beads showed a small increase in fluorescence. This indicated that the peptide was being cleaved and that there was an active protease present. Unfortunately the wells that contained the PfSUB2w beads alongside $MSP1_{rho}$ displayed a similar rise in fluorescence.

These results suggested that the cleavage of the peptide detected in the wells containing the PfSUB2HA beads was not due to active PfSUB2. Instead it appeared that the purification procedure had resulted in the presence of a contaminating protease bound to both the PfSUB2HA and PfSUB2w beads. The rise in fluorescence was small and this suggests that the contaminating protease was either present at a low concentration or unable to cleave $MSP1_{rho}$ efficiently.

The results also suggest that the purified PfSUB2 did not substantially cleave MSP1rho. There are a number of potential reasons for this including the following (1) the purified enzyme was inactive, (2) $MSP1_{rho}$ is not a suitable substrate and cannot be cleaved by PfSUB2, or (3) the concentration of purified PfSUB2 on the beads was too low to detect activity. As explained above, the majority of PfSUB2 purified onto the PfSUB2HA beads was considered likely to be inactive due to the presence of the propeptide or the lack of the catalytic domain. This means it may be difficult to detect activity and several potential substrates may have to be tested before a suitable one is found.

4.5 Use of an unlabelled peptide substrate to detect PfSUB2 activity

The work in the previous section had shown that cleavage of the rhodamine labelled peptide $MSP1_{rho}$ by purified PfSUB2 could not be detected. PfSUB2 is considered to be a sheddase and these enzymes require an accessible, disordered sequence in order to cleave their substrates [81, 82]. It is conceivable that the presence of the rhodamine groups on the peptide may reduce the steric availability of the cleavage site and prevent cleavage by PfSUB2. In order to test this possibility a second peptide based on the MSP1 secondary cleavage site with the sequence

LQGMLNISQH ($MSP1_{Clip}$), was synthesised by P. Fletcher. This time the peptide was not labelled with dye groups. It was hypothesised that if $MSP1_{Clip}$ was cleaved by the purified PfSUB2 it would indicate that the failure to cleave $MSP1_{rho}$ was due to steric hindrance from the rhodamine groups present.

In order to determine if the purified PfSUB2 was capable of cleaving $MSP1_{Clip}$ the PfSUB2HA or PfSUB2w beads were incubated with the peptide at 37°C. Samples of the peptide were taken immediately and after a further 2.5 hours of incubation then subjected to RP-HPLC analysis (Figure 4.7). The $MSP1_{Clip}$ samples taken immediately and incubated with either the PfSUB2HA or PfSUB2w beads were identical and contained predominantly the intact peptide. The RP-HPLC elution profile of samples taken after 2.5 hours incubation with PfSUB2w beads appeared very similar indicating that there had been no significant cleavage of the peptide. Similar results were obtained with samples that had been incubated with the PfSUB2HA beads, indicating that the peptide had not been cleaved by the purified PfSUB2.

In conclusion there was no detection of cleavage of $MSP1_{Clip}$ by the purified PfSUB2. However it could not be determined if the purified PfSUB2 was inactive or if the $MSP1_{Clip}$ was an unsuitable substrate.

4.6 Use of the recombinant PfSUB2 ectodomain to detect PfSUB2 activity

In previous work performed by others, the PfSUB2 ectodomain had been expressed in *Pichia pastoris*, a yeast expression system, where it was shown to be unfolded and inactive [172]. Subtilisins undergo autocatalytic cleavage to remove the propeptide and reveal an active protease [98-101]. PfSUB1 can be expressed in a recombinant active form and this is capable of cleaving inactive PfSUB1 produced by *in vitro* translation [101]. This suggests that if the purified PfSUB2 was active it would be capable of cleaving the inactive recombinant PfSUB2. The recombinant ectodomain was incubated at 37°C with PfSUB2HA or PfSUB2w beads and

Figure 4.7 $MSP1_{Clip}$ is not cleaved by affinity-purified PfSUB2

RP-HPLC analysis of ~ 0.4 mg mL^{-1} $MSP1_{Clip}$ before (A) and after (C) incubation with PfSUB2w beads, and before (B) and after (D) incubation with PfSUB2HA beads. The peak representing intact $MSP1_{Clip}$ is indicated by an asterisk. The slight movement in the position of the $MSP1_{Clip}$ peak is considered due to slight between-run variations in the elution conditions.

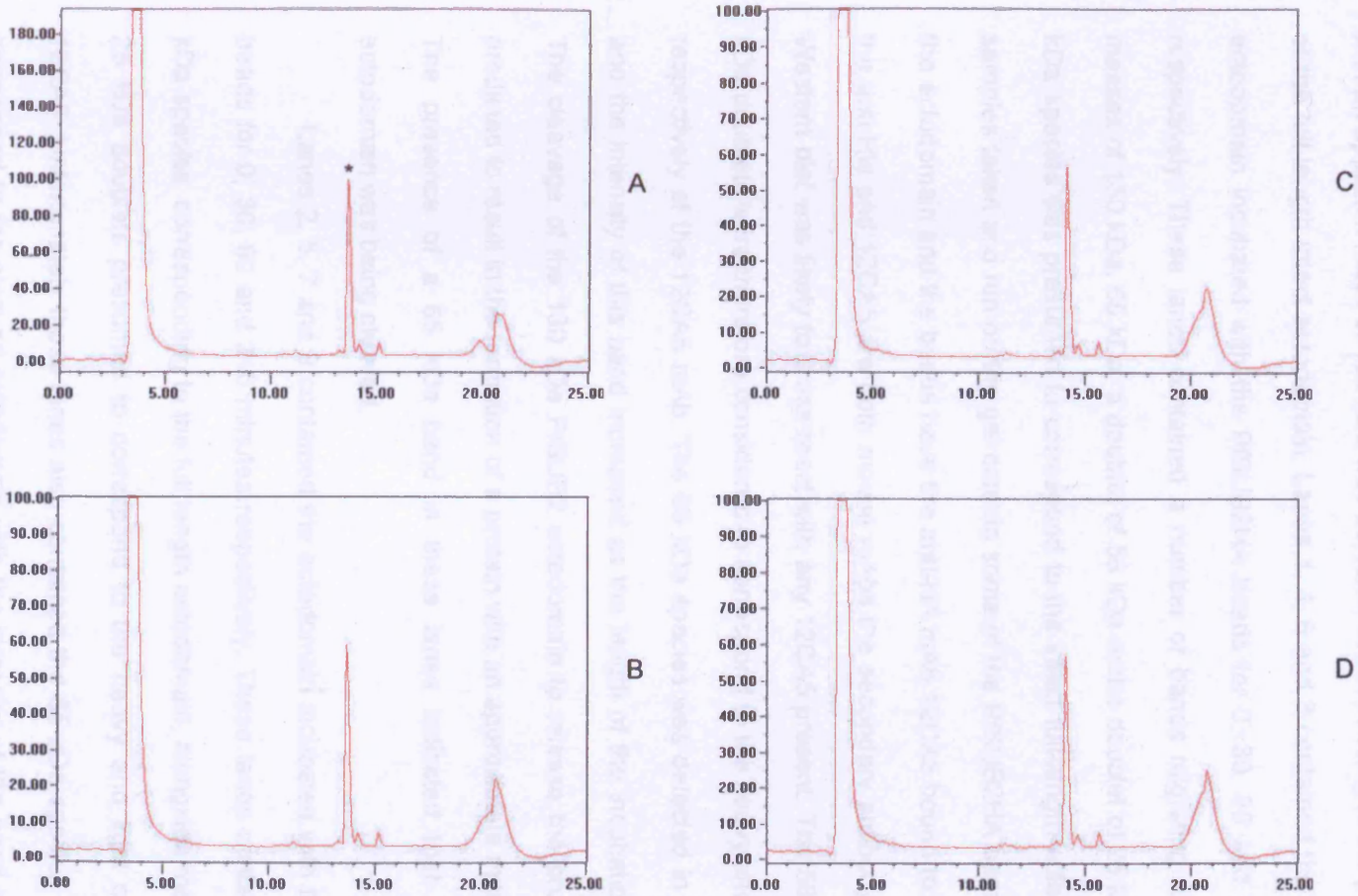
A
B
C
D
0.00
5.00
10.00
15.00
20.00
25.00

samples taken immediately and after 30, 90, and finally 310 minutes incubation. The samples were run on a gel alongside a sample of the ectodomain alone and a Western blot performed using an anti- His_6 mAb to probe the blot (Figure. 4.8). Lane 3 contained the *P. pastoris* derived ectodomain alone and a single species migrating with an apparent mass of 130 kDa was detected corresponding to the predicted size of the full-length intact ectodomain. Lanes 1, 4, 6 and 8 contained the recombinant ectodomain incubated with the PfSUB2HA beads for 0, 30, 90 and 310 minutes respectively. These lanes contained a number of bands migrating with apparent masses of 130 kDa, 65 kDa, a doublet of 56 kDa and a doublet of 25 kDa. The 130 kDa species was presumed to correspond to the intact full-length ectodomain. The samples taken and run on the gel contain some of the PfSUB2HA beads as well as the ectodomain and the beads have the anti-HA mAb 12CA5 bound to them and as the anti-His and 12CA5 are both mouse mAbs the secondary antibody used in the Western blot was likely to cross react with any 12CA5 present. The 56 kDa and 25 kDa doublets were therefore considered to correspond to the heavy and light chains respectively of the 12CA5 mAb. The 65 kDa species was detected in all the lanes and the intensity of this band increased as the length of the incubation increased. The cleavage of the 130 kDa PfSUB2 ectodomain to release the propeptide was predicted to result in the formation of a protein with an approximate mass of 65 kDa. The presence of a 65 kDa band in these lanes indicated that the PfSUB2 ectodomain was being cleaved.

Lanes 2, 5, 7 and 9 contained the ectodomain incubated with the PfSUB2w beads for 0, 30, 90 and 310 minutes respectively. These lanes contained the 130 kDa species, corresponding to the full length ectodomain, alongside the 56 kDa and 25 kDa doublets presumed to correspond to the heavy and light chains of the 12CA5. Unfortunately these lanes also contained the 65 kDa species presumed to correspond to the cleaved ectodomain with the intensity of the band increasing as the length of incubation increased.

Figure 4.8 PfSUB2HA beads do not specifically cleave *P. pastoris* derived PfSUB2 ectodomain

Western blot analysis of *P. pastoris*-derived recombinant PfSUB2 ectodomain with a C-terminus His_6 tag following incubation with either PfSUB2HA or PfSUB2w beads. The blot was and probed with an anti-His6 mAb.

Lanes 2, 5, 7, and 9: recombinant ectodomain incubated at 37°C with PfSUB2w beads for 0, 30, 90 and 310 minutes respectively.

Lanes 1, 4, 6, and 8: recombinant ectodomain incubated at 37°C with PfSUB2HA beads for 0, 30, 90 and 310 minutes respectively.

Lane 3 contains recombinant ectodomain alone.

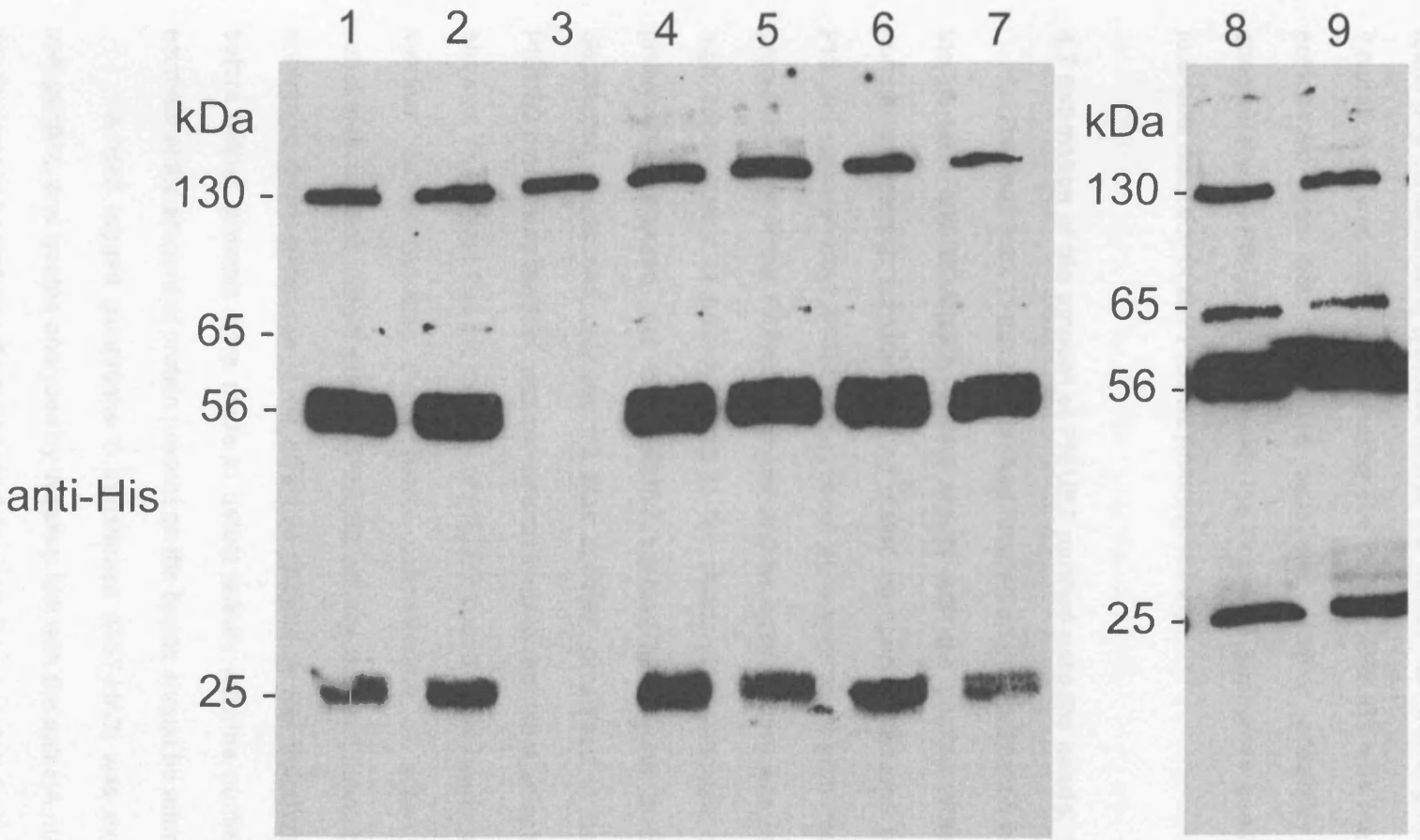
1
2
3
4
5
6
7
8
9
kDa
130
65
56
25
kDa
130
65
56
25
anti-His

The conclusion drawn from this was that no specific PfSUB2 activity could be detected using the recombinant PfSUB2 ectodomain as a substrate. The low-level cleavage that was detected of the recombinant PfSUB2 ectodomain was clearly the result of a contaminating protease or that the ectodomain was degrading during the incubation. It was not known whether the purified PfSUB2 was inactive or if the ectodomain was not a suitable substrate. Another possibility is that the concentration of PfSUB2 purified onto the Protein G Sepharose beads was too low to enable detection of any PfSUB2 protease activity.

4.7 Estimation of the amount of PfSUB2 purified onto the beads.

Previous work in this chapter had focused on the purification of PfSUB2 from the parasite and attempts to detect activity with the purified protein. Despite a number of potential substrates being tested no specific cleavage by the purified PfSUB2 was detected. PfSUB2 is present as a very small proportion of the total protein content of the *P. falciparum* cell and as a result there was unlikely to be a high concentration of protein bound to the beads [114]. Analysis of the purified protein had revealed that four PfSUB2 species had bound to the Protein G Sepharose beads and only the 72 kDa species, presumed to be the terminal PfSUB2 processing product, was considered likely to represent an active form of the enzyme. This meant that the majority of PfSUB2 bound to the beads was likely to be inactive, further reducing the potential concentration of active protein. The substrates used to detect purified PfSUB2 activity may not have been sensitive enough to detect these low levels of active enzyme. It was therefore decided that before further attempts were made to detect activity with the purified PfSUB2 an estimate of the amount of protein present on the beads should be attempted.

A HA3 tagged glutathione S transferase (GST-HA3) was expressed in *E. coli*, purified, and lysates analysed by Western blot with the anti-HA mAb 3F10 (data not shown). In partially purified extracts three species were detected, migrating with

apparent masses of 36 kDa, 33 kDa, and 25 kDa. GST-HA3 is predicted to have a mass of approximately 36 kDa and therefore the largest fragment was presumed to correspond to the full-length protein. The 33 kDa and 25 kDa bands were presumed to correspond to breakdown products.

The next step was to purify the full length GST-HA3 away from the breakdown products. However purification attempts by both gel filtration and HPLC were unsuccessful and were abandoned (data not shown).

The concentration of the purified GST-HA3 was then estimated. A gel was loaded with lanes containing known concentrations of BSA alongside dilutions of the partially purified GST-HA3. The gel was then run and stained with Coomassie blue (Figure 4.9). The intensity of the various BSA bands was used to estimate the concentration of the full length GST-HA3 in the preparation. The 36 kDa band in lane 1 and the band in lane 7 were stained by Coomassie with an equal intensity indicating that these lanes contained the same amount of protein. The 36 kDa band in lane 1 corresponds to the full-length GST-HA3 and lane 7 contains 0.16 mg mL^{-1} BSA. On this basis it was therefore estimated that the GST-HA3 lane contained 0.16 mg mL^{-1} of protein and as 5 µL of GST-HA3 had been loaded the total amount of protein present was calculated as 0.8 µg.

A Western blot was then performed on dilutions of the same GST-HA3 preparation, alongside dilutions of the PfSUB2HA beads and probed with the anti-HA mAb 3F10 (Figure 4.10). The 72 kDa band, presumed to correspond to the active form of PfSUB2, in the initial lane (lane 1) produced a signal with an approximately similar intensity to the lane containing 128 pg of GST-HA3. The amount of 'active' PfSUB2 present in lane 1 was therefore estimated as 128 pg. 10 µL of PfSUB2HA beads had been loaded into this lane and therefore the concentration of active protease bound to the beads was calculated as approximately 12.8 pg μL^{-1}. Although this Figure is likely to be somewhat different from the actual concentration it was considered accurate enough to use as an

Figure 4.9 Quantification of purified recombinant GST-HA3 by comparison with known amounts of pure BSA

Coomassie stained gel of various dilutions of preparations of recombinant GST-HA3 and BSA.

Lane 1, 5 µL purified GST-HA3;

Lane 2, 2.5 µL GST-HA3;

Lane 3, 1.25 µL GST-HA3;

Lane 4, 0.625 µL GST-HA3;

Lane 5, 0.64 mg mL^{-1} BSA;

Lane 6, 0.32 mg mL^{-1} BSA;

Lane 7, 0.16 mg mL^{-1} BSA,

Lane 8, 0.08 mg mL^{-1} BSA;

Lane 9, 0.04 mg mL^{-1} BSA

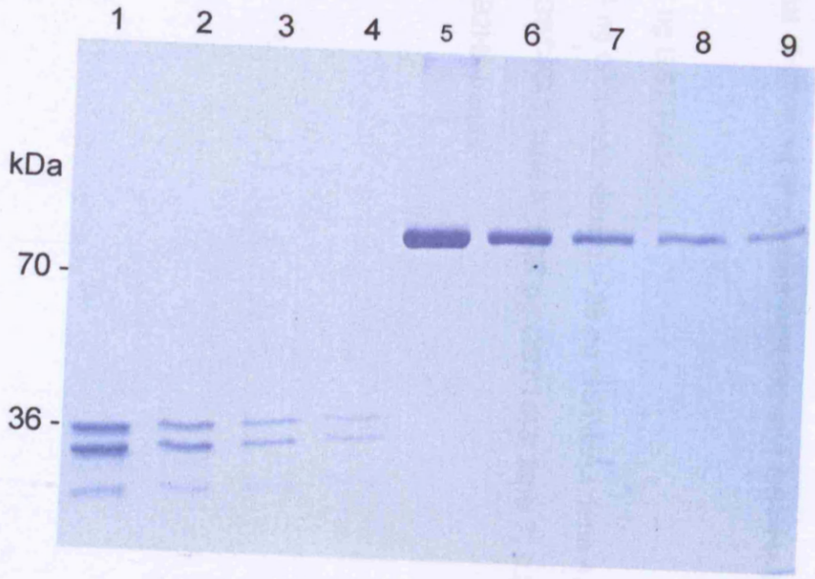
1
2
3
4
5
6
7
8
9
kDa
70 -
36 -

Figure 4.10 The concentration of PfSUB2 can be estimated by comparison with GST-HA3

Western blot of dilutions of purified PfSUB2 and GST-HA3 probed with the anti-HA mAb 3F10.

Lane 1, 3.2 ng GST-HA3;

lane 2, 0.64 ng GST-HA3; lane 3, 128 pg GST-HA3; lane 4, 25.6 pg GST-HA3; lane 5, 5.12 pg GST-HA3; lane 6, 1.02 pg GST-HA3; lane 7, 0.20 pg GST-HA3; lane 8, 10 µL PfSUB2HA beads

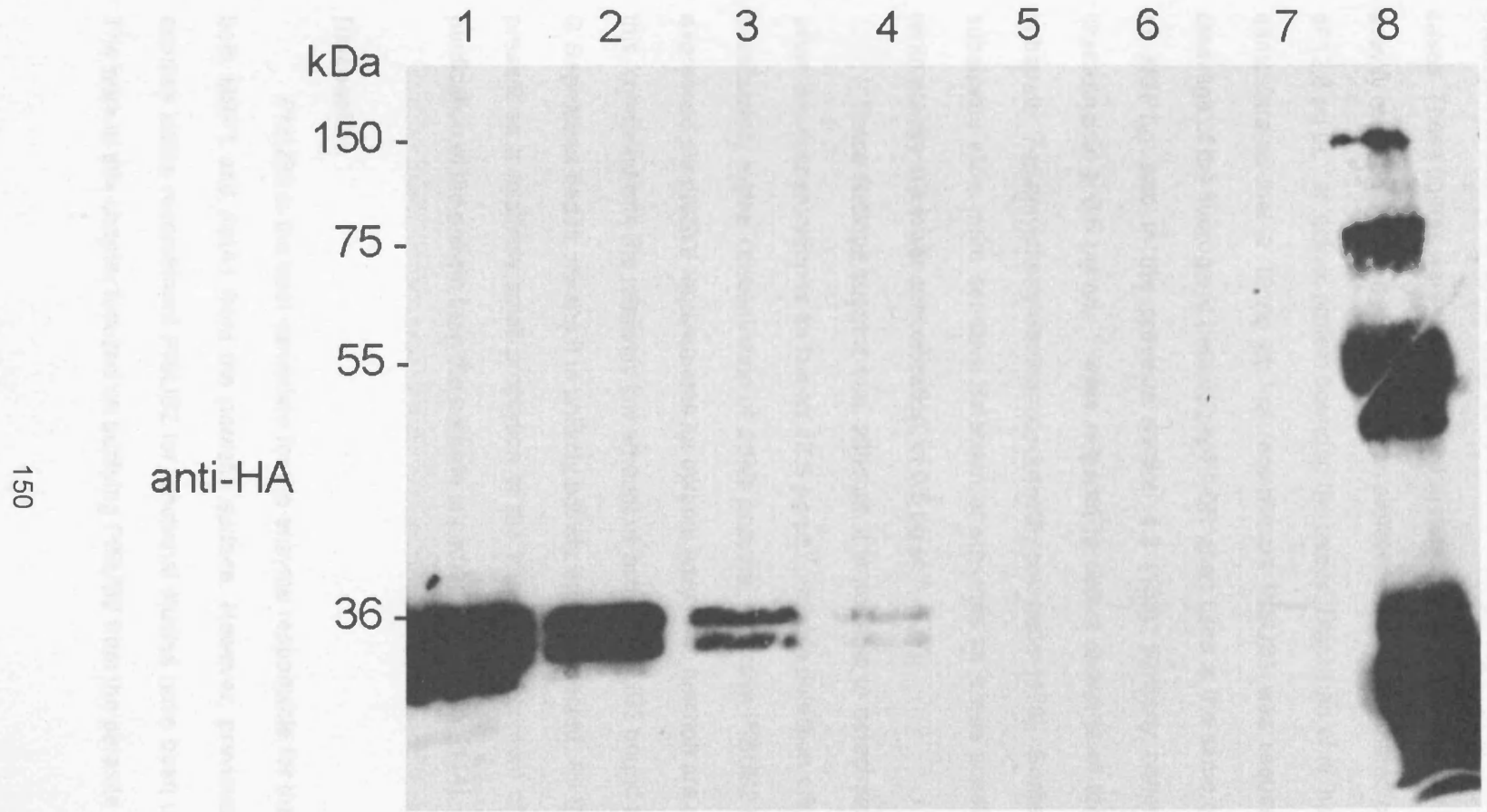
1
2
3
4
5
6
7
8
kDa
150 -
75 -
55 -
anti-HA
36 -

estimation of the amount of 'active' PfSUB2 bound to the Protein G Sepharose beads.

Fluorogenic substrates are widely used to detect protease activity and the minimum amount of enzyme needed to detect activity has been calculated in many cases. These figures were therefore used to determine if it was feasible that PfSUB2 activity could be detected with the purified protein, given the estimated concentration of 12.8 pg μL^{-1} of 'active' protein bound to the beads. Blackman *et al.* had previously demonstrated that ≥ 10 ng μL^{-1} of recombinant PfSUB1 was required to detect cleavage of the fluorogenic peptide pepF1-6R when used at the same concentration as $MSP1_{rho}$ was in the previous section 4.3 [153]. Similarly concentrations of chymotrypsin ≥ 0.5 μg mL^{-1} were required to detect cleavage of the fluorogenic substrate 7-glutarylphenylalaninamido-4-methylcoumarin [176]. Some fluorogenic substrates allow more sensitive detection of enzymes as it was possible to detect renin activity at a lower concentration, of 0.5 pg μL^{-1}, [177].

These findings suggest that, although it is possible to detect some enzymes when the concentration is as low as 12.8 pg μL^{-1}, reliable detection often requires a substantially higher concentration of active enzyme. As active PfSUB2 has yet to be expressed the precise requirements for optimal enzymatic function are unknown and this, combined with the relatively low amount of 'active' PfSUB2 bound to the Protein G Sepharose beads, means it is unlikely activity will be detected. As the PfSUB2 is present as a relatively small proportion of the total protein content of the parasite purification of the protein from the parasite is perhaps unrealistic [114].

Discussion

PfSUB2 is the best candidate for the enzyme responsible for the cleavage of both MSP1 and AMA1 from the parasite surface. However, previous attempts to express active recombinant PfSUB2 for functional studies have been unsuccessful. The work in this chapter focused on purifying PfSUB2 from the parasite by exploiting

the C-terminal tag present in the PfSUB2HA line generated in Chapter 3. It initially appeared that the tag had allowed successful purification of the enzyme from the parasite. However, despite the use of a number of substrates it was not possible to detect PfSUB2 activity and a contaminating protease appeared present.

Although there were a number of potential reasons for the inability to detect activity with the purified PfSUB2 it seemed most likely that the concentration of PfSUB2 bound to the beads was too low. The amount of the 72 kDa form of PfSUB2, predicted to be the active form of the enzyme, purified onto the beads was estimated to be 12.8 pg μL^{-1}. Comparisons with other proteases indicated that with this concentration of enzyme it was unlikely that activity could be detected. Given the relatively small amount of PfSUB2 present in the *P. falciparum* cell it seems unlikely that purification of the protein from the parasite will ever obtain the amounts of protein that may be required to detect activity. Further attempts to obtain active enzyme should focus on over-expression of PfSUB2 within the parasite (see Chapter 5) or preferably the use of unconventional expression systems such as *T. gondii* or *Tetrahymena thermophila* [178]. The A+T rich genome and corresponding codon usage of *T. thermophilia* means it is a good expression system for *P. falciparum* proteins [178].

Chapter 5: Episomal expression of PfSUB2 within *P. falciparum*

Introduction

The expression of *P. falciparum* proteins in heterologous expression systems for structure-function analysis is problematic often as a result of the high A+T content of the parasite genome [136, 178, 179]. A number of approaches have been used to overcome these difficulties including the use of *Tetrahymena thermophila,* another A+T rich protozoan, as an expression system or the re-codonisation of *P. falciparum* genes to reduce the A+T content [136, 178, 180]. Another potential solution to this problem is the use of *P. falciparum* itself to over-express parasite proteins that cannot be expressed in more conventional expression systems. Advances in *P. falciparum* transfection technology have enabled expression of both endogenous and heterogenous proteins from episomes carried by the parasite [121, 124, 132]. Proteins expressed this way fold correctly, undergo normal processing events and, in the case of enzyme expression, exhibit typical activity [124, 130, 132]. At present the factors controlling levels of endogenous protein that can be expressed within the parasite are unknown; for example expression of PfAMA1 from an episome did not result in increased protein levels over untransfected controls, and the majority of protein detected was found to be encoded by the episome suggesting that an episome-derived gene product has dominance over endogenous protein [132]. In *T. gondii* expression of myosin from an episome also resulted in down regulation of the endogenous protein [133]. The choice of promoter for driving protein expression from an episome within the parasite is likely to be critical for correct targeting and localisation although it does not appear to affect correct folding or processing [151, 181].

The study of *P. falciparum* promoter regions has proved challenging. The A+T richness of intergenic regions, combined with their often highly repetitive nature with long homopolymeric adenosine or thymidine (poly(dA)poly(dT)) tracts, has made the identification of regulatory elements difficult; for example the region

upstream of genes often contains many copies of a classical TATA box motif although it is unlikely most are functional [182-186]. In studies investigating promoter structure in *Plasmodium* truncations of the region 5' to a gene usually results in a gradual reduction in promoter activity with no particular motif identifiable as essential for promoter activity [124, 183, 184].

Numerous attempts to express PfSUB2 in an enzymatically active, recombinant form in heterologous expression systems have been unsuccessful despite re-codonisation of the *pfsub2* gene to reduce the A+T content [120, 172]. This chapter focuses on attempts made to overcome this obstacle by over-expression of the protease within the parasite, where correct folding and processing of the protease are expected to proceed efficiently. The *pfsub2* promoter has not previously been studied although the relatively low levels of PfSUB2 found within the parasite suggest it is weak [114]. The aim of the study was to express active PfSUB2 that could then be purified from the parasite and used in enzymatic assays. A stronger promoter could therefore be used to attempt to express higher levels of PfSUB2 than if the wild-type promoter was used as - provided folding and processing of the protein is correct – it is possible that mis-localisation may still result in active protease. The factors controlling the levels of PfSUB2 are unknown and as a result it was considered that it might prove impossible to achieve levels higher than those of wild-type parasites. However, it was also hypothesised that the PfSUB2 expressed from the episome might show dominance over the endogenous PfSUB2. Note that this work was performed before the epitope tagging of PfSUB2 described in Chapter 3.

5.1 Expression of PfSUB2 under the control of the *hsp86* promoter

Four constructs were initially designed to over-express PfSUB2 within *P. falciparum*; these were named pHHT-sub2, pHHT-sub2HA, pHHT-sub2w and pHHT-sub2wHA. Constructs pHHT-sub2 and pHHT-sub2HA contain $pfsub2_{synth}$

gene sequence encoding only the predicted ectodomain of PfSUB2, respectively with or without a single HA epitope tag at the 3' end of the gene. The full-length *pfsub2*$_{synth}$ gene was used in constructs pHHT-sub2w and pHHT-sub2wHA, again with or without a single HA tag. In all these constructs the *pfsub2*$_{synth}$ sequence was under the control of the *P. falciparum* heat shock protein 86 (*hsp86*) promoter which is commonly used in *P. falciparum* transfection constructs [121, 181]. The *hsp86* gene is transcribed at a relatively high level throughout the erythrocytic cycle whereas PfSUB2 is maximally expressed at relatively low levels only at around 40-48 hours post-invasion [19, 114]. Use of the *hsp86* promoter was therefore expected to result in expression of higher levels of PfSUB2 than if the authentic *pfsub2* promoter was used.

Multiple attempts to obtain stable D10 transfectants harbouring the above constructs in episomal form failed while parallel control transfections using pHHT-TK, carried out under identical conditions, were always successful (data not shown) [127]. Eventually, however, parasites apparently harbouring pHHT-sub2HA were detected in thin blood films after 55 days of drug selection. Plasmid was rescued from this line and three clones were selected for restriction digest analysis alongside a sample of the 'original' pHHT-sub2HA plasmid used for the initial transfection (Figure 5.1). Undigested plasmid samples were analysed in parallel to confirm digestion efficiency. *Spe* I digestion of pHHT-sub2HA should release an 887 bp fragment corresponding to the *hsp86* promoter. This band was seen in the digest of the 'original' pHHT-sub2HA but was missing from digests of all 3 recovered clones. Comparison of *Spe* I digested and the corresponding undigested constructs made it clear that one of the *Spe* I sites remained in the recovered clones as the constructs were linearised by digestion. These linearised forms appeared the same size as the *Spe* I digested 'original' pHHT-sub2HA backbone suggesting that re-arrangements had taken place during replication of the plasmid in the parasite, resulting in loss of the majority if not the entire *hsp86* promoter region. Further analysis by IFA and

Figure 5.1 pHHT-sub2HA undergoes re-arrangements within the parasite

Ethidium bromide stained agarose gel of restriction digests of plasmids recovered from D10 parasites after transfection with pHHT-sub2HA.

Lane 1, recovered pHHT-sub2HA clone 1, undigested; lane 2, recovered pHHT-sub2HA clone 2, undigested; lane 3, recovered pHHT-sub2HA clone 3, undigested; lane 4, original pHHT-sub2HA, undigested; lane 5, 1 kb markers (Amersham Pharmacia; sizes are indicated on the left in kb); lane 6, recovered pHHT-sub2HA clone 1 - *Spe* I digested; lane 7, recovered pHHT-sub2HA clone 2 - *Spe* I digested; lane 8, recovered pHHT-sub2HA clone 3 - *Spe* I digested; lane 9, original pHHT-sub2HA – *Spe* I digested.

The band representing the *hsp86* promoter present in lane 9 but absent from lanes 6-8 is indicated.

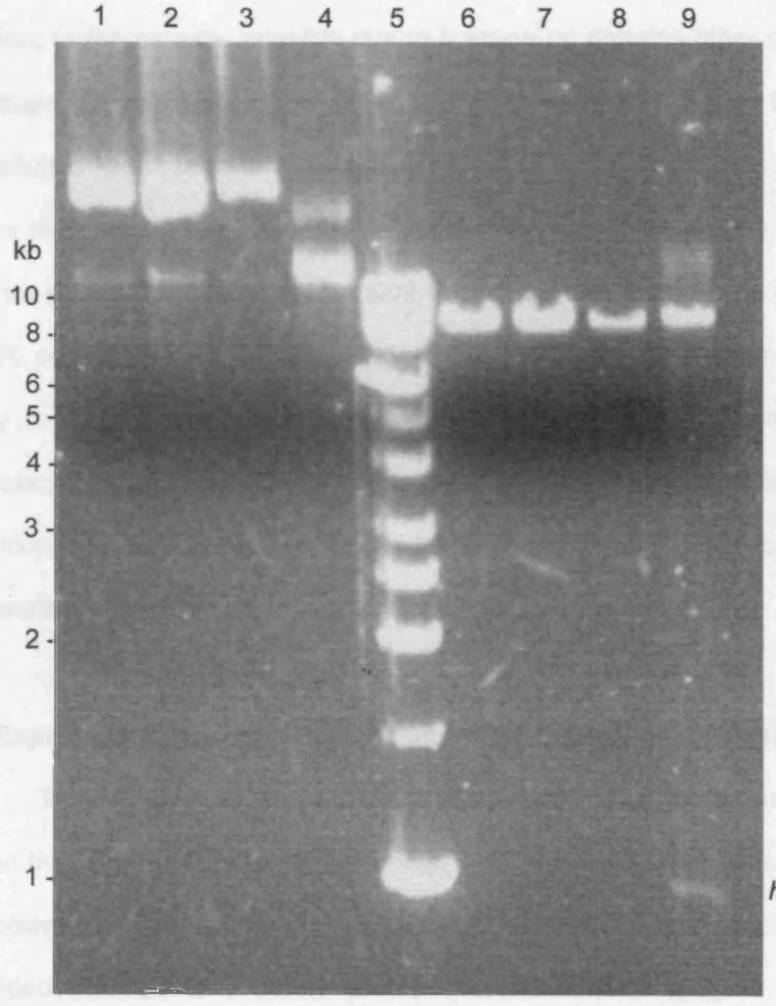
1
2
3
4
5
6
7
8
9
kb
10
8
6
5
4
3
2
1
hsp86 5'

Western blot to try and detect any HA tagged protein were unsuccessful (data not shown), suggesting this deletion had removed all promoter activity.

The selection of a construct that had undergone re-arrangements which effectively eliminated the *hsp86* promoter, together with the prolonged selection period required to obtain a stable, drug-resistant line, suggested that the promoter activity was deleterious to the parasite. There are a number of possible reasons for this, including the following: (1) a simple increase in the levels of active PfSUB2 may be toxic to the parasite possibly due to it acting on proteins other than its authentic substrate; (2) expression of inactive and misfolded PfSUB2 may be toxic; and (3) constitutive expression of PfSUB2 resulting in trafficking to the 'wrong' location within the parasite may be toxic. PfSUB2 is a microneme protein (see Chapter 3) and these organelles are not present throughout the erythrocytic cycle [7]. As the *hsp86* promoter is constitutively active PfSUB2 expressed under this promoter is likely to be trafficked to alternative sub-cellular locations during most of the erythrocytic cycle. The default destination for export of malaria proteins is the PV so it is likely that any PfSUB2 expressed after the merozoite stage is exported to this destination [181, 187].

5.2 Expression of inactive PfSUB2 under the control of the *hsp86* promoter

The results from the previous section implied that expression of PfSUB2 under the control of the *hsp86* promoter was toxic to the parasite. However it was unknown whether the protein expressed was correctly folded and active, or unfolded. PfSUB2 is a serine protease and therefore mutation of $pfsub2_{synth}$ to replace the active site serine (Ser961) with alanine would result in inactive PfSUB2. This could then be placed in the plasmid backbone used before and it was reasoned that if transfections involving these 'inactive' constructs were successful it would imply that the PfSUB2 expressed from the previous constructs was active. On the other hand, if the apparent toxicity was as a result of unfolded protein or simply

incorrect localisation of the PfSUB2 the 'inactive' constructs would also be toxic to the parasite. To test these possibilities, transfections of *P. falciparum* with pHHT-sub2$_i$, pHHT-sub2HA$_i$, pHHT-sub2w$_i$ and pHHT-sub2wHA$_i$ where the PfSUB2 active site serine (Ser961) codon had been substituted with an alanine codon were then performed. However, multiple attempts to obtain stable D10 transfectants harbouring the above 'inactive' constructs in episomal form failed, while parallel pHHT-TK transfections were always successful (data not shown). This suggested that constitutive expression of PfSUB2 throughout the erythrocytic cycle was toxic regardless of protease activity.

From these experiments it was clear that the *hsp86* promoter was not suitable to drive expression of PfSUB2 from an episome. The apparent toxicity appeared to be due to the constitutive nature of the promoter and therefore the use of other promoters was considered for work to proceed.

5.3 Expression of PfSUB2 under the control of the *ama1* promoter

The results described above suggested that expression of PfSUB2 under the control of a constitutively active erythrocytic cycle promoter is toxic to the parasite. Microarray data indicates that AMA1 is expressed at the same time as PfSUB2 but appears to be a more abundant protein [19]. It was therefore postulated that the use of the *ama1* promoter to drive expression of PfSUB2 from an episome might prevent toxicity while resulting in the production of more protein than if the endogenous *pfusb2* promoter was used. In order to test this notion, construct pAMA15'-sub2wHA was prepared. This construct contains the full-length *pfsub2*$_{synth}$ gene, modified with a single C-terminal HA tag, under the control of the *ama1* promoter. Transfections of D10 parasites with the above construct were performed and parasites were detected by thin film after 18 days of drug selection. Plasmid was recovered from this culture and three clones analysed by restriction digest.

There were no rearrangements of the plasmid in any of the clones selected (data not shown). This parasite line was named *ama1*-PfSUB2HA.

Analysis by IFA using the anti-HA mAb 3F10 produced a signal in ~10% of mature schizonts, revealing the presence of a HA tagged protein, with the intensity of the fluorescence varying greatly between individual schizonts (Figure. 5.2). The PfSUB2 expressed from the episome was named PfSUB2epi. Interestingly, the anti-HA signal was quite different to that seen in the PfSUB2HA line (Chapter 3) exhibiting a more diffuse pattern that appeared to be distributed throughout the daughter merozoites, perhaps suggesting a cytoplasmic location for the protein.

P. falciparum carries episomal DNA as trimeric concatamers with multiple concatamers per parasite and parasite replication is associated with rather inefficient segregation of plasmid between daughter merozoites [126, 188]. As a result, it has often been observed that proteins expressed from an episome can only be detected in a proportion of parasites [189]. This is especially true of episomal expression of proteins labelled with GFP where only a proportion of the parasites fluoresce [190, 191]. The lack of detectable PfSUB2epi in the majority of parasites and the large variation in the intensity of the 3F10 signal in those parasites with detectable protein levels was therefore not unexpected, and was probably due to variation in plasmid copy number between individual parasites. It would be predicted that the more copies of plasmid carried by the individual parasite the greater the amount of protein produced and therefore the more intense the signal when detected by IFA. The high intensity of fluorescence seen in some of the *ama1*-PfSUB2HA schizonts compared to clones in which the endogenous *pfsub2* gene had been epitope-tagged (see Chapter 3) suggested that within these parasites the PfSUB2 levels were higher than in wild-type parasites (see Figure 5.2) and that these levels are not immediately toxic to the parasite. However as these 'high expressers' accounted for less than 10% of the population, the overall PfSUB2 l

Figure 5.2 Individual parasites harbouring plasmid pAMA15'-sub2wHA express varying amounts of PfSUB2epi

IFA analysis of *ama1*-PfSUB2HA parasites using the anti-HA mAb 3F10. Parasite nuclei are stained with DAPI (blue). Schizont A appears to express significantly higher levels of PfSUB2epi than schizont B. These images were obtained from the same thin blood film. Magnification 100x.

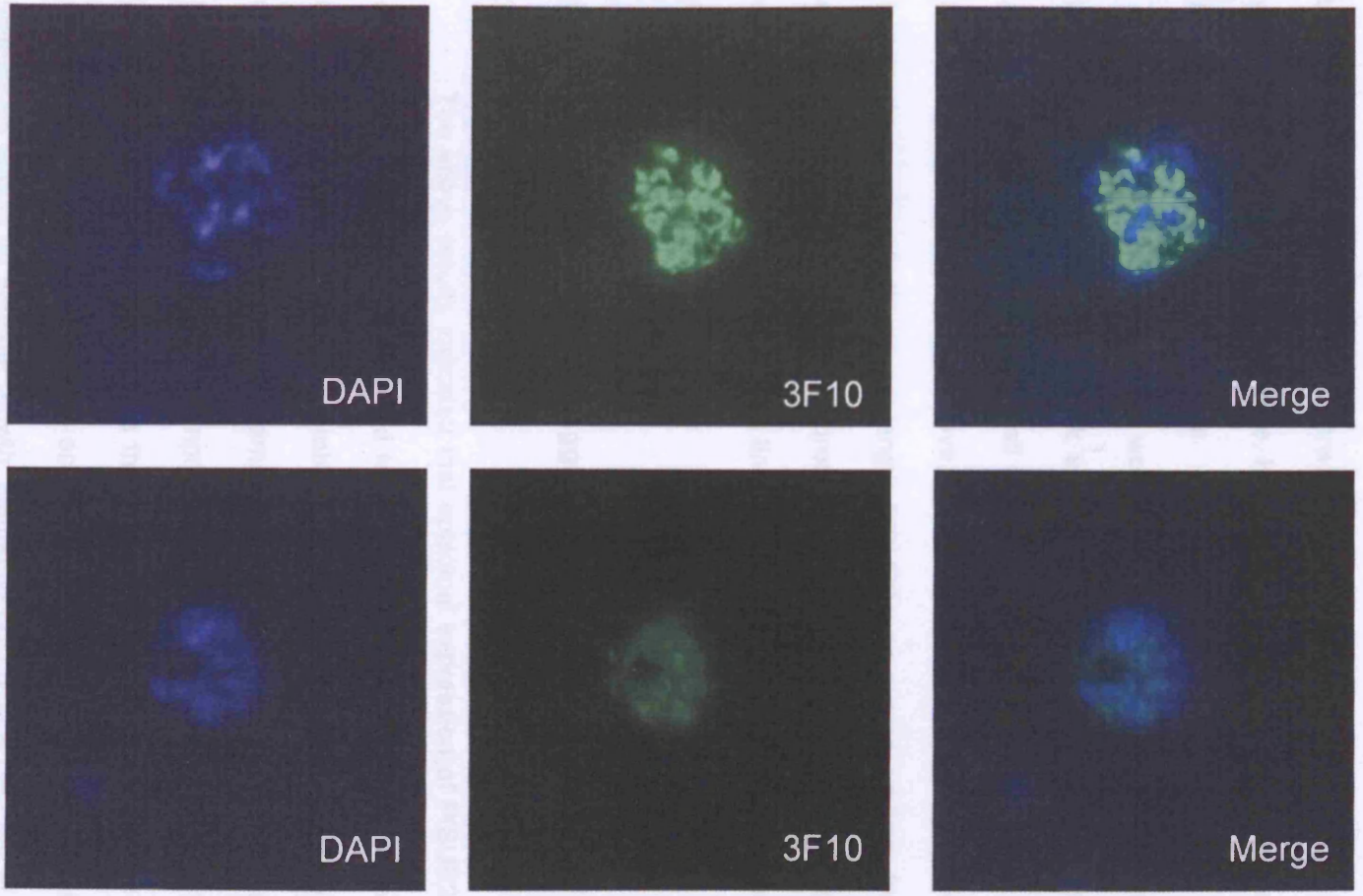
DAPI
3F10
Merge
A
DAPI
3F10
Merge
B

levels were thought unlikely to be significantly greater than those of a wild type population.

PfSUB2epi detection in the *ama1*-PfSUB2HA parasites was also likely hindered by the decision to use a single HA tag as opposed to a HA3 tag, which would allow more sensitive detection. The reason for using a single tag was that, at the point that these experiments were initiated, it was not known whether a HA3 tag would be deleterious to the parasite. However the work described in Chapter 3 has since shown that this is not the case.

Westerns blots with 3F10 were performed on schizont lysates but were inconclusive due to the very weak signals obtained (data not shown). This was probably due to the fact only a small amount of schizonts were carrying detectable levels of protein as discussed above, and the presence of only a single tag. The inability to assess whether a full length PfSUB2 was expressed from the episome and whether it underwent correct processing meant the *ama1*-PfSUB2HA line was of limited use. Further work on this line was abandoned until these issues could be resolved.

5.4 Expression of a triple HA tagged PfSUB2 under the control of the *ama1* promoter

The above results indicated that episomal expression of PfSUB2 under the control of the *ama1* promoter could result in expression of tagged protein but with both segregation and detection problems (see 5.2). Plasmid pAMA15'-sub2wHA was modified to rectify these problems. First, the Rep20 sequence was added as it has previously been shown to improve plasmid segregation between daughter merozoites [122, 192]. Second, as the work from Chapter 3 had in the meantime shown that it is possible to tag the endogenous *pfsub2* with a HA3 tag without any deleterious effects on parasite growth, sequence encoding a HA3 tag at the 3' end

of the *pfsub2*$_{synth}$ gene was included to improve detection of the protein within the parasite.

Transfections were performed with pAMA15'-sub2wHA3Rep20 and parasites were detected in blood smears after 17 days of drug selection. The resulting parasite line was named *ama1*-PfSUB2HA3R. Plasmid was recovered from this line and three clones selected for restriction digest analysis. None of the clones selected showed any re-arrangements (data not shown). Disappointingly the Rep20 sequence did not significantly reduce the time taken for parasites to appear after the start of drug selection (17 days vs. 18 days without Rep20) as it had previously been shown to [122, 190]. This suggests that for this plasmid the presence of the Rep20 sequence does not improve segregation between daughter merozoites.

IFA analysis with the anti-HA mAb 3F10 revealed the presence of a HA tagged protein in schizonts with a higher percentage (~30-50%) of parasites showing a signal compared to the *ama1*-PfSUB2 line. The intensity of the signal in individual schizonts varied greatly as before (data not shown). The protein expressed from this episome was named PfSUB2HA3epi. The variation in intensity of the 3F10 signal provided further evidence that the Rep20 sequence had not improved plasmid segregation as this would be expected to result in a more even distribution of the fluorescence signal. The increase in the proportion of parasites expressing detectable protein was therefore considered likely to be due to improved detection of the protein due to the addition of two further HA tags to the C-terminus of the protein. Once again the small percentage of parasites exhibiting a very intense signal appeared phenotypically normal suggesting that high levels of PfSUB2 are not immediately toxic to the parasite.

The IFA pattern seen using 3F10 in *ama1*-PfSUB2HA3R schizonts was the same as seen with the *ama1*-PfSUB2HA schizonts in 5.2. The signal appeared diffuse and spread within daughter merozoites with no apparent accumulation of protein at the apical end. Dual labelling of the schizonts with anti-RhopH2 and anti-

AMA1 mAbs, markers for rhoptry and microneme organelles respectively, confirmed the absence of an accumulation of PfSUB2 at the apical end of the parasite as there was no co-localisation of either signal with that of 3F10 (see Figure. 5.3) [58, 59, 152]. Similarly, the use of an anti-MSP1 mAb confirmed there was no PfSUB2 found on the parasite surface. Endogenous PfSUB2 is secreted from the micronemes onto the parasite surface upon merozoite release and from here is capped to the posterior end of the parasite (Chapter 3). In order to evaluate whether the same trafficking pattern could be seen with the episomally expressed PfSUB2, free merozoites of the *ama1*-PfSUB2HA3R line were then studied to determine whether the PfSUB2HA3epi re-localised upon merozoite release from the schizont. However, the signal detected in the *ama1*-PfSUB2HA3R free merozoites was the same as that seen in the schizonts, being diffuse and confined within the merozoites (Figure 5.4). Dual labelling with the anti-RhopH2 or anti-MSP1 mAbs again showed no co-localisation with 3F10 in either the rhoptries or on the merozoite surface. In many of the schizonts and merozoites the MSP1 surface signal appeared to encircle the diffuse PfSUB2HA3epi signal. It was therefore concluded that the PfSUB2HA3epi was expressed predominantly in the cytoplasm of both schizonts and free merozoites. It is worth noting that previous studies have shown that AMA1 expressed under the control of the *dhfr-ts* promoter is also found in the parasite cytoplasm and the IFA analyses carried out in that study showed a very similar pattern to that seen here with PfSUB2HA3epi [151].

The mis-localisation of PfSUB2HA3epi observed above was considered probably a result of the use of the *ama1* promoter instead of the authentic *pfsub2* promoter. AMA1 and PfSUB2 are expressed at the same time during the RBC cycle and therefore it had been hoped that using the *ama1* promoter would result in expression of PfSUB2 at the correct time and trafficking to the correct sub-cellular location [19]. However as the ultimate aim of this section of the work was to purify

Figure 5.3 PfSUB2HA3epi expressed by schizonts harbouring plasmid pAMA15'-sub2wHA3Rep20does not locate to the parasite plasma membrane, the micronemes, or rhoptries

IFA analysis of *ama1*-PfSUB2HA3R schizonts. Slides were probed with the anti-HA mAb 3F10 and either mAb 61.3 (anti-RhopH2), mAb 4G2 (anti-AMA1) or mAb X509 (anti-MSP1). Parasite nuclei are stained throughout with DAPI (blue). Magnification 100x.

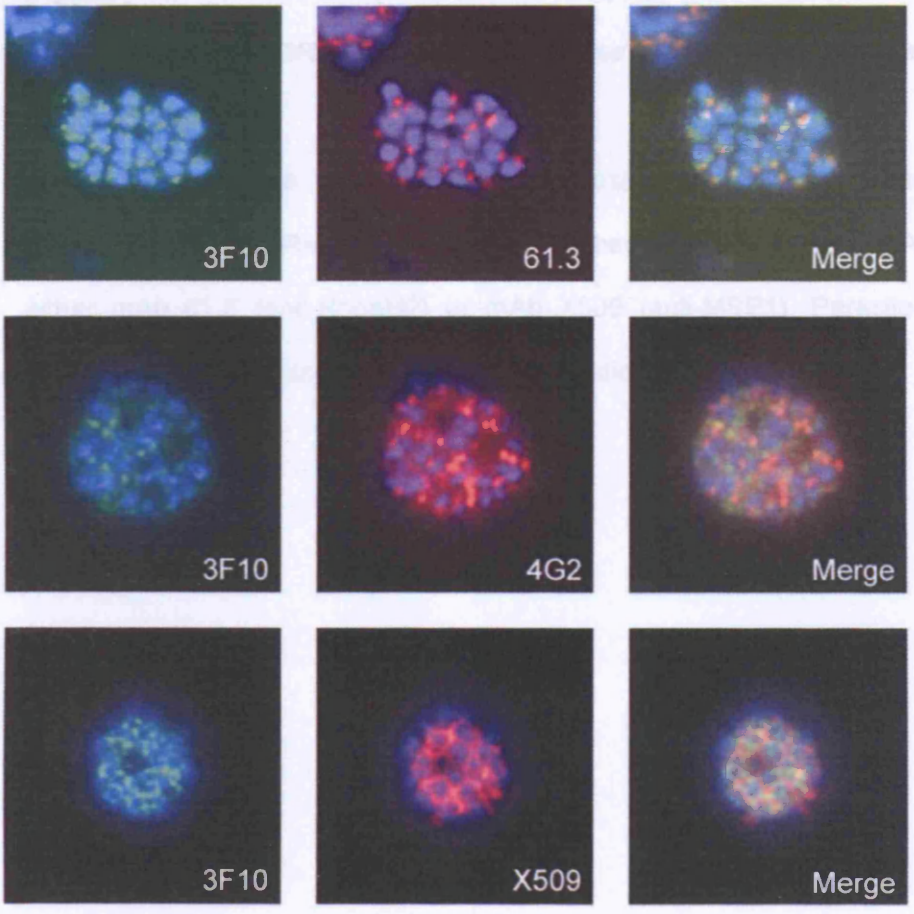
3F10
61.3
Merge
3F10
4G2
Merge
3F10
X509
Merge

Figure 5.4 PfSUB2HA3epi expressed by parasites harbouring plasmid pAMA15'-sub2wHA3Rep20 does not localise to the free merozoite surface or rhoptries

IFA analysis of free merozoites of a parasite culture stably transfected with pAMA15'-sub2wHA3Rep20. Slides were probed with the anti-HA mAb 3F10 and either mAb 61.3 (anti-RhopH2) or mAb X509 (anti-MSP1). Parasites nuclei are stained throughout with DAPI (blue). Magnification 100x.

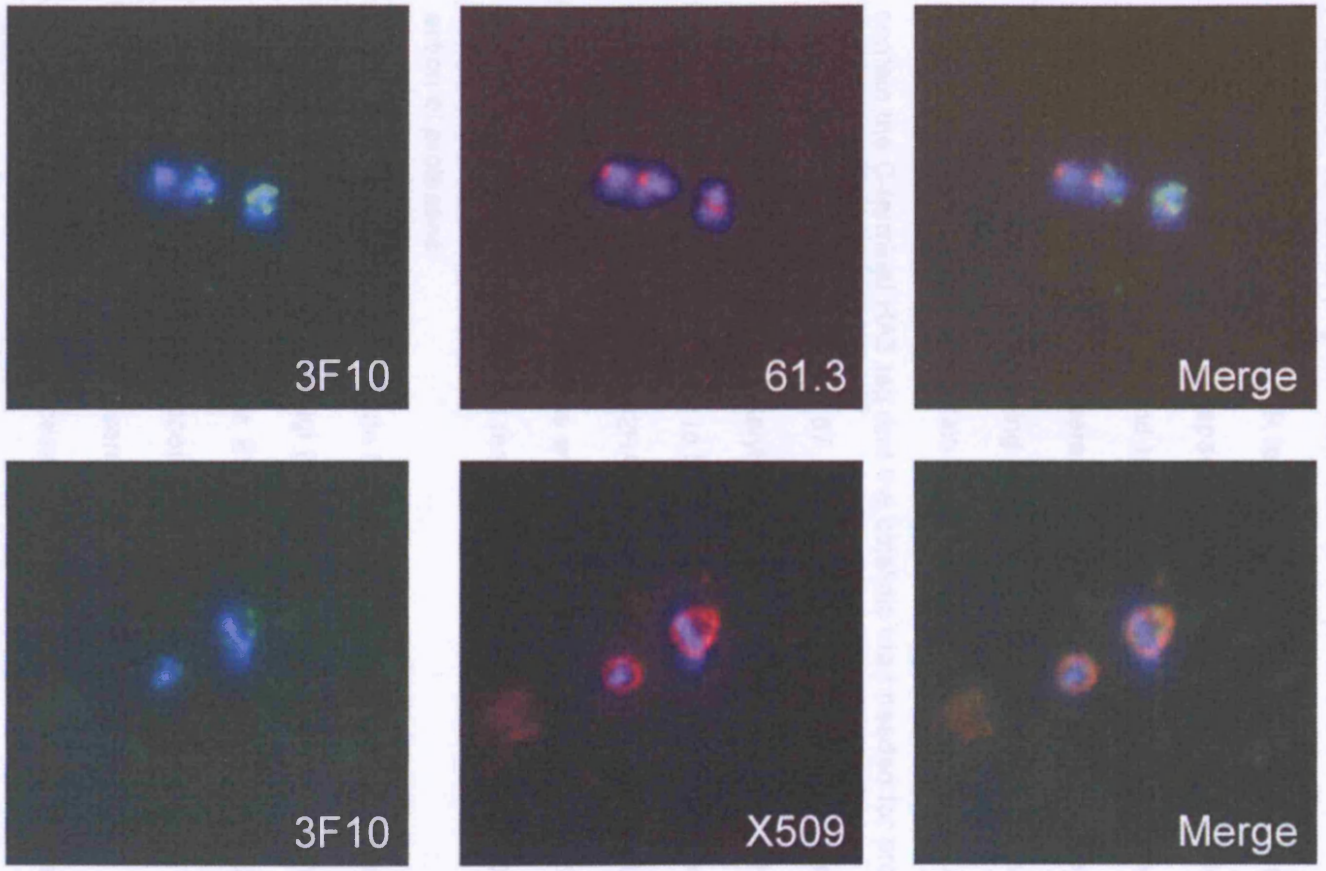
3F10
61.3
Merge
3F10
X509
Merge

the PfSUB2HA3epi from the parasite provided the protein is active, its sub-cellular location was thought unimportant.

Western blots were then performed, using mAbs 3F10 and H5 (anti-Rap2), to probe lysates of *ama1*-PfSUB2HA3R schizonts in parallel with those of PfSUB2HA schizonts (Figure. 5.5). The 3F10 probed blot revealed a number of bands in the *ama1*-PfSUB2HA3R lane, migrating with apparent masses of 150 kDa, 72 kDa, 55 kDa, and a closely spaced triplet of 38 to 36kDa. The 150 kDa and 72 kDa species probably correspond to the full length PfSUB2 and processed, 'active' PfSUB2 respectively, as they were exactly the same size as those bands seen in the PfSUB2HA line. The remaining polypeptides are detected on a western blot and are therefore most likely to contain the HA3 tag. In order for a PfSUB2 fragment to contain the C-terminal HA3 tag and the catalytic triad needed for protease activity it is predicted to have a mass of 67 kDa. As the bands are all smaller than this it is unlikely that they contain the catalytic triad and are therefore probably inactive. They were therefore considered likely to be breakdown products. The 55 kDa and 36 kDa bands were seen in the PfSUB2HA lane as well as the *ama1*-PfSUB2HA3R lane. This other two 38-36 kDa bands were unique to the *ama1*-PfSUB2HA3R lane and were thought possibly to be the result of differences in sample preparation and the action of proteases.

Cleavage of the propeptide from the catalytic domain of eukaryotic subtilases usually occurs in the ER or Golgi [193, 194]. In the case of furin, for example, the propeptide is first cleaved in the ER but full activation of the protease only occurs after further cleavage of the propeptide in the Golgi to dissociate it from the rest of the protein [161]. In the presence of brefeldin A, an inhibitor of anterograde transport from ER to Golgi, processing of PfSUB2 to the 74 kDa species occurs but further cleavage to the 72 kDa terminal processing product is blocked [195]. This indicates that, while the propeptide is cleaved within the ER the final processing step, potentially indicating full activation, occurs outside this compartment. PfSUB2

Figure 5.5 PfSUB2HA3epi undergoes typical processing.

Western blots were performed on extracts of PfSUB2HA clone 2D, and of schizonts stably transfected with construct pAMA15'-sub2wHA3Rep20. Blots were probed with the anti-HA mAb 3F10 or the anti-Rap2 mAb H5. Species corresponding to the various processed forms of PfSUB2 are arrowed and indicated.

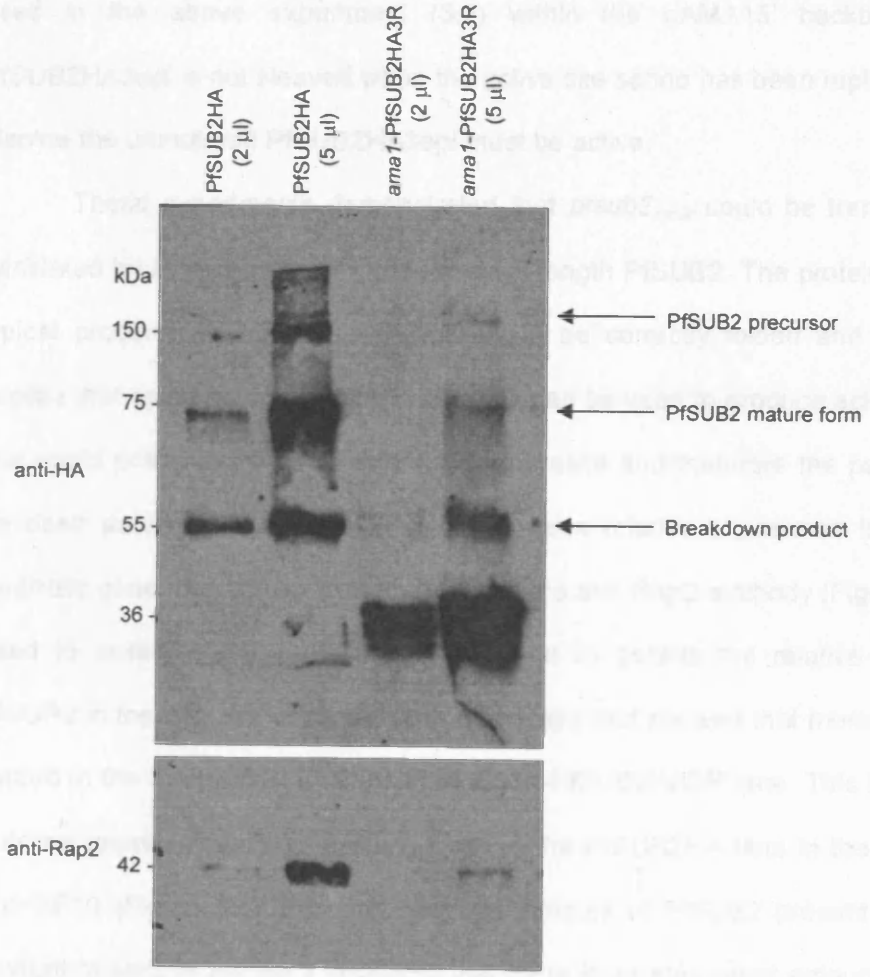
PfSUB2HA (2 µl)
PfSUB2HA (5 µl)
ama1-PfSUB2HA3R (2 µl)
ama1-PfSUB2HA3R (5 µl)
kDa
150
75
55
36
anti-HA
PfSUB2 precursor
PfSUB2 mature form
Breakdown product
anti-Rap2
42

is therefore likely to be fully active only after it has left the ER. PfSUB2HA3epi and the endogenous PfSUB2 are likely to be found together in the ER and Golgi before trafficking to distinct locations within the merozoite. If PfSUB2 is not fully active until after the ER the observed processing of PfSUB2HA3epi is unlikely to be due to the action of the endogenous PfSUB2 *in trans*, and is therefore most likely autocatalytic, indicating that it is catalytically active. Experimental confirmation of this could be achieved through the use of the 'inactive' active-site Ser-to-Ala *pfsub2*$_{synth}$ mutant used in the above experiment (5.2) within the pAMA15' backbone. If the PfSUB2HA3epi is not cleaved when the active site serine has been replaced with an alanine the unmutated PfSUB2HA3epi must be active.

These experiments demonstrated that *pfsub2*$_{synth}$ could be transcribed and translated by *P. falciparum* to produce a full length PfSUB2. The protein undergoes typical processing and is therefore likely to be correctly folded and active. This implies that episomal expression of PfSUB2 can be used to produce active protease that could potentially be purified from the parasite and therefore the parasite could be used as an expression system. To assess relative expression levels of the synthetic gene product, the blot probed with the anti-Rap2 antibody (Figure 5.5) was used to assess the loading of the gels and to assess the relative amounts of PfSUB2 in the different parasite lanes. The Rap2 blot showed that more protein was loaded in the PfSUB2HA lane than the *ama1*-PfSUB2HA3R lane. This is consistent with the greater amount of PfSUB2 seen in the PfSUB2HA lane in the blot probed with 3F10 (Figure 5.5). By comparing the amount of PfSUB2 present against the amount of sample loaded it appeared that there is an equivalent amount of PfSUB2 in both the *ama1*-PfSUB2HA3R and PfSUB2HA lines. Of course as the endogenous PfSUB2 in the *ama1*-PfSUB2HA3R line was not tagged it would not have been detected in these blots and the *ama1*-PfSUB2HA3R parasites might actually be expressing higher levels of PfSUB2. Alternatively, as found by Healer *et al.* in the a previous study referred to above [132], the PfSUB2HA3epi may show dominance

over the endogenous PfSUB2 resulting in the majority of PfSUB2 originating from the episome.

As only a fraction of the schizonts in the *ama1*-PfSUB2HA3R line expressed detectable levels of PfSUB2HA3epi it was perhaps not surprising that the levels seen were equivalent to those seen in the PfSUB2HA line despite the use of the *ama1* promoter to drive protein expression. It seems likely that, until the segregation problems seen with episomal expression can be rectified, over-expression of parasite proteins within *P. falciparum* will not be possible. As the PfSUB2HA3epi levels were not significantly different to the levels of PfSUB2 detected in PfSUB2HA, attempts to purify the protein were abandoned.

5.5 Characterisation of the *pfsub2* promoter

Attempts to 'knock-out' the *pfsub2* gene in the parasite have been unsuccessful suggesting the protein plays an essential function in blood-stages of the parasite [117]. Functional studies involving mutagenesis of the *pfsub2* gene are therefore made difficult as any that alter the normal activity, trafficking or movement of the protease might be lethal to the parasite and therefore the effects would be impossible to detect. The expression of a mutant tagged form of PfSUB2 from an episome could be used to overcome these difficulties as the endogenous PfSUB2 would remain unaltered and therefore the parasites would remain viable whatever manipulations were made to the episomal copy of the gene. The effect of the mutations on the episomally encoded protein could then be studied. However before such an approach can be considered possible, PfSUB2 must be expressed from an episome and shown to be processed and trafficked in a manner that mimics that of the endogenous protein. As shown above, PfSUB2 expressed from an episome under the control of the *ama1* promoter is correctly processed and therefore is presumably correctly folded and active. However the sub-cellular localisation of the protein was found to be incorrect. One possible explanation for this mis-trafficking is

the use of a heterologous promoter, and so work was initiated to characterise the endogenous *pfsub2* promoter in order that it could be used for future studies of this type [128, 181].

CAT is an *E. coli* enzyme that acetylates chloramphenicol, inactivating the antibiotic and therefore conferring resistance to it. CAT is a robust and highly processing enzyme, readily detected using a simple assay, and the CAT reporter system is commonly used to identify *P. falciparum* intergenic regions with promoter activity [121, 124]; the ability of intergenic regions to drive expression of CAT can be quantitatively assessed by detection of CAT expression in the parasite. Six fragments of the region 5' to the *pfsub2* gene F1 (-1459 to –1 bp), F2 (-1267 to -1 bp), F3 (-1054 to -1 bp), F4 (-824 to –1 bp), F5 (-624 to –1 bp) and F6 (-286 to –1 bp) were amplified from parasite DNA. This upstream sequence appears typical of *P. falciparum* intergenic regions, with an A+T content of 85% and a number of poly(dA)/poly(dT) tracts [182, 184, 185]. Each PCR fragment was placed upstream of the *cat* gene within the vector backbone of pHC1-CAT and the resulting constructs transfected into the parasite alongside the positive control pHC1-CAT (where the *cat* gene is under the control of the *cam* promoter) and the negative control plasmid pHC1-no 5'UTR (a control plasmid supplied by R. O'Donnell, which is identical to pHC1-CAT except that it lacks a promoter for the *cat* gene) [130]. Stable lines carrying all of the plasmids mentioned above were established and the ability of each 5' fragment to drive reporter gene expression was then assessed by CAT assay.

The results of these assays are shown in Figure 5.6. Acetylated forms of chloramphenicol were observed in the positive control lanes (bacterial CAT and pHC1-CAT) as well as the F1, F2, F3, F4 and F5 lanes. These results suggest that the *pfsub2* 5' fragments F1, F2, F3, F4 and F5 all contain elements capable of driving expression of CAT in the parasite and therefore exhibit promoter activity. However, the intensity of the acetylated chloramphenicol bands decreased as the

Figure 5.6 The *pfsub2* 5' UTR displays promoter activity

CAT assay performed on extracts of *P. falciparum* cultures stably transfected with constructs pHC1-CATF1 (F1), pHC1-CATF2 (F2), pHC1-CATF3 (F3), pHC1-CATF4 (F4), pHC1-CATF5 (F5), pHC1-CATF6 (F6), pHC1-CAT (CAT) and pHC1-no 5'UTR (NP). The lane marked (Neg) is the negative control. The lanes marked (Pos) are the positive control containing bacterial CAT. The species on the film correspond to (a) non-acetylated residual substrate, (b) 1-acetyl-chloramphenicol and (c) 1,3 acetyl chloramphenicol.

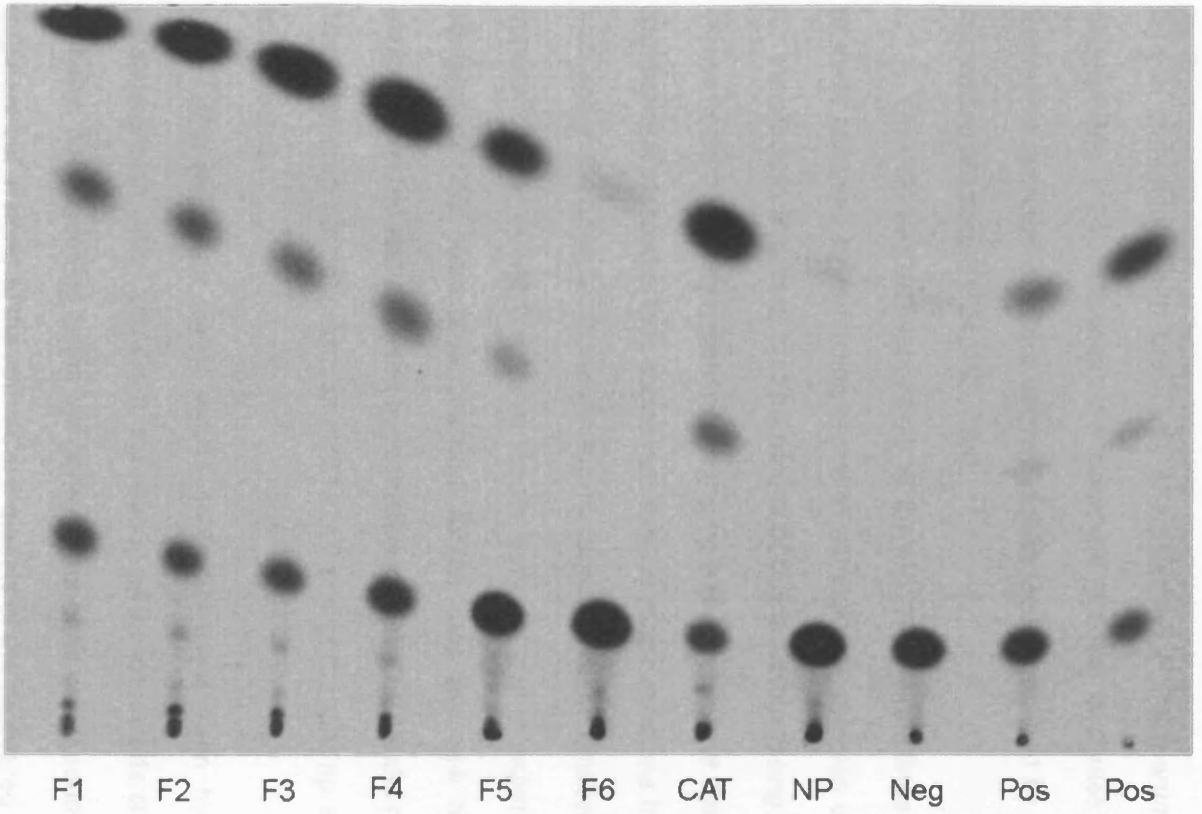
c
b
a
F1
F2
F3
F4
F5
F6
CAT
NP
Neg
Pos
Pos

fragments decrease in size from the F1, F2 and F3 lanes, which were equally intense, to the weaker bands seen in the F4 lane and the weaker still in the F5 lane. This suggests that the F1, F2 and F3 fragments can act as equally strong promoters. As the F3 fragment is 405 bp shorter than the F1 fragment this suggests that the region between –1459 to –1054 bp has no major promoter activity. The F6 fragment was the only *pfsub2* 5' fragment to show no activity, and given its small size in comparison with previously characterised *P. falciparum* promoters this is unsurprising [124]. Overall, the observed gradual decrease in activity as the fragments decrease in size is consistent with results obtained by others with other *P. falciparum* promoters [124, 183, 184].

Plasmid was recovered from all the pHC1-CATprom lines and several clones of each analysed by restriction digest in parallel with samples of the plasmid used for transfection (Figure 5.7). The results of this were surprising. All the recovered clones could be readily linearised, migrating with an apparent size identical to that of the parental plasmids. This suggested that no major deletions had occurred during passage in the parasite. However, further digestion of the recovered plasmid proved impossible. To confirm that these results were not due to experimental error, fresh samples of DNA were produced from all the lines and new clones of recovered plasmid selected and analysed by restriction digest. The results remained the same. The recovered control plasmids pHC1-CAT and pHC1-CATnp also failed to digest as expected.

The restriction digest results contradict those seen by CAT assays and parasite growth. *Xho* I and *Cel* II digestion of all the constructs should release a 793 bp band, corresponding to the *cat* gene, and a band corresponding to the promoter fragment but in none of the *Xho* I/*Cel* II digests of the recovered clones were bands of these sizes released, suggesting re-arrangements of the plasmid. However the selected parasites clearly expressed a functional CAT as seen in the CAT assays. The fact that the parasite lines were pyrimethamine resistant also implies the

Figure 5.7 Restriction digest analysis of recovered pHC1-CATprom plasmids gives unexpected results

Agarose gels stained with ethidium bromide of restriction digest analysis of recovered clones of pHC1-CATF1 and pHC1-no 5'UTR. Plasmids are undigested unless marked otherwise. *Xho* I/*Cel* II digests of pHC1-CATF1 is expected to produce bands of 793 bp, 1.459 kb and 6.597 kb as can be seen in the lane (arrowed) containing the input plasmid. *Xho* I/*Cel* II digests of pHC1-no 5'UTR is predicted to produce bands of 793 bp and 6.597 kb as can be seen in the lane containing this input plasmid (asterisked). *Pst* I/*EcoR* I digests of pHC1-no 5'UTR should produce bands of 361 bp, 467 bp, 1.008 kb, 1.391 kb, 1.454 kb and 2.709 kb as can be seen in the input plasmid (double asterisked). As can be seen, none of the clones isolated from recovered DNA produced the expected restriction fragment pattern upon digestion.

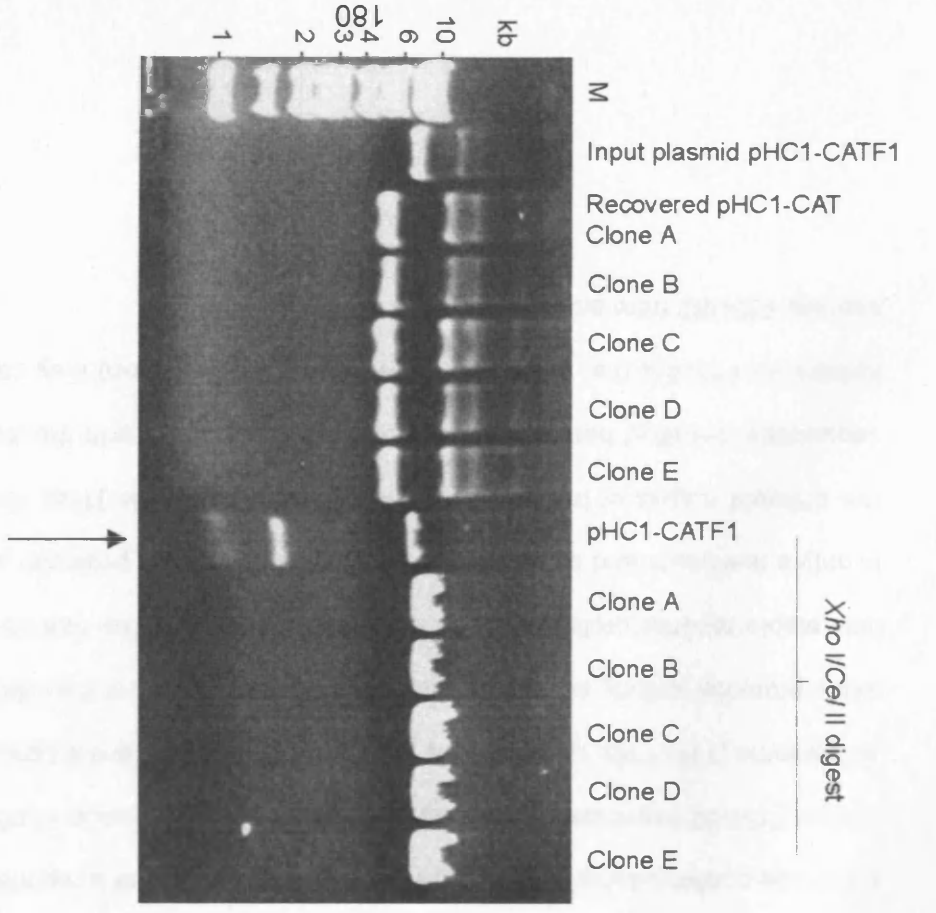
kb
10
6
4
3
2
1
M
Input plasmid pHC1-CATF1
Recovered pHC1-CAT
Clone A
Clone B
Clone C
Clone D
Clone E
pHC1-CATF1
Clone A
Clone B
Clone C
Clone D
Clone E
Xho I/Cel II digest

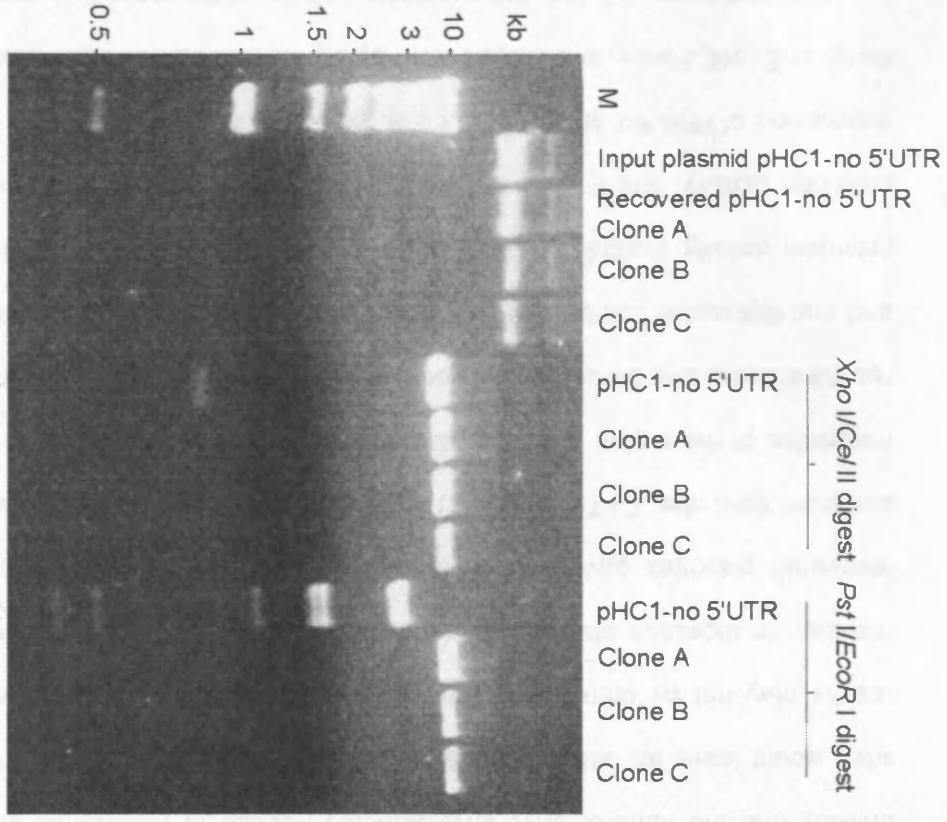
kb
10
3
2
1.5
1
0.5
M
Input plasmid pHC1-no 5'UTR
Recovered pHC1-no 5'UTR
Clone A
Clone B
Clone C
*
pHC1-no 5'UTR
Clone A
Clone B
Clone C
**
pHC1-no 5'UTR
Clone A
Clone B
Clone C
Xho I/Cel II digest
Pst I/EcoR I digest

presence in each plasmid of a functional drug resistance cassette. It seems most unlikely that the number of re-arrangements needed to remove all the restriction sites would leave an unaltered cassette. This suggested that the restriction digest results may not be correct and that the plasmid DNA had become in some way resistant to digestion after replication in the parasite. Although the analysis of the recovered plasmids gave unexpected results this does not invalidate the results obtained from the CAT assays. The aim of these experiments was to identify fragments of the region 5' to the *pfsub2* gene that possess promoter activity. The results showed that the region between –1459 to –1 bp can drive protein expression and that this region can be reduced by 405 bp (–1054 to -1 bp) with no major drop in promoter activity. Further deletions of the region downstream of –1054 bp reduced promoter activity. The F1, F2 or F3 fragments could therefore all be used to drive expression of PfSUB2 although as F3 is the smallest it would possibly be easier to clone in *E. coli*. However previous work by others has shown that reductions in the 5' region of a gene can alter the expression profile of the respective protein [128]. It should be confirmed that the F3 fragment drives expression of a reporter gene at the time of PfSUB2 expression before being used to drive expression of $pfsub2_{synth}$ from an episome [114, 116]. Unfortunately the stability of CAT means it cannot be used to study promoter activity accurately within the different stages of the RBC cycle and a less stable reporter protein such as luciferase is required. The half life of luciferase is only a few hours and can therefore be used to distinguish promoter activity during the different stages of the 48 hour *P. falciparum* RBC cycle [196]. Once the DNA sequences identified here are shown to express luciferase with the same temporal kinetics as PfSUB2 (i.e. peaking at 40-48 hours post invasion) they can be used to express PfSUB2 from an episome.

Discussion

Initially the work in this chapter focused on use of *P. falciparum* to over-express PfSUB2 in a bid to obtain a source of correctly folded active protein. The choice of promoter to drive expression of PfSUB2 is important; expression under the control of a constitutive promoter was found to be toxic to the parasite while use of a late stage promoter resulted in the production of a correctly processed and therefore – it is presumed - folded and enzymatically active PfSUB2. In individual *ama1*-PfSUB2HA3R parasites high levels of PfSUB2 were detected by IFA and these parasites appeared phenotypically normal suggesting that high levels of the protease are not necessarily toxic to the parasite. However within the population as a whole the amount of PfSUB2HA3epi produced was approximately the same as the amount of PfSUB2 expressed in the PfSUB2HA line, likely as result of poor segregation of plasmid between daughter merozoites. Until these segregation problems are resolved it seems unlikely that high levels of PfSUB2 can be expressed within the parasite.

Our results confirm previous studies that the use of alternative promoters to express a malarial protein from an episome can result in its mis-localisation. In order to develop a system for driving PfSUB2 expression from an episome whilst obtaining correct localisation, the *pfsub2* promoter was studied. A number of fragments of the region 5' to the *pfsub2* gene have been found which possess promoter activity. Once the ability of these sequences to control expression of the protein at the correct stages of the RBC cycle has been assessed, they can be used to continue the work on expression of PfSUB2 from an episome. It may then be possible to use this system to study the effects of mutations within the episome-encoded PfSUB2, and in this way assess the proteins function.

Discussion

PfSUB2 is considered to be MESH, the protease involved in shedding MSP1 and AMA1 from the merozoite surface, and is therefore a good candidate for future drug design. However, previous work on PfSUB2 has been hampered by the difficulties in detecting the protein within the parasite and the inability to express it in an active recombinant form. The work described in this thesis focused on utilising transfection technology to further understand the role of PfSUB2 within the parasite.

Overview

Epitope tagging of the PfSUB2 C-terminus allowed unambiguous localisation of the protein to the micronemes of the mature schizont. This differs from the dense granule location previously described but is consistent with the observation that PfSUB2 is released onto the parasite surface at or prior to invasion as dense granules are not believed to release their contents until invasion is complete [116]. This is not the first instance of mis-localisation of *P. falciparum* proteins as AMA1 was initially localised to the rhoptries before reassignment to the micronemes [132]. The accurate detection of PfSUB2 within the parasite has allowed the protein to be studied during schizogony and eventual merozoite release and has resulted in the following model. Initially PfSUB2 accumulates in the micronemes of the mature schizont. The protease undergoes processing in the ER but may remain associated with the propeptide to prevent the cleavage of proteins within the microneme. Upon merozoite release active PfSUB2 is secreted onto the parasite surface where it engages with an actin-based motor. It is unlikely that this interaction is via the PfSUB2 cytoplasmic domain as this region is unconserved amongst *Plasmodium* species, lacks the residues associated with TRAP and MIC2 interaction with actin and – as shown by this study - can be modified by the addition of a tag without deleterious effects on parasite growth [39, 40]. It is possible that PfSUB2 may interact with the actinomyosin motor through ectoplasmic interactions with other

micronemal proteins that are themselves connected to the motor. An example of this is seen in *T. gondii* where MIC2-associated protein (M2AP) remains complexed to MIC2 throughout secretion, translocation and release. This interaction with MIC2 causes the capping of TgM2AP which itself lacks a transmembrane domain [197].

Once on the surface of the merozoite PfSUB2 is pulled to the posterior of the cell, in the process encountering and cleaving MSP1 and AMA1 from the surface of the parasite. However in this work this capping movement has only been studied in the absence of invasion. It is possible that on invading merozoites PfSUB2 movement occurs during the parasites entry into the nascent parasitophorous vacuole and that the protease concentrates at the moving junction. PfSUB2 is then carried into the RBC on the parasite surface where it eventually appears to diffuse back over the parasite surface perhaps as a result of the actinomyosin motor stopping once invasion is complete. By a few hours post invasion PfSUB2 is no longer detected and this may reflect turnover of the protease following completion of its role during invasion.

Future work

PfSUB2 is the first example of a merozoite protein that undergoes capping and the protein behaves in the way predicted for MESH. However, many questions remain unanswered and work is still needed to further dissect the role of the protein during invasion. At present the precise location of PfSUB2 as the parasite invades the RBC is unknown. The small size of the *P. falciparum* merozoite makes studies of the moving junction, even using IEM, extremely challenging. One approach to overcoming this obstacle would be to fuse the reporter protein GFP to PfSUB2. This would allow studies in real time to determine the timing and dynamics of PfSUB2 movement as invasion proceeds.

It would also be interesting to further investigate the interaction between PfSUB2 and the actinomyosin motor within the parasite, for example defining the

regions of the protein required for movement. The episomal expression of PfSUB2 developed in Chapter 5 could be used with the fragments of the *pfsub2* 5' region shown to have promoter activity controlling expression of the $pfsub2_{synth}$ gene. Initially it would have to be confirmed that the sub-cellular location, time of expression and processing of the episomally expressed PfSUB2 matched that of the endogenous PfSUB2. The effect of various mutations on the movement of PfSUB2 could then be assessed. It is perhaps worthy of note that the region between the catalytic triad and predicted transmembrane domain of PfSUB2 is relatively large and extremely well conserved amongst *Plasmodium* species (see Figure 1.5). The function of this region is unknown but given the level of conservation it is likely to be functionally important. If this region is involved in interactions with other proteins, mutations of conserved residues may affect these interactions and prevent PfSUB2 capping. This approach could also be used to mutate residues around the sites at which processing is predicted to occur in an attempt to prevent it. This would reveal the precise processing sites and allow the propeptide to be accurately defined. Although PfSUB2 is predicted to have a relaxed substrate specificity it is unlikely the enzyme can cleave every sequence and by mutating the residues at the cleavage site to prevent processing the sequence specificity of the enzyme could be examined. A similar approach has been used with some success in the case of PfSUB1 [112].

Conclusion

While the ability to transfect *P. falciparum* and modify PfSUB2 has increased our understanding of the protein there are still many questions left to answer about its role during invasion. However it is clear that PfSUB2 is a good candidate for drug design. Protease inhibitors are used to treat infections such as Human Immunodeficiency Virus (HIV). However, as with *P. falciparum,* the emergence of drug resistant forms of the virus has reduced the efficacy of these drugs. This has

been combated with the use of combination therapy involving several drugs aimed at different targets which reduces the rate at which resistance occurs. White *et al* discussed using a similar approach with *P. falciparum* infections as combination therapy is predicted to prolong the efficacy of antimalarials [4]. A protease inhibitor would be a useful addition to current pool of antimalarials and could be used in combination therapy.

1. WHO, *WHO, 'Roll Back Malaria.'* http://www.rbm.who.int/cmc_upload/0/000/015/370/RBMInfosheet_3.htm.
2. Snow, R.W., et al., *The global distribution of clinical episodes of Plasmodium falciparum malaria.* Nature, 2005. **434**(7030): p. 214-7.
3. Gallup, J.L. and J.D. Sachs, *The economic burden of malaria.* Am J Trop Med Hyg, 2001. **64**(1-2 Suppl): p. 85-96.
4. White, N.J., et al., *Averting a malaria disaster.* Lancet, 1999. **353**(9168): p. 1965-7.
5. Breman, J.G., *The ears of the hippopotamus: manifestations, determinants, and estimates of the malaria burden.* Am J Trop Med Hyg, 2001. **64**(1-2 Suppl): p. 1-11.
6. Blackman, M.J., *Proteases involved in erythrocyte invasion by the malaria parasite: function and potential as chemotherapeutic targets.* Curr Drug Targets, 2000. **1**(1): p. 59-83.
7. Bannister, L.H., et al., *A brief illustrated guide to the ultrastructure of Plasmodium falciparum asexual blood stages.* Parasitol Today, 2000. **16**(10): p. 427-33.
8. Aikawa, M., et al., *Erythrocyte entry by malarial parasites. A moving junction between erythrocyte and parasite.* J Cell Biol, 1978. **77**(1): p. 72-82.
9. Dvorak, J.A., et al., *Invasion of erythrocytes by malaria merozoites.* Science, 1975. **187**(4178): p. 748-50.
10. Carruthers, V.B. and L.D. Sibley, *Sequential protein secretion from three distinct organelles of Toxoplasma gondii accompanies invasion of human fibroblasts.* Eur J Cell Biol, 1997. **73**(2): p. 114-23.
11. Culvenor, J.G., K.P. Day, and R.F. Anders, *Plasmodium falciparum ring-infected erythrocyte surface antigen is released from merozoite dense granules after erythrocyte invasion.* Infect Immun, 1991. **59**(3): p. 1183-7.
12. Miller, L.H., et al., *Interaction between cytochalasin B-treated malarial parasites and erythrocytes. Attachment and junction formation.* J Exp Med, 1979. **149**(1): p. 172-84.
13. Pinder, J.C., et al., *Actomyosin motor in the merozoite of the malaria parasite, Plasmodium falciparum: implications for red cell invasion.* J Cell Sci, 1998. **111 (Pt 13)**: p. 1831-9.
14. Dobrowolski, J.M. and L.D. Sibley, *Toxoplasma invasion of mammalian cells is powered by the actin cytoskeleton of the parasite.* Cell, 1996. **84**(6): p. 933-9.
15. Dobrowolski, J.M., V.B. Carruthers, and L.D. Sibley, *Participation of myosin in gliding motility and host cell invasion by Toxoplasma gondii.* Mol Microbiol, 1997. **26**(1): p. 163-73.
16. Bumstead, J. and F. Tomley, *Induction of secretion and surface capping of microneme proteins in Eimeria tenella.* Mol Biochem Parasitol, 2000. **110**(2): p. 311-21.
17. Pinder, J., et al., *Motile systems in malaria merozoites: how is the red blood cell invaded?* Parasitol Today, 2000. **16**(6): p. 240-5.
18. Wesseling, J.G., M.A. Smits, and J.G. Schoenmakers, *Extremely diverged actin proteins in Plasmodium falciparum.* Mol Biochem Parasitol, 1988. **30**(2): p. 143-53.

19. Le Roch, K.G., et al., *Discovery of gene function by expression profiling of the malaria parasite life cycle.* Science, 2003. **301**(5639): p. 1503-8.
20. Field, S.J., et al., *Actin in the merozoite of the malaria parasite, Plasmodium falciparum.* Cell Motil Cytoskeleton, 1993. **25**(1): p. 43-8.
21. Wetzel, D.M., et al., *Actin filament polymerization regulates gliding motility by apicomplexan parasites.* Mol Biol Cell, 2003. **14**(2): p. 396-406.
22. Dobrowolski, J.M., I.R. Niesman, and L.D. Sibley, *Actin in the parasite Toxoplasma gondii is encoded by a single copy gene, ACT1 and exists primarily in a globular form.* Cell Motil Cytoskeleton, 1997. **37**(3): p. 253-62.
23. Schuler, H., A.K. Mueller, and K. Matuschewski, *Unusual properties of Plasmodium falciparum actin: new insights into microfilament dynamics of apicomplexan parasites.* FEBS Lett, 2005. **579**(3): p. 655-60.
24. Meissner, M., D. Schluter, and D. Soldati, *Role of Toxoplasma gondii myosin A in powering parasite gliding and host cell invasion.* Science, 2002. **298**(5594): p. 837-40.
25. Bergman, L.W., et al., *Myosin A tail domain interacting protein (MTIP) localizes to the inner membrane complex of Plasmodium sporozoites.* J Cell Sci, 2003. **116**(Pt 1): p. 39-49.
26. Menard, R., *Gliding motility and cell invasion by Apicomplexa: insights from the Plasmodium sporozoite.* Cell Microbiol, 2001. **3**(2): p. 63-73.
27. Sultan, A.A., et al., *TRAP is necessary for gliding motility and infectivity of plasmodium sporozoites.* Cell, 1997. **90**(3): p. 511-22.
28. Kappe, S., et al., *Conservation of a gliding motility and cell invasion machinery in Apicomplexan parasites.* J Cell Biol, 1999. **147**(5): p. 937-44.
29. Huynh, M.H., et al., *Trans-genera reconstitution and complementation of an adhesion complex in Toxoplasma gondii.* Cell Microbiol, 2004. **6**(8): p. 771-82.
30. Dessens, J.T., et al., *CTRP is essential for mosquito infection by malaria ookinetes.* Embo J, 1999. **18**(22): p. 6221-7.
31. Robson, K.J., et al., *A highly conserved amino-acid sequence in thrombospondin, properdin and in proteins from sporozoites and blood stages of a human malaria parasite.* Nature, 1988. **335**(6185): p. 79-82.
32. Wan, K.L., et al., *Molecular characterisation of an expressed sequence tag locus of Toxoplasma gondii encoding the micronemal protein MIC2.* Mol Biochem Parasitol, 1997. **84**(2): p. 203-14.
33. Robson, K.J., et al., *Thrombospondin-related adhesive protein (TRAP) of Plasmodium falciparum: expression during sporozoite ontogeny and binding to human hepatocytes.* Embo J, 1995. **14**(16): p. 3883-94.
34. Carruthers, V.B., O.K. Giddings, and L.D. Sibley, *Secretion of micronemal proteins is associated with toxoplasma invasion of host cells.* Cell Microbiol, 1999. **1**(3): p. 225-35.
35. Gantt, S., et al., *Antibodies against thrombospondin-related anonymous protein do not inhibit Plasmodium sporozoite infectivity in vivo.* Infect Immun, 2000. **68**(6): p. 3667-73.

36. Carruthers, V.B. and L.D. Sibley, *Mobilization of intracellular calcium stimulates microneme discharge in Toxoplasma gondii.* Mol Microbiol, 1999. **31**(2): p. 421-8.
37. Tomley, F.M. and D.S. Soldati, *Mix and match modules: structure and function of microneme proteins in apicomplexan parasites.* Trends Parasitol, 2001. **17**(2): p. 81-8.
38. Wang, J., D.R. Tolan, and L. Pagliaro, *Metabolic compartmentation in living cells: structural association of aldolase.* Exp Cell Res, 1997. **237**(2): p. 445-51.
39. Buscaglia, C.A., et al., *Sites of interaction between aldolase and thrombospondin-related anonymous protein in plasmodium.* Mol Biol Cell, 2003. **14**(12): p. 4947-57.
40. Jewett, T.J. and L.D. Sibley, *Aldolase forms a bridge between cell surface adhesins and the actin cytoskeleton in apicomplexan parasites.* Mol Cell, 2003. **11**(4): p. 885-94.
41. Brossier, F., et al., *C-terminal processing of the toxoplasma protein MIC2 is essential for invasion into host cells.* J Biol Chem, 2003. **278**(8): p. 6229-34.
42. Carruthers, V.B., G.D. Sherman, and L.D. Sibley, *The Toxoplasma adhesive protein MIC2 is proteolytically processed at multiple sites by two parasite-derived proteases.* J Biol Chem, 2000. **275**(19): p. 14346-53.
43. Opitz, C., et al., *Intramembrane cleavage of microneme proteins at the surface of the apicomplexan parasite Toxoplasma gondii.* Embo J, 2002. **21**(7): p. 1577-85.
44. Sibley, L.D., S. Hakansson, and V.B. Carruthers, *Gliding motility: an efficient mechanism for cell penetration.* Curr Biol, 1998. **8**(1): p. R12-4.
45. Russell, D.G. and R.E. Sinden, *The role of the cytoskeleton in the motility of coccidian sporozoites.* J Cell Sci, 1981. **50**: p. 345-59.
46. Adams, J.H., et al., *An expanding ebl family of Plasmodium falciparum.* Trends Parasitol, 2001. **17**(6): p. 297-9.
47. Duraisingh, M.T., et al., *Erythrocyte-binding antigen 175 mediates invasion in Plasmodium falciparum utilizing sialic acid-dependent and -independent pathways.* Proc Natl Acad Sci U S A, 2003. **100**(8): p. 4796-801.
48. Sim, B.K., et al., *Receptor and ligand domains for invasion of erythrocytes by Plasmodium falciparum.* Science, 1994. **264**(5167): p. 1941-4.
49. Gilberger, T.W., et al., *The cytoplasmic domain of the Plasmodium falciparum ligand EBA-175 is essential for invasion but not protein trafficking.* J Cell Biol, 2003. **162**(2): p. 317-27.
50. Silvie, O., et al., *A role for apical membrane antigen 1 during invasion of hepatocytes by Plasmodium falciparum sporozoites.* J Biol Chem, 2004. **279**(10): p. 9490-6.
51. Triglia, T., et al., *Apical membrane antigen 1 plays a central role in erythrocyte invasion by Plasmodium species.* Mol Microbiol, 2000. **38**(4): p. 706-18.
52. Narum, D.L., et al., *Immunization with parasite-derived apical membrane antigen 1 or passive immunization with a specific*

monoclonal antibody protects BALB/c mice against lethal Plasmodium yoelii yoelii YM blood-stage infection. Infect Immun, 2000. **68**(5): p. 2899-906.
53. Malkin, E.M., et al., *Phase 1 clinical trial of apical membrane antigen 1: an asexual blood-stage vaccine for Plasmodium falciparum malaria.* Infect Immun, 2005. **73**(6): p. 3677-85.
54. Saul, A., et al., *A human phase 1 vaccine clinical trial of the Plasmodium falciparum malaria vaccine candidate apical membrane antigen 1 in Montanide ISA720 adjuvant.* Vaccine, 2005. **23**(23): p. 3076-83.
55. Hehl, A.B., et al., *Toxoplasma gondii homologue of plasmodium apical membrane antigen 1 is involved in invasion of host cells.* Infect Immun, 2000. **68**(12): p. 7078-86.
56. Narum, D.L. and A.W. Thomas, *Differential localization of full-length and processed forms of PF83/AMA-1 an apical membrane antigen of Plasmodium falciparum merozoites.* Mol Biochem Parasitol, 1994. **67**(1): p. 59-68.
57. Howell, S.A., et al., *Proteolytic processing and primary structure of Plasmodium falciparum apical membrane antigen-1.* J Biol Chem, 2001. **276**(33): p. 31311-20.
58. Bannister, L.H., et al., *Plasmodium falciparum apical membrane antigen 1 (PfAMA-1) is translocated within micronemes along subpellicular microtubules during merozoite development.* J Cell Sci, 2003. **116**(Pt 18): p. 3825-34.
59. Healer, J., et al., *Independent translocation of two micronemal proteins in developing Plasmodium falciparum merozoites.* Infect Immun, 2002. **70**(10): p. 5751-8.
60. Howell, S.A., et al., *A single malaria merozoite serine protease mediates shedding of multiple surface proteins by juxtamembrane cleavage.* J Biol Chem, 2003. **278**(26): p. 23890-8.
61. Hodder, A.N., et al., *The disulfide bond structure of Plasmodium apical membrane antigen-1.* J Biol Chem, 1996. **271**(46): p. 29446-52.
62. Tordai, H., L. Banyai, and L. Patthy, *The PAN module: the N-terminal domains of plasminogen and hepatocyte growth factor are homologous with the apple domains of the prekallikrein family and with a novel domain found in numerous nematode proteins.* FEBS Lett, 1999. **461**(1-2): p. 63-7.
63. Pizarro, J.C., et al., *Crystal structure of the malaria vaccine candidate apical membrane antigen 1.* Science, 2005. **308**(5720): p. 408-11.
64. Kato, K., et al., *Domain III of Plasmodium falciparum apical membrane antigen 1 binds to the erythrocyte membrane protein Kx.* Proc Natl Acad Sci U S A, 2005. **102**(15): p. 5552-7.
65. Fraser, T.S., et al., *Erythrocyte-binding activity of Plasmodium yoelii apical membrane antigen-1 expressed on the surface of transfected COS-7 cells.* Mol Biochem Parasitol, 2001. **117**(1): p. 49-59.
66. Mitchell, G.H., et al., *Apical membrane antigen 1, a major malaria vaccine candidate, mediates the close attachment of invasive merozoites to host red blood cells.* Infect Immun, 2004. **72**(1): p. 154-8.

67. Mital, J., et al., *Conditional Expression of Toxoplasma gondii Apical Membrane Antigen-1 (TgAMA1) Demonstrates That TgAMA1 Plays a Critical Role in Host Cell Invasion.* Mol Biol Cell, 2005. **16**(9): p. 4341-9.
68. Herrera, S., et al., *A conserved region of the MSP-1 surface protein of Plasmodium falciparum contains a recognition sequence for erythrocyte spectrin.* Embo J, 1993. **12**(4): p. 1607-14.
69. Goel, V.K., et al., *Band 3 is a host receptor binding merozoite surface protein 1 during the Plasmodium falciparum invasion of erythrocytes.* Proc Natl Acad Sci U S A, 2003. **100**(9): p. 5164-9.
70. O'Donnell, R.A., et al., *Functional conservation of the malaria vaccine antigen MSP-119across distantly related Plasmodium species.* Nat Med, 2000. **6**(1): p. 91-5.
71. Dutta, S., et al., *Merozoite surface protein 1 of plasmodium vivax induces a protective response against Plasmodium cynomolgi challenge in rhesus monkeys.* Infect Immun, 2005. **73**(9): p. 5936-44.
72. Gerold, P., et al., *Structural analysis of the glycosyl-phosphatidylinositol membrane anchor of the merozoite surface proteins-1 and -2 of Plasmodium falciparum.* Mol Biochem Parasitol, 1996. **75**(2): p. 131-43.
73. Holder, A.A., et al., *Processing of the precursor to the major merozoite surface antigens of Plasmodium falciparum.* Parasitology, 1987. **94 (Pt 2)**: p. 199-208.
74. Blackman, M.J., et al., *A single fragment of a malaria merozoite surface protein remains on the parasite during red cell invasion and is the target of invasion-inhibiting antibodies.* J Exp Med, 1990. **172**(1): p. 379-82.
75. Blackman, M.J. and A.A. Holder, *Secondary processing of the Plasmodium falciparum merozoite surface protein-1 (MSP1) by a calcium-dependent membrane-bound serine protease: shedding of MSP133 as a noncovalently associated complex with other fragments of the MSP1.* Mol Biochem Parasitol, 1992. **50**(2): p. 307-15.
76. Blackman, M.J., et al., *Proteolytic processing of the Plasmodium falciparum merozoite surface protein-1 produces a membrane-bound fragment containing two epidermal growth factor-like domains.* Mol Biochem Parasitol, 1991. **49**(1): p. 29-33.
77. Morgan, W.D., et al., *Solution structure of an EGF module pair from the Plasmodium falciparum merozoite surface protein 1.* J Mol Biol, 1999. **289**(1): p. 113-22.
78. Chitarra, V., et al., *The crystal structure of C-terminal merozoite surface protein 1 at 1.8 A resolution, a highly protective malaria vaccine candidate.* Mol Cell, 1999. **3**(4): p. 457-64.
79. Hooper, N.M., E.H. Karran, and A.J. Turner, *Membrane protein secretases.* Biochem J, 1997. **321 (Pt 2)**: p. 265-79.
80. Sisodia, S.S., *Beta-amyloid precursor protein cleavage by a membrane-bound protease.* Proc Natl Acad Sci U S A, 1992. **89**(13): p. 6075-9.
81. Franzke, C.W., et al., *Shedding of collagen XVII/BP180: structural motifs influence cleavage from cell surface.* J Biol Chem, 2004. **279**(23): p. 24521-9.

82. Schwager, S.L., et al., *Cleavage of disulfide-bridged stalk domains during shedding of angiotensin-converting enzyme occurs at multiple juxtamembrane sites.* Biochemistry, 2001. **40**(51): p. 15624-30.
83. Brakebusch, C., et al., *Structural requirements for inducible shedding of the p55 tumor necrosis factor receptor.* J Biol Chem, 1994. **269**(51): p. 32488-96.
84. Alfalah, M., et al., *A point mutation in the juxtamembrane stalk of human angiotensin I-converting enzyme invokes the action of a distinct secretase.* J Biol Chem, 2001. **276**(24): p. 21105-9.
85. Barrett, A.J. and N.D. Rawlings, *Families and clans of serine peptidases.* Arch Biochem Biophys, 1995. **318**(2): p. 247-50.
86. Wu, Y., et al., *Data-mining approaches reveal hidden families of proteases in the genome of malaria parasite.* Genome Res, 2003. **13**(4): p. 601-16.
87. Clausen, T., C. Southan, and M. Ehrmann, *The HtrA family of proteases: implications for protein composition and cell fate.* Mol Cell, 2002. **10**(3): p. 443-55.
88. Dowse, T.J. and D. Soldati, *Rhomboid-like proteins in Apicomplexa: phylogeny and nomenclature.* Trends Parasitol, 2005. **21**(6): p. 254-8.
89. Freeman, M., *Proteolysis within the membrane: rhomboids revealed.* Nat Rev Mol Cell Biol, 2004. **5**(3): p. 188-97.
90. Urban, S., J.R. Lee, and M. Freeman, *Drosophila rhomboid-1 defines a family of putative intramembrane serine proteases.* Cell, 2001. **107**(2): p. 173-82.
91. Urban, S. and M. Freeman, *Substrate specificity of rhomboid intramembrane proteases is governed by helix-breaking residues in the substrate transmembrane domain.* Mol Cell, 2003. **11**(6): p. 1425-34.
92. Brossier, F., et al., *A spatially localized rhomboid protease cleaves cell surface adhesins essential for invasion by Toxoplasma.* Proc Natl Acad Sci U S A, 2005. **102**(11): p. 4146-51.
93. Dowse, T.J., et al., *Apicomplexan rhomboids have a potential role in microneme protein cleavage during host cell invasion.* Int J Parasitol, 2005. **35**(7): p. 747-56.
94. Zhou, X.W., et al., *Proteomic analysis of cleavage events reveals a dynamic two-step mechanism for proteolysis of a key parasite adhesive complex.* Mol Cell Proteomics, 2004. **3**(6): p. 565-76.
95. Carruthers, V.B. and M.J. Blackman, *A new release on life: emerging concepts in proteolysis and parasite invasion.* Mol Microbiol, 2005. **55**(6): p. 1617-30.
96. Howell, S.A., et al., *Distinct mechanisms govern proteolytic shedding of a key invasion protein in apicomplexan pathogens.* Mol Microbiol, 2005. **57**(5): p. 1342-56.
97. Siezen, R.J., et al., *Homology modelling and protein engineering strategy of subtilases, the family of subtilisin-like serine proteinases.* Protein Eng, 1991. **4**(7): p. 719-37.
98. Siezen, R.J. and J.A. Leunissen, *Subtilases: the superfamily of subtilisin-like serine proteases.* Protein Sci, 1997. **6**(3): p. 501-23.

99. Nebes, V.L. and E.W. Jones, *Activation of the proteinase B precursor of the yeast Saccharomyces cerevisiae by autocatalysis and by an internal sequence.* J Biol Chem, 1991. **266**(34): p. 22851-7.
100. Espenshade, P.J., et al., *Autocatalytic processing of site-1 protease removes propeptide and permits cleavage of sterol regulatory element-binding proteins.* J Biol Chem, 1999. **274**(32): p. 22795-804.
101. Sajid, M., C. Withers-Martinez, and M.J. Blackman, *Maturation and specificity of Plasmodium falciparum subtilisin-like protease-1, a malaria merozoite subtilisin-like serine protease.* J Biol Chem, 2000. **275**(1): p. 631-41.
102. Kessler, E. and M. Safrin, *The propeptide of Pseudomonas aeruginosa elastase acts an elastase inhibitor.* J Biol Chem, 1994. **269**(36): p. 22726-31.
103. Fugere, M., et al., *Inhibitory potency and specificity of subtilase-like pro-protein convertase (SPC) prodomains.* J Biol Chem, 2002. **277**(10): p. 7648-56.
104. Ikemura, H., H. Takagi, and M. Inouye, *Requirement of pro-sequence for the production of active subtilisin E in Escherichia coli.* J Biol Chem, 1987. **262**(16): p. 7859-64.
105. Li, Y., et al., *Functional analysis of the propeptide of subtilisin E as an intramolecular chaperone for protein folding. Refolding and inhibitory abilities of propeptide mutants.* J Biol Chem, 1995. **270**(42): p. 25127-32.
106. Yabuta, Y., et al., *Folding pathway mediated by an intramolecular chaperone: propeptide release modulates activation precision of pro-subtilisin.* J Biol Chem, 2001. **276**(48): p. 44427-34.
107. Marie-Claire, C., et al., *Folding pathway mediated by an intramolecular chaperone: the structural and functional characterization of the aqualysin I propeptide.* J Mol Biol, 2001. **305**(1): p. 151-65.
108. Hidaka, Y., et al., *Dual function of the propeptide of prouroguanylin in the folding of the mature peptide: disulfide-coupled folding and dimerization.* J Biol Chem, 2000. **275**(33): p. 25155-62.
109. Blackman, M.J., et al., *A subtilisin-like protein in secretory organelles of Plasmodium falciparum merozoites.* J Biol Chem, 1998. **273**(36): p. 23398-409.
110. O'Donnell, R. and M. Blackman, *Unpublished results.*
111. Yeoh, S., et al., *Unpublished results.*
112. Withers-Martinez, C., et al., *Expression of recombinant Plasmodium falciparum subtilisin-like protease-1 in insect cells. Characterization, comparison with the parasite protease, and homology modeling.* J Biol Chem, 2002. **277**(33): p. 29698-709.
113. O'Donnell, R., F. Hackett, and M. Blackman, *Unpublished results.*
114. Hackett, F., et al., *PfSUB-2: a second subtilisin-like protein in Plasmodium falciparum merozoites.* Mol Biochem Parasitol, 1999. **103**(2): p. 183-95.
115. Uzureau, P., et al., *Gene targeting demonstrates that the Plasmodium berghei subtilisin PbSUB2 is essential for red cell invasion and reveals spontaneous genetic recombination events.* Cell Microbiol, 2004. **6**(1): p. 65-78.

116. Barale, J.C., et al., *Plasmodium falciparum subtilisin-like protease 2, a merozoite candidate for the merozoite surface protein 1-42 maturase.* Proc Natl Acad Sci U S A, 1999. **96**(11): p. 6445-50.
117. O'Donnell, R.A., M.J. Blackman, and B.S. Crabb, *Unpublished results.*
118. Han, Y.S., et al., *Molecular interactions between Anopheles stephensi midgut cells and Plasmodium berghei: the time bomb theory of ookinete invasion of mosquitoes.* Embo J, 2000. **19**(22): p. 6030-40.
119. Florens, L., et al., *A proteomic view of the Plasmodium falciparum life cycle.* Nature, 2002. **419**(6906): p. 520-6.
120. Harris, P.K., et al., *Molecular Identification of a Malaria Merozoite Surface Sheddase.* PLOS Pathogen, 2005. **In Press**.
121. Wu, Y., et al., *Transfection of Plasmodium falciparum within human red blood cells.* Proc Natl Acad Sci U S A, 1995. **92**(4): p. 973-7.
122. O'Donnell, R.A., et al., *A genetic screen for improved plasmid segregation reveals a role for Rep20 in the interaction of Plasmodium falciparum chromosomes.* Embo J, 2002. **21**(5): p. 1231-9.
123. Wu, Y., L.A. Kirkman, and T.E. Wellems, *Transformation of Plasmodium falciparum malaria parasites by homologous integration of plasmids that confer resistance to pyrimethamine.* Proc Natl Acad Sci U S A, 1996. **93**(3): p. 1130-4.
124. Crabb, B.S. and A.F. Cowman, *Characterization of promoters and stable transfection by homologous and nonhomologous recombination in Plasmodium falciparum.* Proc Natl Acad Sci U S A, 1996. **93**(14): p. 7289-94.
125. Fidock, D.A. and T.E. Wellems, *Transformation with human dihydrofolate reductase renders malaria parasites insensitive to WR99210 but does not affect the intrinsic activity of proguanil.* Proc Natl Acad Sci U S A, 1997. **94**(20): p. 10931-6.
126. O'Donnell, R., et al., *An alteration in concatameric structure is associated with efficient segregation of plasmids in transfected Plasmodium falciparum parasites.* Nucleic Acids Res, 2001. **29**(3): p. 716-24.
127. Duraisingh, M.T., T. Triglia, and A.F. Cowman, *Negative selection of Plasmodium falciparum reveals targeted gene deletion by double crossover recombination.* Int J Parasitol, 2002. **32**(1): p. 81-9.
128. Wickham, M.E., J.K. Thompson, and A.F. Cowman, *Characterisation of the merozoite surface protein-2 promoter using stable and transient transfection in Plasmodium falciparum.* Mol Biochem Parasitol, 2003. **129**(2): p. 147-56.
129. Triglia, T., et al., *Allelic exchange at the endogenous genomic locus in Plasmodium falciparum proves the role of dihydropteroate synthase in sulfadoxine-resistant malaria.* Embo J, 1998. **17**(14): p. 3807-15.
130. Crabb, B.S., et al., *Stable transgene expression in Plasmodium falciparum.* Mol Biochem Parasitol, 1997. **90**(1): p. 131-44.
131. Crabb, B.S., et al., *Targeted gene disruption shows that knobs enable malaria-infected red cells to cytoadhere under physiological shear stress.* Cell, 1997. **89**(2): p. 287-96.
132. Healer, J., et al., *Allelic polymorphisms in apical membrane antigen-1 are responsible for evasion of antibody-mediated inhibition in Plasmodium falciparum.* Mol Microbiol, 2004. **52**(1): p. 159-68.

133. Meissner, M., et al., *Modulation of myosin A expression by a newly established tetracycline repressor-based inducible system in Toxoplasma gondii.* Nucleic Acids Res, 2001. **29**(22): p. E115.
134. Meissner, M., et al., *Tetracycline analogue-regulated transgene expression in Plasmodium falciparum blood stages using Toxoplasma gondii transactivators.* Proc Natl Acad Sci U S A, 2005. **102**(8): p. 2980-5.
135. Cowman, A.F., et al., *Functional analysis of the Plasmodium falciparum genome using transfection.* Methods in Microbiology, ed. B. Wren. Vol. 33. 2002: Elsevier. 383-96.
136. Withers-Martinez, C., et al., *PCR-based gene synthesis as an efficient approach for expression of the A+T-rich malaria genome.* Protein Eng, 1999. **12**(12): p. 1113-20.
137. Ho, S.N., et al., *Site-directed mutagenesis by overlap extension using the polymerase chain reaction.* Gene, 1989. **77**(1): p. 51-9.
138. Horton, R.M., et al., *Engineering hybrid genes without the use of restriction enzymes: gene splicing by overlap extension.* Gene, 1989. **77**(1): p. 61-8.
139. Craven, R.A., et al., *Vectors for the expression of tagged proteins in Schizosaccharomyces pombe.* Gene, 1998. **221**(1): p. 59-68.
140. Miller, S.K., et al., *A subset of Plasmodium falciparum SERA genes are expressed and appear to play an important role in the erythrocytic cycle.* J Biol Chem, 2002. **277**(49): p. 47524-32.
141. Trager, W. and J.B. Jensen, *Human malaria parasites in continuous culture.* Science, 1976. **193**(4254): p. 673-5.
142. Lambros, C. and J.P. Vanderberg, *Synchronization of Plasmodium falciparum erythrocytic stages in culture.* J Parasitol, 1979. **65**(3): p. 418-20.
143. Tosta, C.E., et al., *Plasmodium yoelii and Plasmodium berghei: isolation of infected erythrocytes from blood by colloidal silica gradient centrifugation.* Exp Parasitol, 1980. **50**(1): p. 7-15.
144. Bejon, P.A., et al., *A role for microtubules in Plasmodium falciparum merozoite invasion.* Parasitology, 1997. **114 (Pt 1)**: p. 1-6.
145. Wasserman, M., C. Alarcon, and P.M. Mendoza, *Effects of Ca++ depletion on the asexual cell cycle of Plasmodium falciparum.* Am J Trop Med Hyg, 1982. **31**(4): p. 711-7.
146. Shaw, M.K., et al., *Microtubules, but not actin filaments, drive daughter cell budding and cell division in Toxoplasma gondii.* J Cell Sci, 2000. **113 (Pt 7)**: p. 1241-54.
147. Laine, J., et al., *Differential regulation of Akt kinase isoforms by the members of the TCL1 oncogene family.* J Biol Chem, 2002. **277**(5): p. 3743-51.
148. Neill, J.D., et al., *Epitope-tagged gonadotropin-releasing hormone receptors heterologously-expressed in mammalian (COS-1) and insect (Sf9) cells.* Mol Cell Endocrinol, 1997. **127**(2): p. 143-54.
149. Ling, I.T. and A.A. Holder, *Unpublished results.*
150. Blackman, M.J., H. Whittle, and A.A. Holder, *Processing of the Plasmodium falciparum major merozoite surface protein-1: identification of a 33-kilodalton secondary processing product which is*

shed prior to erythrocyte invasion. Mol Biochem Parasitol, 1991. **49**(1): p. 35-44.
151. Kocken, C.H., et al., *Precise timing of expression of a Plasmodium falciparum-derived transgene in Plasmodium berghei is a critical determinant of subsequent subcellular localization.* J Biol Chem, 1998. **273**(24): p. 15119-24.
152. Holder, A.A., et al., *Isolation of a Plasmodium falciparum rhoptry protein.* Mol Biochem Parasitol, 1985. **14**(3): p. 293-303.
153. Blackman, M.J., et al., *Structural and biochemical characterization of a fluorogenic rhodamine-labeled malarial protease substrate.* Biochemistry, 2002. **41**(40): p. 12244-52.
154. Deans, J.A., et al., *Biosynthesis of a putative protective Plasmodium knowlesi merozoite antigen.* Mol Biochem Parasitol, 1984. **11**: p. 189-204.
155. Klemba, M., et al., *Trafficking of plasmepsin II to the food vacuole of the malaria parasite Plasmodium falciparum.* J Cell Biol, 2004. **164**(1): p. 47-56.
156. Mattsson, J.G. and D. Soldati, *MPS1: a small, evolutionarily conserved zinc finger protein from the protozoan Toxoplasma gondii.* FEMS Microbiol Lett, 1999. **180**(2): p. 235-9.
157. Khan, F., et al., *Cyclin-dependent kinase TPK2 is a critical cell cycle regulator in Toxoplasma gondii.* Mol Microbiol, 2002. **45**(2): p. 321-32.
158. Sehgal, A., et al., *Translocation of ribosomal protein P0 onto the Toxoplasma gondii tachyzoite surface.* Int J Parasitol, 2003. **33**(14): p. 1589-94.
159. Yung, S., T.R. Unnasch, and N. Lang-Unnasch, *Analysis of apicoplast targeting and transit peptide processing in Toxoplasma gondii by deletional and insertional mutagenesis.* Mol Biochem Parasitol, 2001. **118**(1): p. 11-21.
160. Field, J., et al., *Purification of a RAS-responsive adenylyl cyclase complex from Saccharomyces cerevisiae by use of an epitope addition method.* Mol Cell Biol, 1988. **8**(5): p. 2159-65.
161. Anderson, E.D., et al., *Activation of the furin endoprotease is a multiple-step process: requirements for acidification and internal propeptide cleavage.* Embo J, 1997. **16**(7): p. 1508-18.
162. Golightly, L.M., et al., *3' UTR elements enhance expression of Pgs28, an ookinete protein of Plasmodium gallinaceum.* Mol Biochem Parasitol, 2000. **105**(1): p. 61-70.
163. Ward, G.E., et al., *Staurosporine inhibits invasion of erythrocytes by malarial merozoites.* Exp Parasitol, 1994. **79**(3): p. 480-7.
164. Gros, P., K.H. Kalk, and W.G. Hol, *Calcium binding to thermitase. Crystallographic studies of thermitase at 0, 5, and 100 mM calcium.* J Biol Chem, 1991. **266**(5): p. 2953-61.
165. Coue, M., et al., *Inhibition of actin polymerization by latrunculin A.* FEBS Lett, 1987. **213**(2): p. 316-8.
166. MacLean-Fletcher, S. and T.D. Pollard, *Mechanism of action of cytochalasin B on actin.* Cell, 1980. **20**(2): p. 329-41.
167. Valderrama, F., et al., *Actin microfilaments facilitate the retrograde transport from the Golgi complex to the endoplasmic reticulum in mammalian cells.* Traffic, 2001. **2**(10): p. 717-26.

168. Poulsen, N.C., et al., *Diatom gliding is the result of an actin-myosin motility system.* Cell Motil Cytoskeleton, 1999. **44**(1): p. 23-33.
169. Makioka, A., et al., *Entamoeba invadens: enhancement of excystation and metacystic development by cytochalasin D.* Exp Parasitol, 2001. **98**(3): p. 145-51.
170. Cramer, L.P. and T.J. Mitchison, *Myosin is involved in postmitotic cell spreading.* J Cell Biol, 1995. **131**(1): p. 179-89.
171. Jean, L., et al., *Functional characterization of the propeptide of Plasmodium falciparum subtilisin-like protease-1.* J Biol Chem, 2003. **278**(31): p. 28572-9.
172. Yeoh, S., S. Fleck, and M.J. Blackman, *Unpublished data.*
173. Geoghegan, K.F., P.J. Rosner, and L.R. Hoth, *Dye-pair reporter systems for protein-peptide molecular interactions.* Bioconjug Chem, 2000. **11**(1): p. 71-7.
174. Packard, B.Z., et al., *Profluorescent protease substrates: intramolecular dimers described by the exciton model.* Proc Natl Acad Sci U S A, 1996. **93**(21): p. 11640-5.
175. Corrie, J.E. and J.S. Craik, *Synthesis and Characterisation of Pure Isomers of Iodoacetamidotetramethylrhodamine.* J Chem Soc Perkin Trans, 1994. **1**: p. 2967-2973.
176. Zimmerman, M., G. Patel, and N.J. Patel Gay, *A new fluorogenic substrate for chymotrypsin.* Anal Biochem, 1976. **70**(1): p. 258-62.
177. Wang, G.T., et al., *A continuous fluorescence assay of renin activity.* Anal Biochem, 1993. **210**(2): p. 351-9.
178. Peterson, D.S., et al., *The circumsporozoite protein of Plasmodium falciparum is expressed and localized to the cell surface in the free-living ciliate Tetrahymena thermophila.* Mol Biochem Parasitol, 2002. **122**(2): p. 119-26.
179. Sayers, J.R., et al., *AGA/AGG codon usage in parasites: implications for gene expression in Escherichia coli.* Parasitol Today, 1995. **11**(9): p. 345-6.
180. Kocken, C.H., et al., *High-level expression of the malaria blood-stage vaccine candidate Plasmodium falciparum apical membrane antigen 1 and induction of antibodies that inhibit erythrocyte invasion.* Infect Immun, 2002. **70**(8): p. 4471-6.
181. Rug, M., et al., *Correct promoter control is needed for trafficking of the ring-infected erythrocyte surface antigen to the host cytosol in transfected malaria parasites.* Infect Immun, 2004. **72**(10): p. 6095-105.
182. Porter, M.E., *The DNA polymerase delta promoter from Plasmodium falciparum contains an unusually long 5' untranslated region and intrinsic DNA curvature.* Mol Biochem Parasitol, 2001. **114**(2): p. 249-55.
183. Polson, H.E. and M.J. Blackman, *A role for poly(dA)poly(dT) tracts in directing activity of the Plasmodium falciparum calmodulin gene promoter.* Mol Biochem Parasitol, 2005. **141**(2): p. 179-89.
184. Dechering, K.J., et al., *Isolation and functional characterization of two distinct sexual-stage-specific promoters of the human malaria parasite Plasmodium falciparum.* Mol Cell Biol, 1999. **19**(2): p. 967-78.

185. Horrocks, P. and B.J. Kilbey, *Physical and functional mapping of the transcriptional start sites of Plasmodium falciparum proliferating cell nuclear antigen.* Mol Biochem Parasitol, 1996. **82**(2): p. 207-15.
186. Holloway, S.P., et al., *Isolation of alpha-tubulin genes from the human malaria parasite, Plasmodium falciparum: sequence analysis of alpha-tubulin.* Mol Microbiol, 1989. **3**(11): p. 1501-10.
187. Adisa, A., et al., *The signal sequence of exported protein-1 directs the green fluorescent protein to the parasitophorous vacuole of transfected malaria parasites.* J Biol Chem, 2003. **278**(8): p. 6532-42.
188. van Dijk, M.R., et al., *Replication, expression and segregation of plasmid-borne DNA in genetically transformed malaria parasites.* Mol Biochem Parasitol, 1997. **86**(2): p. 155-62.
189. O'Donnell, R.A., *Personal communication.*
190. Tonkin, C.J., et al., *Localization of organellar proteins in Plasmodium falciparum using a novel set of transfection vectors and a new immunofluorescence fixation method.* Mol Biochem Parasitol, 2004. **137**(1): p. 13-21.
191. Kadekoppala, M., et al., *Rapid recombination among transfected plasmids, chimeric episome formation and trans gene expression in Plasmodium falciparum.* Mol Biochem Parasitol, 2001. **112**(2): p. 211-8.
192. Sato, S. and R.J. Wilson, *The use of DsRED in single- and dual-color fluorescence labeling of mitochondrial and plastid organelles in Plasmodium falciparum.* Mol Biochem Parasitol, 2004. **134**(1): p. 175-9.
193. Nagahama, M., et al., *Biosynthetic processing and quaternary interactions of proprotein convertase SPC4 (PACE4).* FEBS Lett, 1998. **434**(1-2): p. 155-9.
194. Zhou, A. and R.E. Mains, *Endoproteolytic processing of proopiomelanocortin and prohormone convertases 1 and 2 in neuroendocrine cells overexpressing prohormone convertases 1 or 2.* J Biol Chem, 1994. **269**(26): p. 17440-7.
195. Withers-Martinez, C., L. Jean, and M.J. Blackman, *Subtilisin-like proteases of the malaria parasite.* Mol Microbiol, 2004. **53**(1): p. 55-63.
196. Thompson, J.F., L.S. Hayes, and D.B. Lloyd, *Modulation of firefly luciferase stability and impact on studies of gene regulation.* Gene, 1991. **103**(2): p. 171-7.
197. Rabenau, K.E., et al., *TgM2AP participates in Toxoplasma gondii invasion of host cells and is tightly associated with the adhesive protein TgMIC2.* Mol Microbiol, 2001. **41**(3): p. 537-47.